Statistical Mechanics From Unitary Dynamics

Jonathon Riddell

A Thesis Submitted to the School of Graduate Studies in
Partial Fulfilment of the Requirements for the Degree Doctor of Philosophy

September 12, 2022

McMaster University
Doctor of Philosophy (2022)
Hamilton, Ontario (Department of Physics and Astronomy)

TITLE: Statistical Mechanics From Unitary Dynamics
AUTHOR: Jonathon Riddell
SUPERVISOR: Dr. Erik S. Sørensen
NUMBER OF PAGES: 112

Acknowledgements

No story of success is complete without acknowledging the support system one had while completing a difficult task. Throughout my scientific career I have been lucky to work with amazing people who offered me support, guidance and encouragement. I would like to thank my supervisor Erik, for giving me the opportunity to take on this path, allowing me the room to grow and explore my interests and being a regular pillar of support throughout my time at McMaster. Truthfully there were moments where without Erik, I may have left the program and abandoned my passion for physics. It's a real shame we couldn't get you the supervisor of the year award, it would have been well deserved. I'd like to again, personally thank you for helping me navigate the department and the university with issues relating to my health, and always inserting your voice into conversations when I needed an ally. You have undoubtedly allowed me to grow into the researcher I am today. I would also like to thank Álvaro for being a positive influence on my trajectory as well. I will always look back fondly on the day long collaboration meetings we had at PI! I'd also like to thank you for your patience during the many breaks we had to take for my degree requirements. I look forward to many future collaborations! Throughout the years I've had the pleasure of collaborating with many researchers, some resulting in publications and some not. Regardless of outcomes I am grateful I had the the chance to interact with all of you and share your passion and excitement about the field. Lastly, I would like to thank my committee members Sung-Sik and Duncan. I've always looked forward to chatting with you both about my projects.

I'd like to also thank my family and friends for the support and encouragement they've provided me along the way. My health has had a lot of ups and downs and my family in particular are the crutches I have leaned on throughout my time here. It's impossible to overstate their contribution. I would like to specifically thank three people who are constantly there for me and provide me with invaluable support. Firstly my wife Alejandra. Day in and day out you make bad days easier and my good days better, you are my constant. Secondly my mother Sharon, you are always available and supportive for me, you are my rock. Thirdly my little sister Gabriela, my number one hype-man, you are a big source of my confidence.

You three are the shoulders I stand on, my strength and inspiration. I'd also like to extend a special thanks to my friends Nathan, James, and Steve. You three have been a constant outlet for conversations, black board talks and more throughout the years to talk about the problems and questions I've had about research. I'd also like to thank Mica for being a constant presence in my life and a constant reminder that life exists outside of my research world, and sometimes, usually, watching a cat eat her food is more important than that next line of code.

Contents

Chapter 1

Publications and contributed work

In this chapter I will briefly review all of my work that is published or in the process of publication. If the work is not yet published I will indicate where it is currently submitted to.

1.1 Published work

In this section I list my publications which have gone through peer review. All articles listed below are not contributions to but were published during my graduate studies.

1. Jonathon Riddell, Markus P. Müller. Generalized eigenstate typicality in translation-invariant quasifree fermionic models. *Phys. Rev. B*, 97:035129, Jan 2018.

2. Jonathon Riddell, Erik S. Sørensen, Out-of-time ordered correlators and entanglement growth in the random field xx spin chain. *Phys. Rev. B*, 99:054205, Feb 2019.

3. Jonathon Riddell, Erik S. Sørensen, Out-of-time-order correlations in the quasiperiodic Aubry-André model. *Phys. Rev. B*, 101:024202, Jan 2020.

4. Álvaro M. Alhambra, Jonathon Riddell, Luis Pedro García-Pintos, Time evolution of correlation functions in quantum many-body systems. *Phys. Rev. Lett*. 124:110605, Mar 2020.

1.2 Contributed work

In this section I list all the contributed works to this thesis. All articles contributed as chapters are currently in the peer review process. Throughout the introduction I will refer to these articles as ”Contribution x” where x will be the number in the list below.

1. Jonathon Riddell, Luis Pedro García-Pintos, Álvaro M. Alhambra. Relaxation of non-integrable systems and correlation functions. arxiv:2112.09475, Dec 2021, submitted to Phys. Rev. E. Presented in chapter 3.

2. Jonathon Riddell, Nathan Pagliaroli, Álvaro M. Alhambra. Concentration of quantum equilibration and an estimate of the recurrence time, arXiv:2206.07541, Jun 2022, submitted to Phys. Rev. Lett. Presented in chapter 4.

3. Jonathon Riddell, Wyatt Kirkby, D. H. J. O'Dell, Erik S. Sørensen. Scaling at the OTOC Wavefront: Integrable versus chaotic models, arXiv:2111.01336, Nov 2021, in preparation for Phys. Rev. B. Presented in chapter 5.

Chapter 2

Introduction

2.1 Static equilibrium from unitary dynamics

Statistical mechanics and thermodynamics were initially developed in the 1800s through the desire to describe the macroscopic properties of physical systems. Insights from these two fields have contributed significantly to our understanding and development of topics in engineering, material sciences and more. Despite much success our understanding of statistical mechanics from a foundational point of view is still lacking, with many open questions remaining unanswered. In the past two decades the age old question of how closed quantum systems approach thermodynamic equilibrium has seen a resurgence of interest. The recent uptick in interest in the foundational arguments of statistical mechanics has been largely ignited novel by experiments in ultracold atomic gases as well as new insights from quantum information theory, giving us new experimental insight and theoretical tools to investigate the emergence of statistical mechanics in isolated quantum systems [1–10].

The typical starting point for the construction of statistical mechanics begins with a closed, isolated system governed by some Hamilton $\hat{H}$, typically a classical system. To derive the typical ensembles of statistical mechanics one might make an assumption on the dynamics of the system, such as Ergodicity or one introduces the principle of equal a-priori probability which allows you to assign the microcanonical distribution to the energetically accessible microstates of the system [11, 12]. In this thesis we will keep with the spirit of this approach. We will begin our discussion with a closed, isolated system governed by some Hamiltonian H. We will however make a stronger demand than the typical constructions that one might find in a textbook. The key difference is insisting that static equilibrium and statistical mechanics must emerge from the dynamics of quantum mechanics, as it is the more fundamental theory of reality. So let us begin our discussion by considering some generic

Hamiltonian H governing the dynamics of some quantum system initialized in the pure state $|\psi\rangle$ which is normalized $|\langle\psi|\psi\rangle|^2 = 1$. We will take the convention that the initialization time will be set at $t = 0$. We will also throughout this document take the convention that $\hbar = 1$ and $k_B = 1$. We will assume that the Hamiltonian has a spectral decomposition of the form,

$$\hat{H} = \sum_m E_m |E_m\rangle\langle E_m|, \tag{2.1}$$

where for convenience we will assume that the spectrum is finite. It is helpful then to imagine our system is constructed by some d dimensional local Hilbert space and we have N total lattice sites, giving us a Hilbert space size of d^N. The thermodynamic limit is then recovered when we take $N \to \infty$. While this construction isn't necessary for what follows, this condition is satisfied in a number of interesting models. For example magnetic systems like the spin 1/2 Heisenberg model where $d = 2$, or other lattice models with local degrees of freedom which have a finite local Hilbert space dimension. We will also assume our model does not have any additional symmetries apart from energy avoiding potential problems like sets of non-commuting conserved quantities, degeneracy and integrability [1, 13–22].

We may express our initial state $|\psi\rangle$ in the energy eigenbasis in the following way,

$$|\psi\rangle = \sum_m c_m |E_m\rangle, \quad c_m = \langle\psi|E_m\rangle. \tag{2.2}$$

Dynamics in this system will be generated by the Schrödinger equation,

$$i\frac{d}{dt}|\psi\rangle = \hat{H}|\psi\rangle, \tag{2.3}$$

which admits the energy eigenkets as time independent states as time evolution of these states simply picks up a global phase,

$$i\frac{d}{dt}|E_k\rangle = \hat{H}|E_k\rangle = E_k|E_k\rangle, \quad \implies |E_k(t)\rangle = e^{-iE_k t}|E_k\rangle. \tag{2.4}$$

This then allows us to write the time evolution of our pure state as,

$$|\psi(t)\rangle = \sum_m c_m e^{-iE_m t}|E_m\rangle. \tag{2.5}$$

The time evolution in equation 2.5 is called unitary because the evolution is generated by a unitary operator,

$$\boxed{|\psi(t)\rangle = U(t)|\psi\rangle \text{ with } \quad U(t) = e^{-i\hat{H}t}}. \tag{2.6}$$

The first thing to notice is that the time evolution of equation 2.5 will not be sufficient on it's own to define static equilibrium. What we have here is a normalized vector with entries rotating in the complex plain with frequencies E_m. So on it's own $|\psi(t)\rangle$ will not relax to some notion of static equilibrium. So we must track something else to investigate the emergence of static equilibrium. Intuitively we will introduce an observable $\hat{A}$, and track it's expectation value in time. We say that equilibration has occurred if the expectation value of $\hat{A}$ settles down to a stationary value in time,

$$\langle \hat{A}(t) \rangle \to A(\infty). \tag{2.7}$$

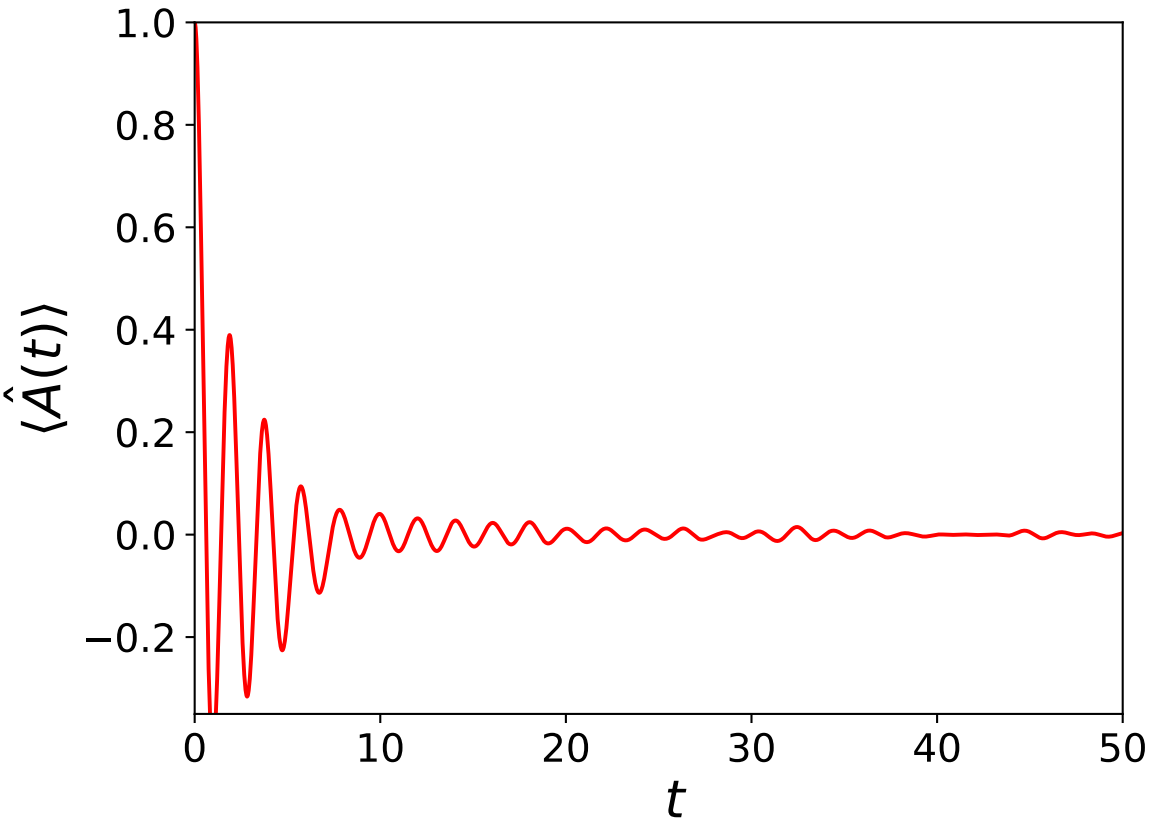

Figure 2.1: Typical expectation value of an observable in time, relaxing to an approximate equilibrium. Numerics were performed on a spin 1/2 J1-J2 type model in one dimension for $L = 22$ lattice sites. To see further details see Contribution 1 in chapter 3. The dynamics presented here are from observable state pair $\langle A_1(t) \rangle_{|\psi\rangle}$ in Contribution 1.

We call the equilibrium value $A(\infty)$ however it's important to note we have yet to demon-

strate it's existence. First let us expand the expectation value of A in the energy eigenbasis,

$$\langle \hat{A}(t) \rangle = \sum_{m,n} \bar{c}_m c_n \hat{A}_{m,n} e^{i(E_m - E_n)t}. \tag{2.8}$$

From equation 2.8 we can see that our expression that we have a quasi-periodic function, so it doesn't make sense to for example define $A(\infty) = \lim_{t\to\infty} \langle \hat{A}(t) \rangle$, as in general this limit does not exist. Instead, if we expect $\langle \hat{A}(t) \rangle$ to relax to equilibrium and stay there, it must equilibrate and sit at the value of $A(\infty)$ for most times t.Therefore the equilibrium value will also be the average value of our expectation value taken over all time, assuming equilibration did indeed occur. We can then define the equilibrium value in the following way [2, 23–28],

$$A(\infty) = \lim_{\tau\to\infty} \frac{1}{\tau} \int_0^\tau \langle \hat{A}(t) \rangle dt. \tag{2.9}$$

This form has a few advantages, firstly, if we assume our Hamiltonian has a non-degenerate spectrum, then we can evaluate this limit easily and recover,

$$A(\infty) = \sum_k |c_k|^2 A_{k,k}. \tag{2.10}$$

Equation 2.10 tells us that the equilibrium value only depends on the diagonal terms of the observable in the energy eigenbasis, which is time independent. Secondly we can introduce the diagonal ensemble from this expression. To see this define the density matrix $\rho(t) = |\psi(t)\rangle\langle\psi(t)|$, then we define the diagonal ensemble as,

$$\boxed{\omega = \lim_{\tau\to\infty} \frac{1}{\tau} \int_0^\tau \rho(t) dt = \sum_k |c_k|^2 |E_k\rangle\langle E_k|}. \tag{2.11}$$

This allows us to rewrite the equilibrium value as,

$$\boxed{A(\infty) = \text{Tr}\left[\hat{A}\omega\right]}. \tag{2.12}$$

This is true for all observables where their expectation value reaches some static value in time after an initial out of equilibrium period. Next we need to understand under what conditions this equilibration process can occur. One way to make progress is to consider the average distance of $\langle \hat{A}(t) \rangle$ and the equilibrium value $A(\infty)$ in time. To study this, we define the following quantity [6, 24, 27],

$$\sigma_A^2 = \lim_{\tau\to\infty} \frac{1}{\tau} \int_0^\tau |\operatorname{Tr}\left[\hat{A}\left(\rho(t) - \omega\right)\right]|^2 dt \quad . \tag{2.13}$$

Note here that this is an infinite time average statement, and does not tell us anything about finite time dynamics. This quantity can be interpreted in a few ways. Firstly we may consider it the average distance squared between $\langle \hat{A}(t) \rangle$ and $A(\infty)$ over all time. So if this quantity is small, we expect that $\langle \hat{A}(t) \rangle$ spends the majority of it's time arbitrarily close to to it's equilibrium value. It might also be interpreted as the second moment of the following probability distribution,

$$P(x) = \lim_{\tau\to\infty} \int_0^\tau \frac{\mathrm{d}t}{\tau} \delta(x - f(t)) \quad . \tag{2.14}$$

$P(x)$ can be understood as the probability that, if we pick a random time $t \in [0, \infty)$, the value of $f(t)$ is exactly x (see also [29–31]). Figure 2.2 is an example of $P(x)$ forming as we take $\tau \to \infty$. The moments of this distribution can be written as [31],

$$\kappa_q = \lim_{\tau\to\infty} \frac{1}{\tau} \int_0^\tau (\langle \hat{A}(t) \rangle - A(\infty))^q dt \quad , \tag{2.15}$$

where we identify the case of $\kappa_2 = \sigma_A^2$. Interestingly σ_A^2 can be bounded quite tightly. To do this let us make a slightly stronger assumption on the energies E_k. We will assume that we have non-degenerate energy gaps,

$$E_m + E_n = E_l + E_k \implies \{m, n\} = \{k, l\}, \tag{2.16}$$

where we demand this holds for all indices. This property is expected to hold for example in quantum chaotic models with level repulsion [1, 2, 32, 33]. With this assumption one can derive the following bound [24, 27],

$$\sigma_A^2 \leq ||\hat{A}||^2 \operatorname{Tr}\left[\omega^2\right] . \tag{2.17}$$

Where $||\hat{A}||$ should be interpreted as the largest singular value of $\hat{A}$. For most relevant initial conditions we expect that $\operatorname{Tr}[\omega^2]$ will be exponentially small in system size [2, 24, 27, 31]. This bound can also be generalized to cases where the Hamiltonian has degenerate gaps and to cases where the initial state is mixed [6, 24, 34, 35].

For the higher moments k_q one can derive a generic bound. First we need to generalize the non-degenerate gaps condition given in equation 2.16 to larger sums of energies,

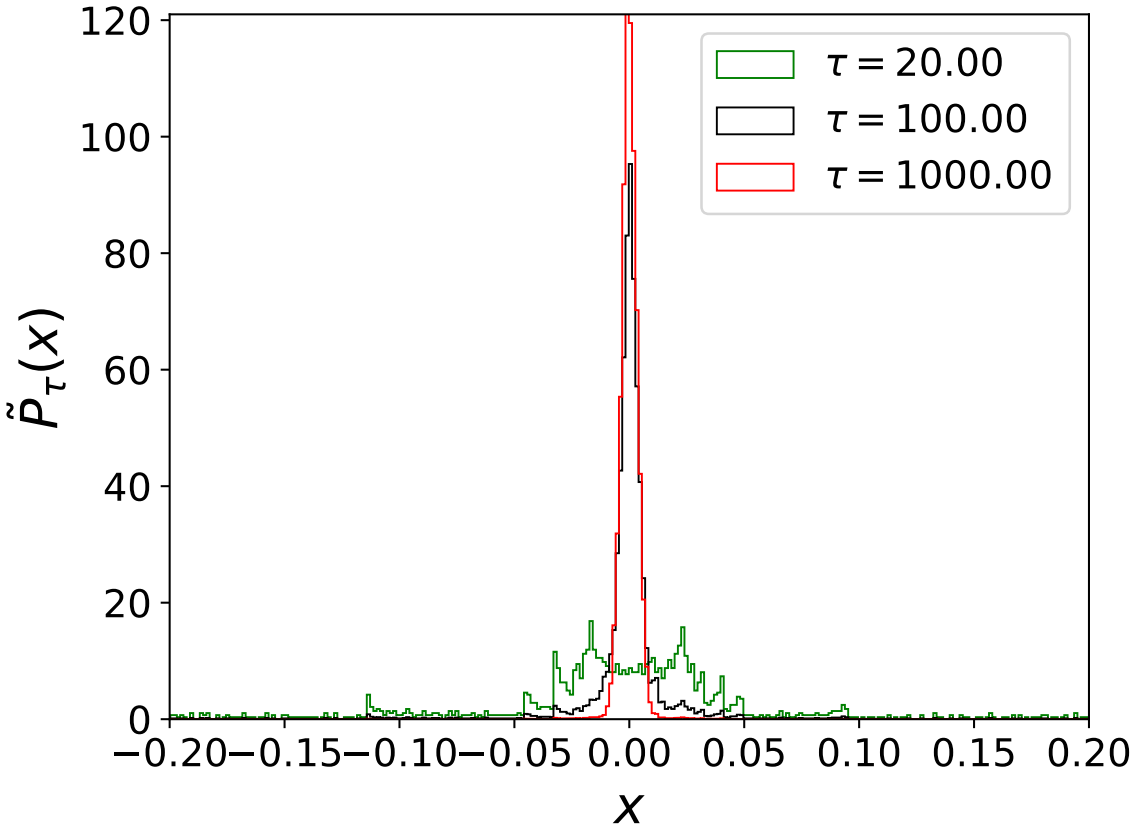

Figure 2.2: Example of $P_\tau(x)$ converging to $P(x)$ where $P_\tau(x) = \int_0^\tau \frac{\mathrm{d}t}{\tau}\delta(x - \langle A(t)\rangle)$ and $P(x)$ is recovered as $\tau \to \infty$. $\tilde{P}_\tau(x)$ represents the approximation of $P_\tau(x)$ by binning samples and constructing a histogram. See Contribution 2 figure 1 for further details.

$$\sum_{i=1}^{q} E_{m_i} = \sum_{i=1}^{q} E_{n_i} \implies \{m_i\} = \{n_i\}. \tag{2.18}$$

This condition is quite strong. A possible mathematical justification for it is that the set of Hermitian matrices that fit this condition have full Lebesgue measure in the set of possible $d^N \times d^N$ matrices, Contribution 2 [31]. A more physical argument for this condition is that it is expected to hold in non-integrable and chaotic models such as those with Wigner-Dyson level statistics [9,36–38]. It is important to note that this assumption further restricts the class of systems we are talking about, but allows us to in return make stronger statements. Using this assumption on the energies we can derive the following bound on the moments of $P(x)$,

Contribution 2 [31],

$$|\kappa_q| \leq \left(q||A||\sqrt{\mathrm{Tr}\left[\omega^2\right]}\right)^q. \tag{2.19}$$

Using equation 2.19 in conjunction with our probability distribution $P(x)$ we can further provide a concentration bound on equilibrium, Contribution 2 [31],

$$\Pr\left[\left|\langle A(t)\rangle - A(\infty)\right| \geq \delta\right] \leq 2e \times \exp\left(-\frac{\delta}{e||A||\sqrt{\mathrm{Tr}[\omega^2]}}\right). \tag{2.20}$$

If $\mathrm{Tr}\left[\omega^2\right] \sim 1/d^N$, then the right hand side of equation 2.20 decays doubly exponentially fast. This can be compared with previous bounds where the result is exponentially tight [24, 27, 31, 39].

One can see right away that the bound for the moments in equation 2.19 is not as tight as it could be. For example equation 2.19 is off by a constant factor of 4 compared to 2.17. One can follow the general procedure of [24] to recover 2.17 to also derive a tighter bound on κ_3 or any κ_q. Let us briefly derive the case for κ_3 to see this. First let us assume that $A(\infty) = 0$. Then,

$$\kappa_3 = \lim_{\tau\to\infty}\frac{1}{\tau}\int_0^\tau dt \sum_{m,n} A_{m,n}\bar{c}_m c_n e^{i(E_m-E_n)t}\sum_{k,l} A_{k,l}\bar{c}_k c_l e^{i(E_k-E_l)t}\sum_{p,q} A_{p,q}\bar{c}_p c_q e^{i(E_p-E_q)t} \tag{2.21}$$

expanding out we have,

$$\kappa_3 = \lim_{\tau\to\infty}\frac{1}{\tau}\int_0^\tau dt \sum_{m,n,k,l,p,q} A_{m,n}A_{k,l}A_{p,q}\bar{c}_m c_n \bar{c}_k c_l \bar{c}_p c_q e^{i(E_m+E_k+E_p-E_n-E_l-E_q)t} \tag{2.22}$$

From here we use our assumption on the energy eigenstates defined in equation 2.18. This means we only have the following surviving terms,

$$\kappa_3 = \sum_{m,k,p} |c_m|^2|c_k|^2|c_p|^2(A_{m,m}A_{k,k}A_{p,p} + A_{m,m}A_{k,p}A_{p,k} + A_{m,k}A_{k,m}A_{p,p} + \tag{2.23}$$

$$A_{m,p}A_{k,m}A_{p,k} + A_{m,k}A_{k,p}A_{p,m} + A_{m,p}A_{k,k} + A_{p.m}) \tag{2.24}$$

Here, we see that due to the equilibrium expectation value being zero, we can eliminate the first three, and the final term, leaving us with,

$$\kappa_3 = \sum_{m,k,p} |c_m|^2|c_k|^2|c_p|^2(A_{m,p}A_{k,m}A_{p,k} + A_{m,k}A_{k,p}A_{p,m}) \tag{2.25}$$

And this can be further compressed to be,

$$\kappa_3 = 2\,\mathrm{Tr}\left[A\omega A\omega A\omega\right]. \tag{2.26}$$

So now that we have a nice expression, we continue by bounding it. First let's apply Cauchy-Schwarz with $\mathrm{Tr}\left[A^\dagger B\right] \leq \sqrt{\mathrm{Tr}\left[A^\dagger A\right]}\sqrt{\mathrm{Tr}\left[B^\dagger B\right]}$, this leaves us with (using the fact that all of our matrices will be Hermitian),

$$|\kappa_3| \leq 2\sqrt{\mathrm{Tr}\left[AA\omega^2\right]}\sqrt{\mathrm{Tr}\left[\omega A\omega A^2\omega A\omega\right]} \tag{2.27}$$

We will shift a few terms around in the second square root,

$$|\kappa_3| \leq 2\sqrt{\mathrm{Tr}\left[AA\omega^2\right]}\sqrt{\mathrm{Tr}\left[A^2\omega A\omega^2 A\omega\right]}. \tag{2.28}$$

In the first square root we have A^2 and ω^2 as positive operators, and in the second we have A^2 and $\omega A\omega^2 A\omega = (\omega A\omega)^2$ as positive operators. For any positive operators P, Q we have that, $\mathrm{Tr}\left[PQ\right] \leq ||P||\,\mathrm{Tr}\left[Q\right]$, allowing us to write,

$$|\kappa_3| \leq 2\sqrt{||A||^2\,\mathrm{Tr}\left[\omega^2\right]}\sqrt{||A||^2\,\mathrm{Tr}\left[\omega^2 A\omega^2 A\right]}. \tag{2.29}$$

Next we can use the Cauchy-Schwarz inequality and the positive operator norm bound one more time and arrive at,

$$|\kappa_3| \leq 2||A||^3\sqrt{\mathrm{Tr}\left[\omega^2\right]}\sqrt{\mathrm{Tr}\left[\omega^4\right]}. \tag{2.30}$$

It can be shown that, Contribution 2 [31],

$$\mathrm{Tr}\left[\omega^q\right] \leq \sqrt{\mathrm{Tr}\left[\omega^2\right]}^q, \tag{2.31}$$

which leads us to conclude that,

$$|\kappa_3| \leq 2||A||^3\sqrt{\mathrm{Tr}\left[\omega^2\right]}\sqrt{\mathrm{Tr}\left[\omega^4\right]} \leq 2||A||^3\sqrt{\mathrm{Tr}\left[\omega^2\right]}^3, \tag{2.32}$$

indicating that equation 2.19 can be most likely improved on a case by case basis.

The bounds in equations 2.17, 2.19 and 2.20 give us an intuitive way to understand when equilibration can emerge for an observable. By assumption we have begun our dynamics in a pure state and this property is conserved in time,

$$\mathrm{Tr}\left[\rho(t)\right] = \mathrm{Tr}\left[\rho(t)^2\right] = 1. \tag{2.33}$$

This is a general property of pure states. Mixed states such as ω however do not have this property. We can define the purity of a quantum density matrix as,

$$\gamma = \text{Tr}\left[\sigma^2\right], \tag{2.34}$$

where σ is some density matrix. Using d^N as the Hilbert space dimension we have that,

$$\frac{1}{d^N} \leq \gamma \leq 1, \tag{2.35}$$

where the lower bound is saturated when σ is the maximally mixed state,

$$\sigma = \frac{1}{d^N} \sum_{i=1}^{d} |\psi_i\rangle\langle\psi_i|. \tag{2.36}$$

$|\psi_i\rangle$ is chosen to be a complete orthonormal basis for the Hilbert space. We have $\gamma = 1$ precisely when we have a pure state. We can therefore see from equation 2.17 that the upper bound on our average distance to equilibrium will be very small if our diagonal ensemble ω is very mixed. Recalling the definition of ω,

$$\omega = \lim_{\tau\to\infty} \frac{1}{\tau} \int_0^\tau \rho(t)dt = \sum_k |c_k|^2 |E_k\rangle\langle E_k|. \tag{2.37}$$

ω will be very mixed when we have a large number of eigenstates contributing to the dynamics $|c_k|^2 > 0$ but each individual term $|c_k|^2$ is small. So with the condition of $\text{Tr}\left[\omega^2\right]$ being small, we have a strong criteria for equilibration to occur on average, over an infinite interval. In figure 2.3 we see three example states and how the purity $\gamma = \text{Tr}\left[\omega^2\right]$ decays exponentially fast with system size.

Now clearly we can never have $\rho = \omega$ as one is a pure state and the other is a mixed state, so the full system will never become ω. They can however become indistinguishable for certain observables and subsystems. So far we have focused on single observables such that $\langle\psi|\hat{A}(t)|\psi\rangle \to \text{Tr}\left[\hat{A}\omega\right]$. The bound in equation 2.17 can be used to show that sufficiently small subsystems of our quantum system equilibrate under unitary dynamics [6, 24, 34]. To see this we need to introduce some extra machinery to setup the problem. Suppose we split our total system into two subsystems. Let us call them S, B for the subsystem and the bath, such that $N = N_S + N_B$. Then our subsystem has dimension d^{N_S} and our bath has dimension d^{N_B}. The state of the subsystem is given by tracing out the degrees of freedom of the bath, so we define the subsystem states with the following partial trace $\rho_S(t) = \text{Tr}_B\left[\rho(t)\right]$ and $\omega_S = \text{Tr}_B\left[\omega\right]$. The final ingredient we need is the trace distance between two density matrices, which characterizes the difficulty of distinguishing two states experimentally. For any two quantum states ρ_1, ρ_2 the trace distance is defined as,

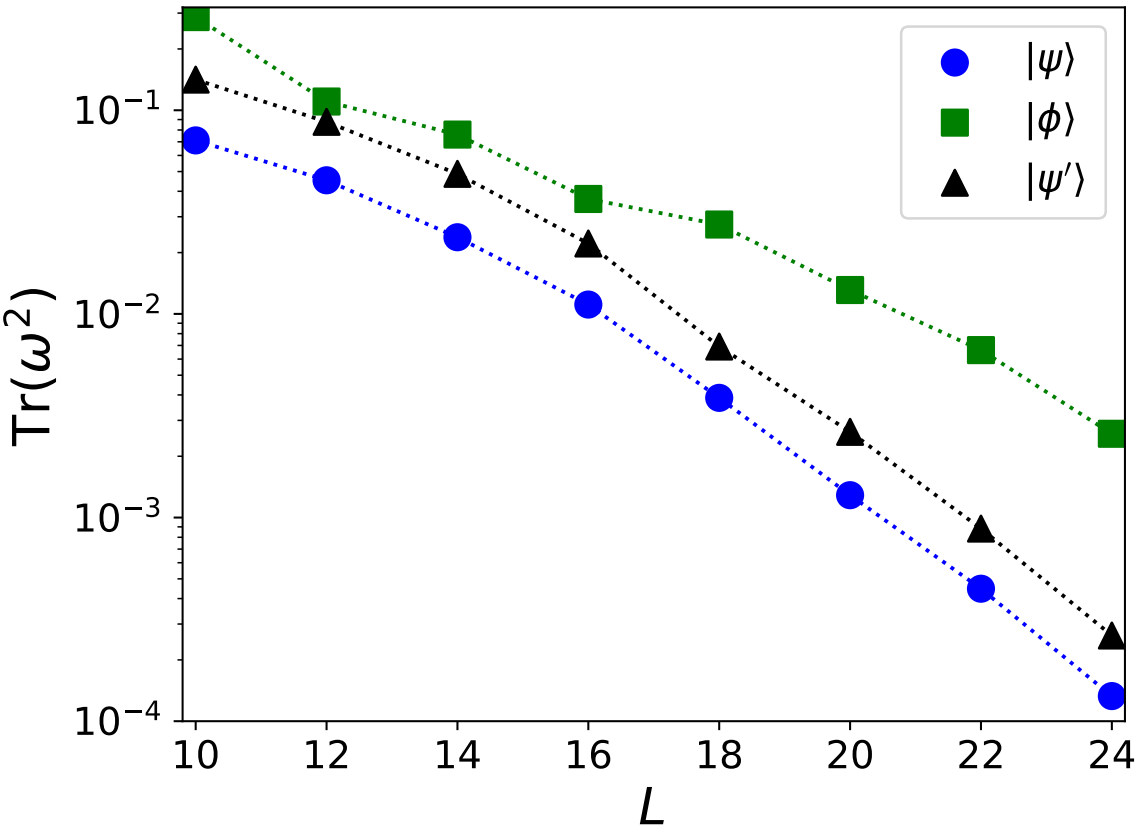

Figure 2.3: Purity of the diagonal ensemble for a variety of system sizes L and states. To see further details see Contribution 2 in chapter 4 figure 2.

$$D(\rho_1, \rho_2) = \frac{1}{2} \mathrm{Tr}\left[\sqrt{(\rho_1 - \rho_2)^2}\right]. \tag{2.38}$$

Then it is possible to show that [6, 34],

$$\lim_{\tau\to\infty} \frac{1}{\tau} \int_0^\tau D(\rho_S(t), \omega_S) dt \leq \frac{1}{2} \sqrt{d^{N_S} \mathrm{Tr}\left[\omega_B^2\right]} \leq \frac{1}{2} \sqrt{d^{2N_S} \mathrm{Tr}\left[\omega^2\right]}, \tag{2.39}$$

which tells us that the subsystem S equilibrates when $\mathrm{Tr}\left[\omega^2\right]$ is sufficiently small (or more importantly when it is small enough to drown out the size of d^{2N_S}), or when a large number of eigenstates contribute to the dynamics in a non-negligible way.

By appealing to infinite time averages we have demonstrated that equilibration can occur, and we expect some notion of static equilibrium to emerge, most notably with expectation

values given to us for observables in equilibrium as $\text{Tr}\left[\hat{A}\omega\right]$ for subsystems. This doesn't tell us much about how long such processes might take. It is then desirable to extend our understanding to allow for statements about finite time processes during equilibration. For example a bound of the form,

$$|\,\text{Tr}\left[\hat{A}\left(\rho(t)-\omega\right)\right]|^2 \leq f(t), \tag{2.40}$$

where $f(t)$ is some decreasing function of time. One could also investigate the finite time average,

$$\sigma_A^2(\tau) = \frac{1}{\tau}\int_0^\tau |\,\text{Tr}\left[\hat{A}\left(\rho(t)-\omega\right)\right]|^2. \tag{2.41}$$

Solving this problem in general is quite difficult. To see this let's consider again the general expression for our observable evolving in time,

$$\langle\hat{A}(t)\rangle = \sum_{m,n}\bar{c}_m c_n \hat{A}_{m,n} e^{i(E_m-E_n)t}. \tag{2.42}$$

These terms can conveniently be grouped and rewritten as,

$$\langle\hat{A}(t)\rangle = \sum_{\alpha} v_\alpha e^{iG_\alpha t}, \tag{2.43}$$

where $\alpha=(m,n)$, $v_\alpha = \bar{c}_m c_n \hat{A}_{m,n}$ is constant and $G_\alpha = E_m - E_n$. From this expression we see that in general we are trying to understand time dependent properties of a large dephasing problem. We start with some atypical configuration of our complex numbers $v_\alpha e^{iG_\alpha t}$ and as we evolve our system in time these numbers slowly form a dense cloud about $A(\infty)$ on the real line, with complex components canceling. See figure 2.4 for an example of the terms $v_\alpha e^{iG_\alpha t}$ evolving in time.

If the problem lacks transport or "slow equilibration" processes then this process appears to be quite quick, and independent of system size. Initial conditions can be easily found however where equilibration timescales scale with the size of the system Contribution 1 [40], [41–46]. An easy way to see this is by example. Consider the following spin 1/2 Heisenberg like Hamiltonian,

$$H = \sum_{j=1}^{L} J_1\left(S_j^+ S_{j+1}^- + \text{h.c}\right) + \gamma_1 S_j^Z S_{j+1}^Z + J_2\left(S_j^+ S_{j+2}^- + \text{h.c}\right) + \gamma_2 S_j^Z S_{j+2}^Z.$$

Consider tracking the observable $\hat{A} = S^Z_{\frac{L}{4}}$ equilibrating under the Hamiltonian and the initial states,

$$|\psi_1\rangle = |\uparrow\downarrow\uparrow\downarrow\uparrow\ldots\rangle, \tag{2.44}$$

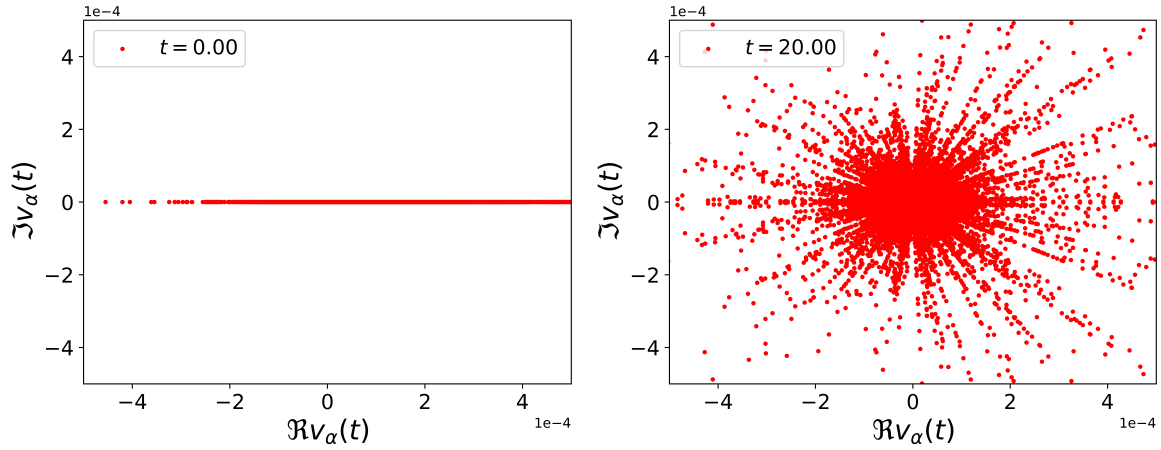

Figure 2.4: Plot of $v_\alpha(t) = v_\alpha e^{iG_\alpha t}$ for an equilibrating observable. Numerics were performed on a spin 1/2 J1-J2 type model in one dimension for $L = 18$ lattice sites. To see further details see Contribution 1 in chapter 3. The dynamics presented here are from observable state pair $\langle A_1(t)\rangle_{|\psi\rangle}$ in Contribution 1.

$$|\psi_2\rangle = |\uparrow\uparrow \ldots \uparrow\downarrow\downarrow \ldots \downarrow\rangle. \tag{2.45}$$

If we let L be even, then the patterns for $|\psi_1\rangle$, $|\psi_2\rangle$ tell us that,

$$\langle\psi_1|S^Z_{\text{tot}}|\psi_1\rangle = \langle\psi_2|S^Z_{\text{tot}}|\psi_2\rangle = 0, \tag{2.46}$$

where,

$$S^Z_{\text{tot}} = \sum_{j=1}^{Z} S^Z_j. \tag{2.47}$$

It turns out that S^Z_{tot} is a conserved quantity since $[H, S^Z_{\text{tot}}] = 0$. Combining this fact with the fact that our model is translation invariant we expect the equilibrium value in both cases for our observable to be,

$$A(\infty) = 0. \tag{2.48}$$

So we have two states that arrive at an identical equilibrium value eventually. The problem in comparing these two dynamical processes directly is that $|\psi_1\rangle$ will see equilibration independent of system size (for sufficiently large systems) while $|\psi_2\rangle$ will have its equilibration time scale with the system size. This is due to the fact that the primary drivers of dynamics will be the spin flipping terms in the dynamics for this observable. $|\psi_1\rangle$ has all spins anti-parallel and will therefore admit spin flip operations on all lattice sites at $t = 0$, while $|\psi_2\rangle$ only admits nearest neighbor spin flip operations in two locations at $t = 0$. We will then see $\langle\psi_2|\hat{A(t)}|\psi_2\rangle$

remain stationary for times proportional to the system size. If it is not immediately obvious it may be instructive to look at the Hadamard formula (see ref. [47] lemma 5.3),

$$e^{sH}\hat{A}e^{-sH} = \hat{A} + s[H,\hat{A}] + \frac{s^2}{2}[H[H,\hat{A}]] + \dots. \tag{2.49}$$

The Hadamard formula tells us that the dynamics can be thought of us nested commutation relations. These nested commutation relations tell us how our local observable will pick up non-local terms in time, smearing it across the lattice. For some initial conditions each new nested commutator will contribute significantly to the dynamics, while for others one doesn't see significant changes until much higher order terms. It is therefore quite difficult to consider initial conditions generically, as this would fail to exclude systems with significant transport.

With these difficulties in mind, little progress has been made on finite time statements [2, 28, 48]. Some results do exist however these techniques restrict us to regimes outside of our interests here like thermal quenches, coupling to a heat bath, integrable models or early times, Contribution 1 [40], [23, 25, 42, 49–57].

Another interesting problem related to equilibration is that of recurrences. Quantum dynamics is both unitary and reversible, and therefore the idea of static equilibrium emerging at all seems to conflict with the nature of quantum theory. This conflict can most naturally be seen by considering the Poincaré recurrence theorem [58–64] which states that, for time independent quantum mechanical systems with discrete (but potentially countably infinite) energy eigenvalues, for every $\epsilon > 0$ and $T_0 > 0$ there exists a $T > T_0$ such that,

$$||\psi(T)\rangle - |\psi(0)\rangle| < \epsilon. \tag{2.50}$$

$|\psi(t)\rangle$ is again the state of the system at time t. This theorem tells us that if we wait long enough our quantum state will return arbitrarily close to it's initial conditions. This theorem calls into question the long lasting and stable equilibrium we are trying to justify in this chapter. To resolve this problem we can appeal to our intuition. Observing the nature around us, it appears as if these recurrences are rare and should take an extremely long time to occur. It is therefore desirable to understand rigorously when such recurrences might occur. Intuitively we would expect these recurrences to occur at later and later times as we add degrees of freedom to the system. This might be observed by the fact that the initial conditions we are interested in look very different from static equilibrium, especially thermodynamic equilibrium. We wouldn't expect to see all of the air in a room collect itself in one corner, even if this was the initial conditions. We therefore expect these recurrences to happen at astronomically large timescales. Interestingly some powerful results can be obtained when one considers the average recurrence time or the average spacing of recurrences. Let t_n

denote a sequence of recurrences labeled by the index n. Then we wish to understand the quantity [65],

$$T_r(u, \Delta) = \lim_{n\to\infty} \frac{t_n}{n}. \tag{2.51}$$

It turns out that we can provide a lower bound on this average recurrence time, Contribution 2 [31],

$$\frac{u}{2e^2}\exp\left(\frac{1-\Delta}{e\mathrm{Tr}[\omega^2]}\right) \leq T_r(u, \Delta), \tag{2.52}$$

where we say a recurrence occurred if $1 - F(t) \leq \Delta$ with a time width of length u. Again we see the purity of the diagonal ensemble as the key ingredient in our expression. This expression matches the scaling of previous estimates in the literature [65, 66].

In this subsection we have demonstrated that purity of the diagonal ensemble $\mathrm{Tr}\left[\omega^2\right]$ is a suitable diagnostic for the emergence of static equilibrium for sub-systems of a total system, and also indicates the robustness of that equilibrium against recurrences. Despite this success ω looks nothing like the usual ensembles of statistical mechanics, so our next task is to relate our ω to the ensembles of statistical mechanics.

2.2 Jaynes' principle

So far we have justified why we expect equilibrium to emerge, first for individual observables and then for sub-systems of our quantum system. Our equilibrium expectation values are given to us by the diagonal ensemble,

$$\langle \hat{A}(\infty)\rangle = \langle \hat{A}\rangle_\omega = \mathrm{Tr}\left[\hat{A}\omega\right]. \tag{2.53}$$

In practice ω isn't something easy to work with, and it is desirable to derive, under reasonable assumptions, a potentially easier to use ensemble in it's place. To do this we employ a method found in a number of statistical mechanics textbooks, Jaynes' principle of maximum entropy [11, 12, 67]. This is sometimes also referred to as Gibbs algorithm. This is a method of statistical inference. Using limited information about our state, like the energy, we pick the most unbiased ensemble to use in place of ω. We will address when we can substitute these maximum entropy ensembles in place of ω in the next section.

In practice we want to take

$$\omega = \sum_k |c_k|^2 |E_k\rangle\langle E_k|, \tag{2.54}$$

and replace $|c_k|^2$ with probabilities that are analytically easier to work with. Jaynes' principle of maximum entropy states that the most unbiased distribution we can assign to $|c_k|^2$ is the one which maximizes the von Neumann entropy [68],

$$S_{vN}(\rho) = -k \,\mathrm{Tr}\left[\rho \ln \rho\right]. \tag{2.55}$$

Plugging in ω gives us the Shannon entropy,

$$S(\omega) = -k \sum_k |c_k|^2 \ln |c_k|^2. \tag{2.56}$$

We want to maximize the entropy in equation 2.55 under several constraints $C_n = 0$ given to us by the time independent properties of ρ. We will throughout this document set $k = k_B = 1$, where k_B is the Boltzmann constant.

An instructive way to approach this problem would be to first include all possible conserved quantities as constraints as our state ρ will keep these properties for all time. Since our eigenvalues are non-degenerate the set of conserved quantities can be listed as $Q_k = |E_k\rangle\langle E_k|$, which are projectors onto the subspace of individual energy eigenkets. We will introduce the ensemble Λ, where $\Lambda_{k,k} = p_k$ is a diagonal density matrix in the energy eigenbasis like ω. Λ will serve as the ensemble we recover from the maximum entropy arguments. We will look for an unbiased distribution p_k such that it obeys the constraints given to us by our pure state ρ. From here we can cast our constraints for Λ in the following way,

$$C_k = \mathrm{Tr}\left[\Lambda Q_k\right] - \mathrm{Tr}\left[\rho Q_k\right] = p_k - |c_k|^2 = 0. \tag{2.57}$$

Then as usual we introduce a Lagrange multiplier for each constraint λ_k. Then we employ the Lagrange multiplier method to maximize the entropy under these constraints. Constructing the Lagrangian function,

$$\mathcal{L}(\Lambda, \lambda_n) = S_{vN}(\Lambda) + \sum_{n=1}^{d^N} \lambda_n C_n. \tag{2.58}$$

We will now arbitrarily set $\lambda_n = 0$ if $|c_k|^2 = 0$. Then performing the optimization we recover the probability distribution,

$$p_k = e^{\lambda_k - 1}, \tag{2.59}$$

or equivalently $\lambda_k = 1 + \ln p_k$. This case however is quite trivial, since we have the constraints of $p_k = |c_k|^2$ giving us straightforwardly that

$$\Lambda = \omega. \tag{2.60}$$

So the diagonal ensemble is the maximum entropy ensemble given to us if we include every single projector onto the energy eigenbasis as our conserved quantities. Interestingly the fact that constraints C_n are linear functionals of the density, one can use Jaynes' principle to coarse grain our constraints, giving us a number of different possible ensembles [69].

We can now move onto more familiar ensembles. Let us assume we still have a non-degenerate Hamiltonian and the energies E_m are ordered by their indices m such that $E_m < E_{m+1}$. Then let us assume we have some state ρ which has support only on the subspace,

$$T_{u,\delta} = \text{span}\{|E_k\rangle | u - \delta \leq \frac{E_k}{N} \leq u\}, \tag{2.61}$$

where δ is assumed to be some small quantity. This may be approximately satisfied by ρ. Then can set $p_k = 0$ if $|E_k\rangle \notin T_{u,\delta}$. Performing the Gibbs algorithm then recovers the microcanonical ensemble [11, 12],

$$\tau_{u,\delta} = \frac{1}{\Omega} \sum_{E_k \in T_{u,\delta}} |E_k\rangle\langle E_k| \tag{2.62}$$

Here $\Omega = \dim T_{u,\delta}$. This gives us the usual starting point for statistical mechanics, that we assign equal probabilities for energetically accessible microstates $p_k = \frac{1}{M}$, where M corresponds to the number of energetically accessible microstates. One can for example recover the Boltzmann entropy by subbing this state into our definition of the entropy,

$$S = k_B \ln \Omega. \tag{2.63}$$

Another important ensemble is recovered when we instead look at a constraint of just the expectation value of energy,

$$\langle E \rangle = \text{Tr}\left[\rho H\right] = \langle \psi | H | \psi \rangle. \tag{2.64}$$

Note that this is usually considered in the context of a system connected to a large bath of energy, but here we treat it again as an isolated system. Completing the optimization problem we find that,

$$p_k = \frac{e^{-\beta E_k}}{Z}, \quad Z = \sum_k e^{-\beta E_k}. \tag{2.65}$$

This is the standard canonical ensemble or the Gibbs state and Z is the partition function. The Lagrange multiplier β is set by demanding the energy of the canonical ensemble matches our

initial conditions,

$$\langle\psi|H|\psi\rangle = \langle E\rangle = \text{Tr}\left[\rho_\beta H\right]. \tag{2.66}$$

We can also rewrite our ensemble in any basis as,

$$\boxed{\rho_\beta = \frac{1}{Z}e^{-\beta H}, \;\; Z = \text{Tr}\left[e^{-\beta H}\right]}. \tag{2.67}$$

For a great review of it's properties see [70]. Inserting this state into our definition of entropy gives,

$$S = k_B \ln Z + \beta\langle E\rangle. \tag{2.68}$$

Interestingly this tells us that,

$$\frac{\partial S}{\partial\langle E\rangle} = \beta, \tag{2.69}$$

and from thermodynamics we can then identify $\beta = \frac{1}{T}$, where T is temperature. Substituting this in, and re-arranging we can write,

$$-T\ln Z = \langle E\rangle - TS, \tag{2.70}$$

which again referencing thermodynamics allows us to identify the free energy,

$$F = -T\ln Z. \tag{2.71}$$

Interestingly the microcanonical ensemble and the canonical ensemble can give equivalent local expectation values under some assumptions. For example keeping the system size of S fixed and growing the bath one can write for translationally invariant locally interacting system [71–74],

$$\lim_{N_B\to\infty} ||\,\text{Tr}_B\left[\tau_{u,\delta}\right] - \text{Tr}_B\left[\rho_\beta\right]\,||_1 = 0. \tag{2.72}$$

Despite $\tau_{u,\delta} \neq \rho_\beta$ we can recover equivalence of these ensembles for subsystems. A notable counter example where the ensembles are not equivalent are long range interacting systems [75–79]. This identification is similar to the conclusion that $\rho(t) \neq \omega$ but they become identical for some subsystem as you grow the bath to an infinite size. Now that we have unbiased guesses to approximate the properties of ω, our next task is to investigate when these guesses give a correct approximation.

2.3 From the diagonal ensemble to statistical mechanics

In the last section we have used Jaynes' principle of maximum entropy to derive the most unbiased ensembles we could based off of limited information about our state. The problem we face now is understanding when we can compare the diagonal ensemble ω with an ensemble from statistical mechanics. Despite ρ_β being the most convenient to use analytically, we will for now compare ω to the microcanonical ensemble $\tau_{u,\delta}$. This is due to the fact that we are dealing with an isolated system, and we expect $\rho(t)$ to have the majority of it's support around some energy density u [11, 72]. A possible justification for this exists again from results relying on concentration bounds. Consider a Hamiltonian which is a sum of n terms, where each term acts at most on k terms. We also impose that the Hamiltonian be written a way where the norm of such terms is less than or equal to unity. Let m be the maximum number of neighbors of any local terms that interact. If we consider a product state ρ with energy $\langle E\rangle = \mathrm{Tr}\left[\rho H\right]$ and some real number $a \geq \sqrt{\frac{\mathbb{O}(m^2)}{n}}$ then [80],

$$\mathrm{Tr}\left[\rho\Pi_{\geq\langle E\rangle+na}\right] \leq e^{-\frac{na^2}{\mathbb{O}(m^2)}} \text{ and } \mathrm{Tr}\left[\rho\Pi_{\leq\langle E\rangle-na}\right] \leq e^{-\frac{na^2}{\mathbb{O}(m^2)}}, \tag{2.73}$$

where $\Pi_{\geq f}$ is the projection onto the subspace of eigenvectors with energy eigenvalues $E_k \geq f$. While this statement doesn't give us the distribution of excited energies, it at least bounds the type of distributions we might be interested in. Energy excitations too far from the mean $\langle E\rangle$ are suppressed like the tails of a Gaussian distribution. See [81] for a discussion on the distribution of $|c_k|^2$ terms.

The goal now will be to understand why we can compare ω to $\tau_{u,\delta}$. It is probably obvious already that trivially $\omega \neq \tau_{u,\delta}$. So let us return to our arbitrary observable A. We then have our infinite time average value,

$$A(\infty) = \sum_k |c_k|^2 A_{k,k}, \tag{2.74}$$

and the microcanonical average,

$$\mathrm{Tr}\left[\tau_{u,\delta}A\right] = \frac{1}{\Omega}\sum_{E_k\in T_{u,\delta}} A_{k,k}. \tag{2.75}$$

In the following subsections we will present two potential explanations for why these two expectation values should be equal. Note that if we define a full set of observables for some subsystem S, and these expectation values are identical, this would constitute equivalence of ensembles for the diagonal ensemble and the microcanonical ensemble,

$$\mathrm{Tr}_B\left[\omega\right] \approx \mathrm{Tr}_B\left[\tau_{u,\delta}\right]. \tag{2.76}$$

2.3.1 The strong eigenstate thermalization hypothesis

The eigenstate thermalization hypothesis is a generalization of arguments seen in quantum chaos. Chaos in the quantum regime was initially studied largely in the single particle regime and reveals that chaotic Hamiltonians can be successfully treated as random matrices [33, 36, 37, 82–96]. If we expressed an observables in the energy eigenbasis of a random Hamiltonian we would in general recover the elements [1],

$$\hat{A}_{m,n} = \bar{\hat{A}}\delta_{m,n} + \sqrt{\frac{\overline{\hat{A}^2}}{d^N}} R_{m,n}, \tag{2.77}$$

where we have kept the convention of our Hilbert space being d^N, $\bar{\hat{A}} = \frac{1}{d^N}\sum_m \hat{A}_{m,m}$ and $R_{m,n}$ is a random variable with zero mean and unit variance. Applying this equation to our definition of our static equilibrium expectation value, we get,

$$A(\infty) = \sum_m |c_m|^2 A_{m,m} = \bar{\hat{A}}. \tag{2.78}$$

This however should feel insufficient to the reader, if we treat our equilibrium problem purely with equation 2.77 then $A(\infty)$ is independent of energy and temperature. To remedy this shortcoming of random matrix theory the eigenstate thermalization hypothesis (ETH) has been proposed [1, 8, 9, 97–100],

$$\boxed{\hat{A}_{m,n} = A(\bar{E})\delta_{m,n} + e^{-S(\bar{E})/2} f(\bar{E}, \alpha) R_{m,n}}. \tag{2.79}$$

Here $\bar{E} = \frac{E_m + E_n}{2}$ is the average energy, $\alpha = E_m - E_n$ is the frequency, $A(\bar{E})$, $f(\bar{E}, \alpha)$ are smooth functions of their arguments and $S(\bar{E})$ is the thermodynamic entropy. This gives us a an expression where the diagonal entries of our observable A is a smooth function of energy up to small corrections, while the off-diagonal elements are exponentially suppressed and behave similar to the off-diagonal given to us by random matrix theory given in equation 2.77. In fact equation 2.79 and equation 2.77 give identical predictions if one focuses on a small enough region of the spectrum. This equation isn't exact for finite systems but for the systems we are interested in for this document we expect that equation 2.79 will hold in the thermodynamic limit.

An interesting thing to distinguish is the diagonal and off-diagonal statements of ETH. If we look again at our pure state dynamics,

$$\langle \hat{A}(t) \rangle = \sum_{m,n} \bar{c}_m c_n \hat{A}_{m,n} e^{i(E_m - E_n)t}. \tag{2.80}$$

Assume non-degenerate energies we can conveniently split our dynamics up,

$$\langle \hat{A}(t) \rangle = \sum_m |c_m|^2 \hat{A}_{m,m} + \sum_{m \neq, n} \bar{c}_m c_n \hat{A}_{m,n} e^{i(E_m - E_n)t}. \tag{2.81}$$

We can then identify important parts of equation 2.79. Firstly the diagonal ETH which applies to the time independent part of our pure state evolution tells us that $\hat{A}_{m,m}$ is a smooth function of energy up to small corrections. These corrections are exponentially suppressed by the thermodynamic entropy $S(\bar{E})$. The second part or the off-diagonal ETH statement tells us that the off-diagonal elements of our observable $\hat{A}_{m,n}$ are all suppressed exponentially by the thermodynamic entropy. The off-diagonal ETH plays an important role in suppressing fluctuations about equilibrium. Let $A(\infty) = 0$, then the fluctuations about equilibrium can be captured by σ_A^2 with $A(\infty) = 0$,

$$\sigma_A^2 = \lim_{\tau \to \infty} \frac{1}{\tau} \int_0^\tau \langle \hat{A}(t) \rangle^2 dt. \tag{2.82}$$

Assuming the model obeys the off-diagonal portion of ETH one can show that [1],

$$\sigma_A^2 \leq \max_{m \neq n} |A_{m,n}|^2 \propto e^{-S(\bar{E})}. \tag{2.83}$$

This observation aligns quite nicely with our analytic bound given in equation 2.17. To see this it is interesting to introduce the Rényi entropies [68],

$$\boxed{S_\alpha(\rho) = \frac{1}{1-\alpha} \ln \mathrm{Tr}\left[\rho^\alpha\right]}, \tag{2.84}$$

where we recover our von Neumann entropy when,

$$\lim_{\alpha \to 1} S_\alpha(\rho) = S_{vN}(\rho). \tag{2.85}$$

From here we can rewrite our bound in equation 2.17 with the second Rényi entropy,

$$\sigma_A^2 \leq ||\hat{A}||^2 \, \mathrm{Tr}\left[\omega^2\right] = ||\hat{A}||^2 e^{-S_2(\omega)}. \tag{2.86}$$

We expect both $S_2(\omega)$ and $S(\bar{E})$ to be extensive in the number of lattice sites N [39, 101–103], giving the same scaling between the ETH ansatz and the analytical argument relying on the diagonal ensemble.

The form in equation 2.79 has been numerically verified in a large range of models [1, 21, 99, 104–126] and is expected to hold in generic non-integrable models. This ansatz is supposed to hold for *relevant* observables, which is usually taken to be local observables,

that is, observables with support on some subsystem of the lattice. There is some evidence that this might be extended out to as much as half the total system size. Despite a large body of numerical evidence there is no analytical proof of the ansatz for any class of models. There has however been some progress. For example one can bound the off-diagonal of the observable's elements as [127, 128],

$$|\langle E_m|\hat{A}|E_n\rangle| \leq \frac{|E_m - E_n|}{R} e^{-\frac{|E_m - E_n| - R}{gk}}, \tag{2.87}$$

where g, k and R are constants. This bound however falls quite short of the $e^{-S(\bar{E})}$ predicted by equation 2.79. There has also been advances in the direction of the diagonal portion of the hypothesis [129, 130].

Returning to the single observable $\hat{A}$, we can see agreement now between $A(\infty)$ and that of the microcanonical ensemble. Let us again assume our pure state $|\psi\rangle$ has the majority of it's support on some microcanonical window defined by u and δ, then we see that,

$$A(\infty) = \sum_k |c_k|^2 \hat{A}_{k,k} \approx A(\bar{E}), \tag{2.88}$$

and likewise the microcanonical average is,

$$\text{Tr}\left[\tau_{u,\delta}\hat{A}\right] \approx A(\bar{E}). \tag{2.89}$$

In fact it can be shown that [9],

$$A(\infty) = \text{Tr}\left[\hat{A}\rho_\beta\right] + \mathbb{O}\left(\frac{1}{N}\right) + \mathbb{O}(\Delta^2) + \mathbb{O}(e^{-S(\bar{E})/2}), \tag{2.90}$$

where Δ is the quantum uncertainty in our energy,

$$\Delta = \sqrt{\sum_k |c_k|^2 (E_k - \langle E\rangle)^2}, \tag{2.91}$$

and we have that $\text{Tr}\left[\omega H\right] = \text{Tr}\left[\rho_\beta H\right]$. We can see that ETH is a sufficient condition for thermalization from unitary dynamics. It turns out that thermalization is not only sufficient but it is necessary, that is, thermalization implies ETH and ETH implies thermalization [131]. An interesting consequence of equation 2.79 is the following. Let us partition our system again into our subsystem S and the bath B. We will assume we have some complete basis of operators $\hat{A}_n$ on S which satisfies equation 2.79. Then assuming $|E_k\rangle \in T_{u,\delta}$,

$$\lim_{N\to\infty} ||\,\text{Tr}_B\left[|E_k\rangle\langle E_k|\right] - \text{Tr}_B\left[\tau_{u,\delta}\right]\,|| = 0. \tag{2.92}$$

This tells us that on subsystems of our total system, the energy eigenstates are identical to the microcanonical ensemble. Assuming we have equivalence of ensembles we will also have,

$$\lim_{N\to\infty} || \operatorname{Tr}_B \left[|E_k\rangle\langle E_k|\right] - \operatorname{Tr}_B \left[\rho_\beta\right] || = 0, \tag{2.93}$$

where we have assumed that $E_k = \operatorname{Tr}\left[H\rho_\beta\right]$. This also leads us to an interesting conclusion. Assume $E_k \approx E_l$, then the local statistics of these energy eigenstates are also identical,

$$\lim_{N\to\infty} || \operatorname{Tr}_B \left[|E_k\rangle\langle E_k|\right] - \operatorname{Tr}_B \left[|E_l\rangle\langle E_l|\right] || = 0. \tag{2.94}$$

These three observations lead us to identify a new ensemble, the eigenstate ensemble $|E_k\rangle\langle E_k|$ that, similar to $\tau_{k,\delta}$, encodes the equilibrium properties of our subsystems.

2.3.2 Eigenstate typicality

The previous section discussed the strong version of ETH, namely that all eigenstates obey the hypothesis. We can make analytic progress by relaxing this statement to typical or the vast majority of eigenstates obey this hypothesis. Doing this is sometimes called the weak ETH or eigenstate typicality. Under certain assumptions a general expression for the weak ETH has been derived and used for a variety of results [49, 132, 133]. The statement is the following, take $0 < \alpha < \frac{1}{D+1}$ where D denotes the dimension of our lattice. Let H be a translation-invariant, non-degenerate Hamiltonian and let ρ be an equilibrium ensemble such that $[\rho, H] = 0$ with a finite correlation length ξ. A state with finite correlation length means that the expectation values of spatially separated observables are bounded by,

$$\max_{\hat{A},\hat{B}} |\langle \hat{A}\hat{B}\rangle - \langle \hat{A}\rangle\langle \hat{B}\rangle| \leq ||\hat{A}||||\hat{B}||e^{-\frac{d(\hat{A},\hat{B})}{\xi}}, \tag{2.95}$$

where $d(\hat{A}, \hat{B})$ is the distance between the lattice support of the two observables. Then taking $\hat{A}$ to be some observable with support on some connected region of at most N^α sites we have [49],

$$\Pr_{E_k\in\rho}\left(|\langle E_k|\hat{A}|E_k\rangle - \operatorname{Tr}\left[\rho\hat{A}\right]| \geq \delta\right) \leq \exp\left(-c\delta N^{\frac{1}{D+1}}\xi^{-\frac{D}{D+1}}\right), \tag{2.96}$$

where c is some constant and $\Pr_{E_k\in\rho}$ is the probability of sampling the energy eigenstate $|E_k\rangle$ from the ensemble ρ. This equation tells us that the probability of finding an eigenstate expectation value of our observable $\hat{A}$, δ away from the ensemble average is exponentially suppressed by both δ and N. Then as we approach the thermodynamic limit it should be

increasingly rare to see energy eigenstates sampled from ρ giving expectation values of $\hat{A}$ which are far from the ensemble average. While it is just a bound, the dimensional dependence of equation 2.96 is interesting, and further work is required to find what the optimal scaling would be for this bound.

While equation 2.96 should not be mistaken for *the* weak ETH, it does single out a class of models where the eigenstates on average do satisfy the condition of ETH where expectations of an observable in the energy eigenbasis are identical to the ensemble average given to us by Jaynes' principle in statistical mechanics. It can be further used to make a statement about the equivalence of our eigenstates and the ensembles of statistical mechanics on subsystems. Let us assume we are in a system that satisfies equation 2.96. We can then bound the probability of sampling an energy eigenstate far from the local description of an equilibrium ensemble ρ,

$$\mathrm{Pr}_{|E_k\rangle\in\rho}\left(||\,\mathrm{Tr}_B\left[|E_k\rangle\langle E_k|\right]-\mathrm{Tr}_B\left[\rho\right]||_1\geq\delta\right), \tag{2.97}$$

Using the union bound we have that,

$$\leq \dim(S)\mathrm{Pr}_{|E_k\rangle\in\rho}\left(\max_{\hat{A}\in S}\mathrm{Tr}\left[A\left(\mathrm{Tr}_B\left[|E_k\rangle\langle E_k|\right]-\mathrm{Tr}_B\left[\rho\right]\right)\right]\geq\delta\right), \tag{2.98}$$

$$\leq \dim(S)\exp\left(-c\delta N^{\frac{1}{D+1}}\xi^{-\frac{D}{D+1}}\right), \tag{2.99}$$

where $\dim(S)$ is the dimension of the subsystem. Putting everything together this tells us that,

$$\mathrm{Pr}_{|E_k\rangle\in\rho}(||\mathrm{Tr}_B\left[|E_k\rangle\langle E_k|\right]-\mathrm{Tr}_B\left[\rho\right]||_1\geq\delta)\leq\dim(S)\exp\left(-c\delta N^{\frac{1}{D+1}}\xi^{-\frac{D}{D+1}}\right), \tag{2.100}$$

where our ensemble might be $\rho=\tau_{u,\delta}$. This demonstrates that with typicality arguments alone, our eigenstates can be shown to have a very high probability of being locally identical to our ensembles from statistical mechanics.

Another interesting thing to investigate would be the average distance between the reduced density matrices,

$$\sum_k \rho_{k,k}||\,\mathrm{Tr}_B\left[|E_k\rangle\langle E_k|\right]-\mathrm{Tr}_B\left[\rho\right]||_1. \tag{2.101}$$

We can bound this in the following way. Let us define $\Delta_k=||\,\mathrm{Tr}_B\left[|E_k\rangle\langle E_k|\right]-\mathrm{Tr}_B\left[\rho\right]||_1$,

$$\sum_k \rho_{k,k}||\,\mathrm{Tr}_B\left[|E_k\rangle\langle E_k|\right]-\mathrm{Tr}_B\left[\rho\right]||_1=\sum_k\rho_{k,k}\Delta_k. \tag{2.102}$$

We partition our sum into two sectors, let $\Delta = \frac{\ln N}{N^{\frac{1}{D+1}}}$,

$$\sum_k \rho_{k,k}\Delta_k = \sum_{\Delta_k \leq \Delta} \rho_{k,k}\Delta_k + \sum_{\Delta_k > \Delta} \rho_{k,k}\Delta_k, \tag{2.103}$$

$$\leq K\frac{\ln N}{N^{\frac{1}{D+1}}} + \max_{\Delta_k > \Delta} \Delta_k \sum_{\Delta_k > \Delta} \rho_{k,k}, \tag{2.104}$$

$$\leq K\frac{\ln N}{N^{\frac{1}{D+1}}} + \dim(S)\exp\left(-c\Delta N^{\frac{1}{D+1}}\xi^{-\frac{D}{D+1}}\right), \tag{2.105}$$

$$\leq K\frac{\ln N}{N^{\frac{1}{D+1}}} + C\dim(S)\left(\frac{1}{N}\right)^{-c'\xi^{-\frac{D}{D+1}}}. \tag{2.106}$$

Then this gives us,

$$\sum_k \rho_{k,k}||\operatorname{Tr}_B\left[|E_k\rangle\langle E_k|\right] - \operatorname{Tr}_B\left[\rho\right]||_1 \leq K\frac{\ln N}{N^{\frac{1}{D+1}}} + C\dim(S)\left(\frac{1}{N}\right)^{-c\xi^{-\frac{D}{D+1}}}, \tag{2.107}$$

where K, C, c are all constants independent of the system size. So we see from these two derivations that in sufficiently large systems, it is extremely unlikely that we sample an eigenstate that does not obey the diagonal portion of ETH. In particular this probability vanishes in the thermodynamic limit. We also have that the average distance between all $\operatorname{Tr}_B\left[|E_k\rangle\langle E_k|\right]$ and $\operatorname{Tr}_B\left[\rho\right]$ decays to zero in the thermodynamic limit.

2.4 Volume law scaling of entanglement

The von Neumann entropy given to us in equation 2.55 can also tell us important properties of the state, like purity and entanglement. Let us briefly recall some properties of S_{vN}. We will not list an exhaustive list but focus on the important concepts for our discussion. For a more complete discussion see [68, 134, 135].

Firstly, $S_{vN}(\rho) = 0$ if and only if ρ is a pure state, making it a test that reveals the purity of our state. Therefore,

$$S_{vN}(|E_k\rangle\langle E_k|) = 0. \tag{2.108}$$

As we have mentioned previously, it is maximized as,

$$S_{vN}(\mathbb{I}/d^N) = N\ln d, \tag{2.109}$$

for the maximally mixed state. Note that this maximal value scales like the number of lattice sites in our system or the volume of our system. We call this behavior a volume law scaling

or refer to the entropy as extensive. S_{vN} is invariant to a change in basis such that $S_{vN}(\rho) = S_{vN}(U\rho U^\dagger)$, where U is a unitary matrix. It is also additive for independent systems,

$$S_{vN}(\rho_S \otimes \rho_B) = S_{vN}(\rho_S) + S_{vN}(\rho_B). \tag{2.110}$$

If our state is pure and our two subsystems are independent, we say they are unentangled. These states are also sometimes called separable. If the state is not separable however we say that the subsystem S is entangled with the bath B. The entanglement entropy is a way of measuring how much entanglement is present between a bi-partition of a system in a pure state, and it is given by,

$$S_{vN}(\rho_S) = S_{vN}(\rho_B). \tag{2.111}$$

The more mixed ρ_S is the more entangled the subsystem and the bath are. This observation has interesting consequences. The von Neumann entropy is sub-additive for systems with entanglement,

$$S_{vN}(\rho) \leq S_{vN}(\rho_S) + S_{vN}(\rho_B). \tag{2.112}$$

In general we expect the thermodynamic entropy to be extensive [1, 11, 12], that is, it scales with the system size,

$$S_{vN}(\tau_{u,\delta}) \propto N. \tag{2.113}$$

Using the sub-additive property of the von Neumann entropy, we therefore expect that the subsystems entropy must also scale like the system size,

$$S_{vN}(\tau_{vN}) \leq S_{vN}(\mathrm{Tr}_S\left[\tau_{vN}\right]) + S_{vN}(\mathrm{Tr}_B\left[\tau_{vN}\right]) \propto N_S + N_B. \tag{2.114}$$

We can now link this back to ETH. We expect that for individual eigenstates satisfying eigenstate thermalization, that,

$$\mathrm{Tr}_B\left[|E_k\rangle\langle E_k|\right] \approx \mathrm{Tr}_B\left[\tau_{u,\delta}\right], \tag{2.115}$$

meaning that the entanglement entropy of our energy eigenstate should follow a volume law,

$$S_{vN}(\mathrm{Tr}_B\left[|E_k\rangle\langle E_k|\right]) \propto N_S. \tag{2.116}$$

This observation is a common test for eigenstate thermalization and has been confirmed in a wide variety of non-integrable models [1, 117, 136–139]. This is contrary to the properties of the ground state energy eigenstate of gapped quantum systems, which has entanglement entropy grow like an area law [140–142]. Models not obeying ETH can also see volume laws

in the entanglement entropy of the eigenstates, however these are only observed for vanishing fractions of the system size N_S/N [16, 117, 143, 144] while ETH models continue to support this volume law for non-vanishing fractions of N_S/N. Due to limitations of numerical studies it is unclear if this volume law holds for subsystems making up half of the system $N_S/N = 1/2$. Some evidence suggests that it does hold for half the system to leading order [136].

Since we expect that $\text{Tr}_B[\omega] \approx \text{Tr}_B[\tau_{u,\delta}]$ it is also expected that [137, 145–151],

$$S_{vN}(\text{Tr}_B[\rho(t)]) \propto N_S \text{ , for sufficiently large t.} \tag{2.117}$$

In fact, models obeying ETH starting from our of equilibrium conditions have linearly increasing entanglement entropy between subsystems [21]. Interestingly random pure states are nearly maximally entangled on average [152].

2.5 Notable counter examples

In this section we will discuss classes of models that do not obey eigenstate thermalization and in most initial conditions, we do not expect the system to relax it's observables to traditional thermal expectation values. The classes of models we will cover here are the so called integrable models. Despite there being some variety to what these can look like we will focus on free fermionic models in the first two subsections and in the third we will briefly make a note of two interacting classes of models which also do not satisfy eigenstate thermalization.

2.5.1 Non-interacting extended models

In this subsection we will focus on free fermionic models and comment briefly on bosonic models at the end of the subsection. We will consider free fermionic models of the form,

$$\hat{H} = \sum_{i,j} M_{i,j} f_i^\dagger f_j, \tag{2.118}$$

where M is the co-efficient matrix that is real symmetric and f_j is a fermionic annihilation operator acting on lattice site j that obeys the canonical anti-commutation relations,

$$\{f_m, f_n\} = \{f_m^\dagger, f_n^\dagger\} = 0, \;\; \{f_m^\dagger, f_n\} = \delta_{m,n}. \tag{2.119}$$

This model can be extended to include terms which include pair creation and annihilation terms of the form,

$$B_{i,j} f_i^\dagger f_j^\dagger + \bar{B}_{i,j} f_i f_j, \tag{2.120}$$

while still being mappable to free, non-interacting fermions. For simplicity we will keep $B = 0$ and mention studies where $B \neq 0$. Our model Hamiltonian is easily solved. Since M is real symmetric we can decompose it into,

$$M = ADA^T, \tag{2.121}$$

where A is a real orthonormal matrix and D is a diagonal matrix with entries of the form $D_{k,k} = \epsilon_k$. This transformation gives us new fermionic operators,

$$d_k = \sum_{j=1}^{L} A_{j,k} f_j, \tag{2.122}$$

which also obey the standard canonical anti-commutation relations,

$$\{d_m, d_n\} = \{d_m^\dagger, d_n^\dagger\} = 0, \;\; \{d_m^\dagger, d_n\} = \delta_{m,n}. \tag{2.123}$$

The interesting aspect of these models is that they have an extensive number of conserved quantities. To see this, consider the Heisenberg equation,

$$\frac{d}{dt}\hat{A} = i[H, \hat{A}]. \tag{2.124}$$

This equation tells us that if we have $[H, \hat{A}] = 0$ then the observable A has it's expectation value conserved in time. In our free fermionic Hamiltonian we can see that,

$$[H, d_k^\dagger d_k] = 0, \;\; \forall k. \tag{2.125}$$

If there are N total lattice sites then there are N conserved quantities in equation 2.118. We can always write the time evolution of a fermionic operator in this class of models as,

$$f_m(t) = \sum_k a_{m,k}(t) f_m, \tag{2.126}$$

where $a_{j,k}(t)$ is the single particle propagator given to us by,

$$\{f_m^\dagger(t), f_n\} = a_{m,n}(t). \tag{2.127}$$

In this section we will work with models which are extensive,

$$A_{j,k} \sim \frac{1}{\sqrt{N}}, \tag{2.128}$$

which tells us that we have delocalizing dynamics such that [31, 49, 56].

$$a_{m,n}(t) \to 0 \text{ as } t \to \infty. \tag{2.129}$$

Equilibration and thermalization have been studied for this class of models as well. The eigenstates of our free Hamiltonian in equation 2.118 are Gaussian states [54, 153], meaning they are fully described by their two point correlation functions,

$$\langle f_m^\dagger f_n \rangle \text{ or } \langle d_k^\dagger d_k \rangle. \tag{2.130}$$

This is due to the eigenstates being constructed from the vacuum state $|0\rangle$ by our fermionic creation operators $d_k^\dagger$. Then it is easy to see that one can apply Wick's theorem [154, 155] to reduce higher order correlation functions to products of two point correlation functions for these states. The thermal ensemble $\rho_\beta = \frac{1}{Z} e^{-\beta H}$ also has this property [155]. Interestingly even if one starts with an out of equilibrium state that does not have this property, and the model has the capacity for delocalizing transport, then most initial pure state ρ will relax to a state with Gaussian statistics [54, 55]. We can therefore focus our attention on two point correlation functions when we study equilibration in this class of models.

With delocalizing dynamics and an initial pure state with decaying correlations in space one can show that [56],

$$\langle f_m^\dagger(t) f_n(t) \rangle - \langle f_m^\dagger(t) f_n(t) \rangle_\infty \sim \frac{1}{t^{\alpha(1+s)}} \text{ as } t \to \infty, \tag{2.131}$$

where α and s are constants and

$$\langle f_m^\dagger(t) f_n(t) \rangle_\infty = \lim_{\tau \to \infty} \frac{1}{\tau} \int_0^\infty \langle f_m^\dagger(t) f_n(t) \rangle dt. \tag{2.132}$$

Similar results were found in [55]. One can also study the probability distribution given to us in equation 2.14, and for example bound it's moments as, Contribution 2 [31],

$$\kappa_q \leq \left(q c^2 \frac{\nu}{N} \right)^q, \tag{2.133}$$

where c and ν are constants and we assume the single particle spectrum is generic. This gives the concentration bound,

$$\Pr\left[\left| \langle f_m^\dagger f_n(t) \rangle - \langle f_m^\dagger f_n(\infty) \rangle \right| \geq \delta \right] \leq 2e \times \exp\left(-\frac{\delta}{e c^2} \sqrt{\frac{L}{\nu}} \right). \tag{2.134}$$

So we see that analytical results in this class of models are much more accessible, strong statements on the decay to equilibrium are possible. Now let us explore what equilibrium looks like.

Due to the presence of the conserved quantities we need to instead derive a maximum entropy ensemble that takes these symmetries into consideration, to properly reflect the equilibrium state. Following Jaynes' principle we can arrive at the generalized Gibbs ensemble,

$$\rho_{\beta_j} = \frac{1}{Z} e^{-\sum_{j=1}^{r} \beta_j \hat{Q}_j}, \tag{2.135}$$

where we have deliberately kept r and Q_j arbitrary. For any given problem r is the number of relevant conserved quantities to conserve and Q_j the set of relevant conserved quantities. In general, if we have a sufficiently well behaved initial condition, the two point correlation functions relax to the generalized Gibbs ensemble defined by [14, 19, 22, 55, 56, 156],

$$Q_k = d_k^\dagger d_k, \forall k, \tag{2.136}$$

giving us N total conserved quantities. This requirement can be relaxed for example in translation invariant systems, where the number of conserved quantities required may be reduced by instead considering current operators as our charges [55],

$$Q_j = \frac{1}{L} \sum_x f_x^\dagger f_{x+j} + \text{h.c} = \frac{1}{L} \sum_l \cos\left(\frac{2\pi l j}{N}\right) d_l^\dagger d_l. \tag{2.137}$$

If we assume the initial state has exponentially decaying correlations with length ξ, then we only have $r \sim \xi$ non-negligible charges or values of $\langle Q_j(t) \rangle = \langle Q_j \rangle$ for the state. While these results do not depend on a generalized form of ETH directly it's possible to derive a generalized weak ETH for such models when they are translation invariant. It can be shown that eigenstates chosen at random give identical expectation values to the generalized Gibbs ensemble in the thermodynamic limit [18, 157]. Let us write the charges as,

$$Q_j = \sum_k q_j(k) d_k^\dagger d_k, \tag{2.138}$$

where $k = 2\pi j/N$, for $1 \leq j \leq N$ and we have deliberately chosen to work in one dimension, analogous results hold for all dimensions d,

$$\langle E_k | f_m^\dagger f_n | E_k \rangle \to \frac{1}{2\pi} \int dk \frac{1}{1 + e^{\sum_j \beta_j q_j(k)}}. \tag{2.139}$$

The above equation tells us that energy eigenstates of translation invariant Hamiltonians of the form given in equation 2.118 have expectation values which agree with the Generalized Gibbs ensemble. These statitics are generalized Fermi-Dirac statistics. Note that the number of conserved quantities in this expression doesn't need to be extensive.

A large body of work has also studied the the entanglement entropy of these free models. Both analytical and numerical work has shown a volume law scaling for small subsystems.

In particular for subsystems such that $N_s/N \to 0$, a volume law is observed [16, 117, 143, 144, 158, 159]. If we assume the model is translation invariant and let $N_S/N = 1/2$ and take $N \to \infty$, it is observed that the average entanglement entropy of the energy eigenstates is no longer maximal [143],

$$\lim_{L\to\infty} 2\langle S\rangle/(L\ln 2) \approx 0.5378\ldots, \tag{2.140}$$

where the maximal value would have been unity and $\langle S\rangle$ is the average entanglement entropy of all eigenstates for a bipartition. It can be shown that this average entanglement entropy can be bounded above and below by [143],

$$N_S \ln 2\left(1-\frac{N_S}{N}\right) \leq \langle S\rangle \leq N_S\ln 2 - \frac{N_S^2}{2N}, \tag{2.141}$$

from this bound it easy to see that the first term on the upper and lower bound is not only the volume law we expect from chaotic eigenstates, but is the maximal value. The correcting terms vanish if we keep N_S fixed and take the system size to the thermodynamic limit, however they are non-negligible when N_S/N is finite.

It is also interesting to explore how things change if instead of fermions, we study bosonic models. Here we present a proof of generalized eigenstate typicality for such models. The derivation is similar to [18, 157]. First consider a Hamiltonian in one dimension (similar results hold for all d),

$$\hat{H} = \sum_{i,j} h_{i,j}\hat{b}_i^\dagger \hat{b}_j. \tag{2.142}$$

Where $\hat{b}_i$ is the bosonic annihilation operator and we assume the coefficient matrix h is translation invariant. These operators obey the commutation relations,

$$[\hat{b}_i, \hat{b}_j^\dagger] = \delta_{ij}, \tag{2.143}$$

$$[\hat{b}_i, \hat{b}_j] = [\hat{b}_i^\dagger, \hat{b}_j^\dagger] = 0. \tag{2.144}$$

The Hamiltonian h can be diagonalized by introducing new momentum bosonic operators of the form,

$$\hat{d}_k = \frac{1}{L^{d/2}}\sum_j e^{ik\cdot j}\hat{b}_j. \tag{2.145}$$

Where $k = \frac{2\pi n}{L}, n = 1, 2, \ldots L$. It is easy to see that as $L \to \infty$ the possible values of k sit on a dense set in the interval $(0, 2\pi)$. Which recovers the Hamiltonian,

$$\hat{H} = \sum_{\vec{k}} \epsilon_k \hat{d}_k^\dagger \hat{d}_k. \tag{2.146}$$

So we see that the eigenstates are completely defined by their distribution of momentum eigenmodes in reciprocal space with $\langle \hat{d}_k^\dagger \hat{d}_k \rangle = 0, 1, 2 \ldots$. Defining the correlations in real space we write the occupation matrix,

$$\langle \hat{b}_m^\dagger \hat{b}_n \rangle = \frac{1}{L^d} \sum_k \langle \hat{d}_k^\dagger \hat{d}_k \rangle e^{ik(m-n)}. \tag{2.147}$$

We can partition the space into a number of cells which contain $g \gg 1$ points and require the cells have enough points such that,

$$\frac{1}{N} \ll \Delta k_x \ll \frac{1}{N_A}. \tag{2.148}$$

Where N_A is the size of the individual subsets of points in k space. This allows us to approximate each cell with a chosen value of $e^{ik(m-n)} \approx e^{i\vec{k}_r(m-n)}$ where r is the label for the subsets of k space. Then we may write,

$$\langle \hat{b}_m \hat{b}_n \rangle = \frac{g}{L^d} \sum_r n_r e^{ik_r(m-n)}. \tag{2.149}$$

Where n_r is the density of bosons in the cell r. Then, consider charges written as,

$$\hat{Q}_i = \sum_k q_{i,k} \hat{d}_k^\dagger \hat{d}_k. \tag{2.150}$$

Such that they are well approximated by,

$$\hat{Q}_i = g \sum_r n_m q_{i,r} \tag{2.151}$$

We wish to count the number of eigenstates that might be fixed by these constraints. So we must figure out how many ways one can distribute gn_r bosons in g places. Note that, $n_m \in [0, \infty)$. The counting problem is the same as the traditional derivation of Bose-Einstein statistics [11]. The total number of ways of distributing the bosons is,

$$w(n_r, g) = \frac{(n_r g + g - 1)!}{n_r g!(g-1)!} \tag{2.152}$$

So the total number of states is,

$$W = \prod_r \frac{(n_r g + g - 1)!}{n_r g!(g-1)!} \approx \frac{(n_r g + g)!}{n_r g!(g)!} \tag{2.153}$$

We then maximize the function below with the constraints of our conserved quantities,

$$\frac{\partial}{\partial n_r}\left(\ln W - \sum_i \lambda_i g \sum_r n_r q_{i,r}\right) = 0 \tag{2.154}$$

Then applying the Stirling approximation and reorganizing gives,

$$n_r = \frac{1}{e^{\sum_i \lambda_i q_{i,r}} - 1}, \tag{2.155}$$

which is a generalized Bose-Einstein statistic. In the thermodynamic limit the summation can be expressed as an integral,

$$\langle \hat{b}_m^\dagger \hat{b}_n \rangle = \frac{1}{2\pi}\int dk \frac{e^{ik(m-n)}}{e^{\sum_i \lambda_i q_{i,k}} - 1} \tag{2.156}$$

So we see that bosonic systems satisfy this notion as well, that is, typical eigenstates converge to this generalized Gibbs ensemble. It is interesting to note that the results for equilibration to a generalized Gibbs ensemble can be extended to bosonic systems as well [55].

2.5.2 Localized free fermions

A counter example to both thermalization and it's generalized form are localized models. There are many ways to induce localization for free models but here we discuss two. Consider the model written as,

$$H = \sum_{j=1}^{N} -\frac{J}{2}(f_j^\dagger f_{j+1} + \text{h.c}) + \lambda_j f_j^\dagger f_{j+1}, \tag{2.157}$$

where J dictates the strength of the nearest neighbor hopping term and λ_i will be an onsite, model dependent disordered potential. The Anderson model is recovered when we draw λ_i from a uniform distribution on the interval $\lambda_i \in [-\lambda, \lambda]$ [160]. Anderson localization (AL) is induced for any disorder parameter $\lambda > 0$ for the one dimensional Anderson insulator [137, 145, 161–163]. AL systems have exponentially suppressed transport. One can see this for example with the Lieb-Robinson bound. In the generic case where we expect ETH to hold we recover the bound [21, 164],

$$|||[A(t), B]||| \leq C||A||||B||e^{-\frac{|x|-vt}{\xi}}, \tag{2.158}$$

where $|x|$ is the distance between the support of A and B on the lattice and v is the Lieb-Robinson velocity. For Anderson localized models we instead get [21, 165, 166],

$$||[A(t), B]|| \leq C||A||||B||e^{-\frac{|x|}{\xi}}, \tag{2.159}$$

where we call ξ in this case the localization length and the Lieb-Robinson velocity is zero. Energy eigenstates of the AL models obey area laws in their entanglement entropy and entanglement entropy is bounded to this area law for all time [21,137,165,167,168]. The single particle eigenstates are localized, giving us the relation [161, 165, 169],

$$A_{m,k} \sim e^{-|k-m|/\xi}. \tag{2.160}$$

In general we don't expect this model to relax it's subsystems to expectation values given by a generalized Gibbs ensemble. The generalized Gibbs ensemble still obeys a volume law for it's subsystems which cannot emerge for an initial pure state evolving under our Anderson localized model [168].

The second model that is interesting is the Aubry-André model [20, 170]. Instead of our onsite potentials being random we now have quasi-periodic terms,

$$\lambda_j = \lambda \cos\left(2\pi\sigma j\right). \tag{2.161}$$

Where now the disorder parameter λ is a multiplicative constant controlling the strength of our quasi-periodic potential. The value σ is responsible for the qausi-periodicity, it is usually taken to be the inverse golden ratio,

$$\sigma = \frac{\sqrt{5}-1}{2}. \tag{2.162}$$

This model has an extended and a localized phase due to it's self-duality with a reciprocal space given by [20, 171],

$$d_k = \frac{1}{\sqrt{L}} \sum_j e^{i2\pi jk\sigma} f_j. \tag{2.163}$$

The critical point between the extended phase and localized phase is located at $\lambda_c = J$ with $\lambda_c < J$ being the extended regime. This model has also seen an extensive amount of research done on it [14, 49, 171–178]. Interestingly if one allows for long range hopping it is possible to induce an energy dependent mobility edge where the model has single particle eigenstates which are both extended and localized [179, 180]. Recent evidence suggests that the localization of the Aubrey-André model is more classical than Anderson localization [174]. This model has been experimentally realized in a number of experiments [181–187]. Despite the differences in localization between the Aubrey-André model

and the Anderson model in the classical limit, the Aubrey-André model still has the typical markers of single particle localization discussed above. It has area laws for it's energy eigenstate's entanglement entropy and obeys a zero velocity Lieb-Robinson bound in its localized phase. In general we also don't expect this model to relax it's subsystems to a generalized Gibbs ensemble description.

2.5.3 Interacting examples

In this section we will discuss one dimensional spin 1/2 Heisenberg type models of the form,

$$H = J\sum_{j=1}^{N}\left(S_j^x S_{j+1}^x + S_j^y S_{j+1}^y + \Delta S_j^z S_{j+1}^z + \lambda_j S_j^Z\right). \tag{2.164}$$

We will assume similar to the Anderson insulator, that λ_i is generated by a uniform distribution on the interval $\lambda_i \in [-\lambda, \lambda]$. Δ is the anisotropy parameter, when $\Delta = 0$ we recover a model that can be mapped to free fermions with the Jordan-Wigner transformation [153]. When $\Delta \neq 0$, the resulting mapping returns a Hamiltonian with interactions between neighboring fermions. In that case we refer to the model as being interacting rather than free.

When $\lambda = 0$ and $\Delta > 0$ this model is solvable by the Bethe ansatz and is therefore integrable [188]. The model has been numerically explored and confirmed to obey the weak eigenstate thermalization hypothesis [189]. This model, similar to free models, has an extensive number of conserved quantities and it is therefore interesting to study the generalized ETH and compare eigenstates to the generalized Gibbs ensemble. A number of studies reveal that this model similarly satisfies the generalized ETH [190–192]. Studies of the entanglement entropy in this model reveal volume laws for small subsystems, and some evidence suggests the scaling is independent of the parameter δ, giving us entanglement entropy scaling on subsystems equivalent to the free case [117].

If instead we instead consider our model with $\lambda > 0$ our model is the typical model to study the many body localization (MBL) transition [21]. When $\lambda > 0$ but is small, the majority of the eigenstates are chaotic, however when $\lambda \gg J$ the model transitions to the MBL phase [21,149,162,193–199] with a critical disorder existing somewhere in the interval $\lambda_c \in [3, 6]$. Intermediate values of λ support a phase coexistence with the so called many body localization edge [21]. In this intermediate regime the middle of the spectrum is expected to obey ETH while the localized states at the edge of the spectrum become more numerous [21]. The MBL phase has localization that is distinct from Anderson localization. The eigenstates have area law entanglement [21, 149, 162, 199], similar to AL however in a non-equilibrium context, it the entanglement between subsystems grows like a logarithm [137, 146, 200–203],

$$S_{vN}(\mathrm{Tr}_B\left[\rho(t)\right]) \sim \ln t. \tag{2.165}$$

MBL phases can equilibrate, however the phase lacks dissipation and therefore the equilibrium properties cannot be well described from the usual ensembles of statistical mechanics [21].

While equation 2.164 is the traditional model to study MBL, it has been numerically observed in a number of models [21, 137, 146, 149, 162, 193–203]. There is also some experimental evidence of it's existence [185]. Despite much progress in our understanding of MBL, it is still an open question if MBL would be stable in the thermodynamic limit and a growing amount of evidence suggests it may just be a prethermalization phenomenon [204–211]. Recent studies might suggest the transition takes place at much larger disorder strengths $\lambda_c > 20$ [210, 211] indicating that it might be necessary to understand the intermediate regime as a prethermal MBL regime, where thermalization timescales grow exponentially with disorder [204].

2.6 Scrambling of quantum information

The process of equilibrating to a thermal expectation value has extremely interesting consequences. Imagine we have two states, $|\psi_1\rangle$ and $|\psi_2\rangle$, each with interesting and distinct properties. We could for example distinguish them by saying that,

$$\langle\psi_1|\hat{A}|\psi_1\rangle \neq \langle\psi_2|\hat{A}|\psi_2\rangle, \tag{2.166}$$

for a local observable A. In principle there would be many observables satisfying this condition. We could also choose these states such that they have roughly equal energy,

$$\langle\psi_1|H|\psi_1\rangle \approx \langle\psi_2|H|\psi_2\rangle. \tag{2.167}$$

Assuming the dynamics generated by H thermalize the expectation value of $\hat{A}$, we conclude that since the energy densities of the two states are very similar, they relax the observables to the same thermal value,

$$A(\infty) = \langle\hat{A}\rangle_\beta. \tag{2.168}$$

From this observation we can see that equilibration to a thermal ensemble effectively "erases" the local information that initially distinguished our states. Quantum mechanics however tells us that information is conserved. Instead of erasing the information, the system has

scrambled the information, making it impossible to determine initial conditions by measuring local observables alone. This mirrors classical chaos, where incomplete information will give us exponential inaccuracy. Studying scrambling then might tell us about quantum chaos, and how to diagnose the differences in dynamics given to us by ETH, integrable and localized models.

A popular function to investigate scrambling is the out of time ordered correlator (OTOC) [151, 212–220],

$$C(x,t) = \langle [\hat{A}(t), \hat{B}]^\dagger [\hat{A}(t), \hat{B}] \rangle \,, \tag{2.169}$$

where the average is usually taken over some equilibrium ensemble. Some studies have considered pure states as well [168, 221, 222]. The variable x is taken to be the distance between the local observables $\hat{A}$ and $\hat{B}$ on the lattice, where one can vary x by moving the support of either observable on the lattice. The OTOC captures how non-local $\hat{A}$ becomes in time, picking up support on farther and farther regions of the lattice as t gets larger. At $t = 0$ we usually have $[\hat{A}, \hat{B}] = 0$ and we will see $C(x,t)$ grow as a function of time as $\hat{A}(t)$ begins pickup terms that do not commute with $\hat{B}$.

If one approaches the classical limit the commutator becomes a Poisson bracket which is a standard diagnostic of classical chaos. We therefore expect the OTOC in non-integrable models to initially grow exponentially fast controlled by the quantum Lyapunov exponent [220],

$$C(0,t) \sim e^{\lambda_L t}, \tag{2.170}$$

where λ_L is upper bounded (assuming a thermal average) by [220],

$$\lambda_L \leq \frac{2\pi k_B T}{\hbar}. \tag{2.171}$$

ETH can be viewed as a generalization of RMT which is a diagnostic of quantum chaos, and we therefore expect that if $C(x,t)$ can diagnose chaos, it must clearly differentiate ETH obeying models and integrable models. If our Hamiltonian H only has local interactions, the initial growth of the OTOC will be a power law when $x \neq 0$ [168, 221, 221, 223–227],

$$C(x,t) \sim t^{l(x)}, \tag{2.172}$$

where $l(x)$ is a linear function of x depending on the structure of the interactions in H, usually derived from the Hadamard formula. After the power law regime is exited we have an OTOC universal wave form, [228–230],

$$C(x,t) \sim \exp\left(-\lambda_L (x/v_B - t)^{1+p}/t^p\right). \tag{2.173}$$

v_B here is the butterfly velocity and p is a constant. This form has been verified in a large class of models [15, 138, 228–238]. For free models one can explicitly derive that $p = 1/2$ and therefore the existence of the waveform given in equation 2.173 is not sufficient to differentiate quantum chaotic models from integrable models [230]. For quantum spin models in general it is believed that $p > 0$ and the form will not reduce to the Lyapunov exponential growth [230]. The form of this universal waveform is usually found by fitting regimes where $C(x,t) \lll 1$ [229, 233]. Despite the appealing form of equation 2.173, it doesn't appear to be a good diagnostic of quantum chaos, Contribution 3 [239], where for example in two dimensions the value of p is identical between chaotic and integrable models [230]. Early results indicate that the waveform of $C(x,t)$ when $x \approx v_B t$ could be a diagnostic of quantum chaos by studying the waveform, Contribution 3 [239],

$$C(x,t) \sim e^{-m(x)(x-v_B t)^2 + b(x)(x-v_B t)}, \tag{2.174}$$

where $m(x), b(x)$ are spatially dependent functions with different scaling in free and chaotic regimes. Notably in free models $m(x), b(x)$ have power law decays, while in non-integrable models they decay exponentially, Contribution 3 [239].

The time it takes $C(x,t) \sim 1$ is referred to as the scrambling time and the late time value of the OTOC does appear to be a diagnostic of chaos. Let $\hat{A}$ and $\hat{B}$ be Hermitian and unitary. Then for a Hamiltonian that satisfies ETH, the late time value of the OTOC is [240, 241],

$$C(x, t \to \infty) = 2 - 2\left(\langle \hat{A}^2 \rangle \langle \hat{B} \rangle^2 + \langle \hat{A} \rangle^2 \langle \hat{B}^2 \rangle - \langle \hat{A} \rangle^2 \langle \hat{B} \rangle^2\right). \tag{2.175}$$

Therefore the exact factorization and late time value of $C(x,t)$ being non-zero can be considered markers of chaos. However some evidence suggests this late time scrambling does not always indicate chaos in the classical limit [242].

Chapter 3

Relaxation of non-integrable systems and correlation functions

Relaxation of non-integrable systems and correlation functions

Jonathon Riddell,[1,2,*] Luis Pedro García-Pintos,[3,†] and Álvaro M. Alhambra[4,‡]

[1] *Department of Physics & Astronomy, McMaster University 1280 Main St. W., Hamilton ON L8S 4M1, Canada.*
[2] *Perimeter Institute for Theoretical Physics, Waterloo, ON N2L 2Y5, Canada*
[3] *Joint Center for Quantum Information and Computer Science and Joint Quantum Institute, NIST/University of Maryland, College Park, Maryland 20742, USA*
[4] *Max-Planck-Institut für Quantenoptik, Hans-Kopfermann-Straße 1, D-85748 Garching, Germany*

(Dated: August 28, 2022)

We investigate early-time equilibration rates of observables in closed many-body quantum systems and compare them to those of two correlation functions, first introduced by Kubo and Srednicki. We explore whether these different rates coincide at a universal value that sets the timescales of processes at a finite energy density. We find evidence for this coincidence when the initial conditions are sufficiently generic, or "typical". We quantify this with the effective dimension of the state and with a "state-observable effective dimension" which estimate the number of energy levels that participate in the dynamics. Our findings are confirmed by proving that these different timescales coincide for dynamics generated by Haar-random Hamiltonians. This also allows to quantitatively understand the scope of previous theoretical results on equilibration timescales and on random matrix formalisms. We approach this problem with exact, full spectrum diagonalization. The numerics are carried out in a non-integrable Heisenberg-like Hamiltonian, and the dynamics are investigated for several observable/state pairs.

The current rate of development of quantum technologies means that experiments on quantum many body systems away from equilibrium are within reach. One of the more easily realizable mechanisms in this context is that of a *quantum quench* [1]. In it, one prepares a simple initial state $|\Psi\rangle$ of a lattice system, such as a low energy eigenstate of Hamiltonian H_0, and the Hamiltonian is suddenly switched to H for which $|\Psi\rangle$ is no longer an eigenstate. This drives the system far from equilibrium, and the subsequent dynamics can be traced through the expectation values of observables A,

$$\langle A(t)\rangle \equiv \langle\Psi|\, e^{-iHt} A e^{iHt}\, |\Psi\rangle\,, \tag{1}$$

where t is the time elapsed after the quench.

The experimental relevance of this setting has triggered a large amount of theoretical work, aimed at describing the complex dynamics of a wide variety of models [2, 3]. One of the most prominent features of these quantum dynamics is that physically relevant observables often thermalize, in the sense that there is some time T such that $\langle A(t)\rangle \sim \langle A\rangle_\beta$ for $t \geq T$, where $\langle A\rangle_\beta = \mathrm{Tr}\left[\frac{e^{-\beta H}}{Z} A\right]$ is the expectation value of a Gibbs ensemble with average energy $\langle\Psi|H|\Psi\rangle$. It is by now established that thermalization occurs generically as a consequence of the *eigenstate thermalization hypothesis* (ETH) [4, 5]. The ETH implies that energy eigenstates within a microcanonical window have thermal expectation values, from which it follows that $\overline{\langle A(t)\rangle} \to \langle A\rangle_\beta$, where $\overline{\langle ...\rangle}$ denotes the long-time average.

Less is known about how fast systems thermalize and about how the ETH affects the approach to thermal equilibrium (also called relaxation or equilibration). It has been argued that the ETH is behind fast relaxation to steady state values [6–14]. It has also been shown to play a role in fluctuation-dissipation relations [3, 15–18], certain kinds of transport [3, 19–21], and in the appearance of random matrix-like phenomena [3, 21–24]. However, our theoretical understanding of these processes, their timescales, and of how the ETH influences them remains far from complete.

Here, we investigate the relaxation timescales of A by numerically analyzing the early-time decay of the expectation value $\langle A(t)\rangle$ for various observables and states. We focus on a non-integrable Heisenberg model that we study via exact diagonalization. For the cases studied, we observe numerically that at early times the expectation value decays as

$$\langle A(t)\rangle \simeq \langle A(0)\rangle e^{-\frac{\sigma_A^2 t^2}{2}} \simeq \langle A(0)\rangle \left(1 - \frac{\sigma_A^2 t^2}{2}\right), \tag{2}$$

for some constant $\sigma_A > 0$. This sets the initial *relaxation rate*, which dominates until later phenomena, such as hydrodynamic tails [21, 25, 26], become relevant. We thus identify σ_A as the object of study of previous works on the timescales of equilibration [8–10, 27, 28].

We study the relaxation rate σ_A, and relate it to those of two correlation functions: $\mathcal{C}(t)$ describing the long-time out of equilibrium fluctuations, introduced by Srednicki [15], and the Kubo function $\mathrm{C}_{\mathrm{Kubo}}(t)$ describing the dissipation of perturbations near thermal equilibrium. We also calculate these rates analytically in a random matrix theory model, for which we show that they coincide up to a d^{-1} error, with d the Hilbert space dimension. Inspired by this result and other insights from random matrix theory frameworks [7, 29], we theorize,

* riddeljp@mcmaster.ca
† lpgp@umd.edu
‡ alvaro.alhambra@mpq.mpg.de

and numerically analyze, that in "generic" situations, the decay rate of all these quantities closely matches. This sets a universal timescale, which may only depend on few parameters such as the temperature [30].

The coincidence of correlation functions introduced by Srednicki and Kubo has been previously referred to as a "fluctuation-dissipation theorem" [3, 16]. With our analysis, we go beyond this connection by exploring how this fluctuation-dissipation relation can already arise at the initial relaxation process of the system. This is also supported by previous results [11, 31] which found other initial conditions under which thermal correlation functions coincide with the post-quench evolution of observables.

To study the relation between the different decay rates, we numerically determine σ_A for different initial conditions and system sizes, up to $L = 24$, and compare it to the rates σ_G and σ_K which characterize the dynamics of the Srednicki and Kubo correlation functions, respectively. We find that they are of the same order of magnitude in all cases studied, and they converge to the same value for at least one of the observables and initial state considered. We also observe that they are closer the more generic or "typical" the initial conditons are, which we quantify with the so-called *effective dimension* [32, 33] of the initial state, and with a modified version of it that also depends on the observable measured.

With these results, we illustrate with exact numerics previous theoretical arguments regarding timescales of relaxation [15, 27, 28], narrowing down their regime of applicability. We conclude that the accuracy of many existing theoretical predictions, (in particular, their ability to predict the relaxation timescale accurately) crucially depends on the typicality of the initial conditions, which appears to be challenging to quantify rigorously. We propose the aforementioned two quantities as figures of merit of this typicality, and we conclude that their value also relates to the validity of random matrix theory models studied in the literature [6, 7, 17, 34–37].

The paper is structured as follows. We define the model, observables, and states considered in our simulations in Sec. I, and we study the decay rates of the observables in Sec. II. In Sec. III, we define the correlation function of Srednicki and in Sec. IV that of Kubo. We compare the different decay rates in Sec. V. In Sec. VI, we show that all timescales coincide for Haar random Hamiltonians of large dimensional systems. In Sec. VII, we further investigate the conditions under which $\langle A(t)\rangle$, $\mathcal{C}(t)$, and $\mathrm{C}_{\mathrm{Kubo}}(t)$ have similar decay rates. We end with some remarks and open questions in Sec. VIII.

I. NON-INTEGRABLE MODEL: HEISENBERG CHAIN

We provide numerical results using a Heisenberg chain with next-nearest neighbour interactions

$$H = \sum_{j=1}^{L} J_1 \left(S_j^+ S_{j+1}^- + \text{h.c}\right) + \gamma_1 S_j^Z S_{j+1}^Z + J_2 \left(S_j^+ S_{j+2}^- + \text{h.c}\right) + \gamma_2 S_j^Z S_{j+2}^Z, \tag{3}$$

where $S_j^Z = |\uparrow\rangle\langle\uparrow| - |\downarrow\rangle\langle\downarrow|$ is the Pauli operator along Z for spin j and $S_j^+ = |\uparrow\rangle\langle\downarrow|$. We characterize this model by the coefficient vector $(J_1, \gamma_1, J_2, \gamma_2)$. It is non-integrable and obeys the ETH for generic parameters. However, it is quasi-free for $(J_1, \gamma_1, J_2, \gamma_2) = (J_1, 0, 0, 0)$ and Bethe-ansatz solvable when $(J_1, \gamma_1, J_2, \gamma_2) = (J_1, \gamma_1, 0, 0)$ [38–40]. Unless otherwise stated, we take $(J_1, \gamma_1, J_2, \gamma_2) = (-1, 1, -0.2, 0.5)$ for the figures.

The Hamiltonian in Eq. (3) has a number of symmetries which allows us to block-diagonalize it. In particular, it preserves total magnetization in the $m_z = \sum_{j=1}^{L} S_j^Z$ direction and is translation invariant. In our numerics, we choose initial states with $\langle m_z\rangle = 0$, which allows to further exploit the Z_2 spin flip symmetry. Our initial states are also chosen such that they have support in the $k = \{0, \pi\}$ translation sectors. This allows us to access exact dynamics from the maximally symmetric blocks of the Hamiltonian using the spatial reflection symmetry.

We investigate two observables of interest,

$$A_1 \coloneqq S_1^Z, \tag{4}$$

$$A_2 \coloneqq \frac{1}{L}\sum_{j=1}^{L} S_j^Z S_{j+1}^Z. \tag{5}$$

Observable A_1 has support on a single site and is therefore not translation invariant. This requires eigenstates from different symmetry sectors of the Hamiltonian to contribute to its dynamics. This is fundamentally different from the translation-invariant observable A_2, for which dynamics are generated only between eigenstates in the same symmetry sector.

We study three initial states that, as we see below, showcase rapid and slow examples of the relaxation process when probed by the observables introduced above. Let,

$$|\psi\rangle \coloneqq |\uparrow\downarrow\uparrow\downarrow\ldots..\rangle, \tag{6}$$

$$|\psi'\rangle \coloneqq \frac{1}{\sqrt{2}}\left(|\uparrow\downarrow\uparrow\downarrow\ldots..\rangle + |\downarrow\uparrow\downarrow\uparrow\ldots..\rangle\right), \tag{7}$$

$$|\phi\rangle \coloneqq \frac{1}{\sqrt{L}}\sum_{r=0}^{L-1} \hat{T}^r |\uparrow\uparrow\ldots\uparrow\downarrow\ldots\downarrow\downarrow\rangle, \tag{8}$$

where $\hat{T}$ is the translation operator shifting the state of each spin by one lattice site.

One expects the Néel-type state $|\psi\rangle$ to rapidly approach equilibrium due to every $\uparrow$ being neighboured by two $\downarrow$ terms. Also, $|\psi'\rangle$ being a superposition of two such states, we expect it to behave similarly, although its "cat state" structure may slightly change the physics. Meanwhile, $|\phi\rangle$ is a translation invariant state where the generating state $|\uparrow\uparrow\ldots\uparrow\downarrow\ldots\downarrow\downarrow\rangle$ only has two points that will initially admit spin flip dynamics. Due to this property, we expect it to exhibit slower equilibration that is more likely to feature hydrodynamic tails associated with transport.

In summary, we focus on the observable-state pairs

$$\langle A_1(t)\rangle_{|\psi\rangle} \coloneqq \langle\psi|A_1(t)|\psi\rangle, \tag{9a}$$
$$\langle A_2(t)\rangle_{|\phi\rangle} \coloneqq \langle\phi|A_2(t)|\phi\rangle, \tag{9b}$$
$$\langle A_2(t)\rangle_{|\psi'\rangle} \coloneqq \langle\psi'|A_2(t)|\psi'\rangle. \tag{9c}$$

II. INITIAL DECAY RATE

We observe that the initial decay of expectations after a quench takes the form

$$\begin{aligned}\langle A(t)\rangle &\simeq (\langle A(0)\rangle - \langle A(\infty)\rangle)\, e^{-\frac{\sigma_A^2 t^2}{2}} + \langle A(\infty)\rangle \\ &\simeq (\langle A(0)\rangle - \langle A(\infty)\rangle)\left(1 - \frac{\sigma_A^2 t^2}{2}\right) + \langle A(\infty)\rangle,\end{aligned} \tag{10}$$

where $\langle A(\infty)\rangle$ represents a late time "equilibrated" value that for simplicity we will take to be $\langle A(\infty)\rangle = 0$ throughout.

A Taylor expansion to second order shows that

$$\begin{aligned}\sigma_A^2 &= -\frac{1}{\langle A(0)\rangle}\frac{d^2\langle A(t)\rangle}{dt^2}\Big|_{t=0} = -\frac{\langle[H,[H,A]]\rangle}{\langle A(0)\rangle} \\ &= \frac{\sum_{j,k} c_j c_k^* A_{jk}(E_j - E_k)^2}{\sum_{j,k} c_j c_k^* A_{jk}},\end{aligned} \tag{11}$$

where in the last line we expand in the energy eigenbasis $\{|E_j\rangle\}$ such that $H = \sum_j E_j |E_j\rangle\langle E_j|$, the initial state is $|\Psi\rangle = \sum_j c_j |E_j\rangle$ and $A_{jk} = \langle E_j| A |E_k\rangle$. This second derivative has previously appeared in the analysis of general equilibration timescales [9].

Since we focus on an early-time regime, both the Gaussian and the quadratic functions give good approximations, with the Gaussian being slightly more accurate in most cases. The accuracy of the approximation is shown in Fig. 1 for the observable-state pair in Eq. (9a) (the other two show similar behaviour). Here, we see that the Gaussian does a marginally better job at approximating the decay in the dynamical region of interest and both functions get progressively worse at approximating the dynamics as t increases. This differs from the exponential decay $\sim e^{-\sigma t}$ associated with Fermi's golden rule found in some regimes [12, 41, 42]. In the cases studied here, a leading linear term is already ruled out from the fact that for our initial states and observables it holds that $[A, |\Psi\rangle\langle\Psi|] = 0$.

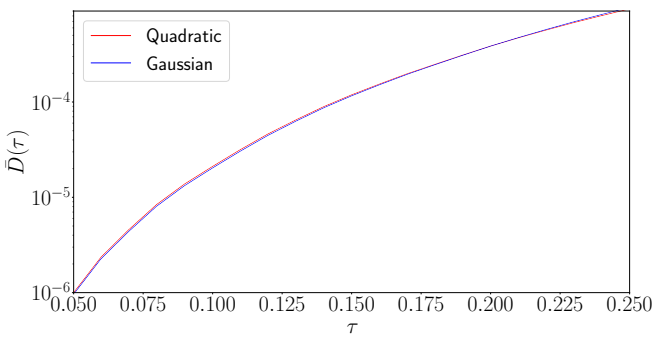

FIG. 1. Early time fit of $\langle A_1(t)\rangle_{|\psi\rangle}$ as defined in Eq. (9a) with respect to a quadratic and a Gaussian. We define a discrete approximation of the functions to be compared at the times $t \in \{n\Delta t | n \in \mathcal{N} \wedge n\Delta t \leq \tau\}$. We take $\bar{D}(\tau) = ||\langle\overrightarrow{A_1}(t)\rangle_{|\psi\rangle} - \overrightarrow{f}(t)||_1 / ||\langle A_1(t)\rangle_{|\psi\rangle}||_1$ where $\overrightarrow{g}(t)$ is the vector with components $g(n\Delta t)$, and $f(t)$ is the fitted function on the discrete interval. Here $\Delta t = 0.01$ and the fits are performed for $L = 24$ dynamics.

We first investigate the dependence of the initial decay rate σ_A with respect to various parameters of the Hamiltonian in Eq. (3). To produce a systematic picture of the dependence of σ_A on the parameters of the Hamiltonian, we take $(J_1, \gamma_1, J_2, \gamma_2) = (J_1, \frac{J_1\Delta}{2}, J_2, \frac{J_2\Delta}{2})$. We further fix the relation $J_2 = \frac{1}{2.7}J_1$. The results are shown in Fig. 2 for $L = 18$. We vary $J_1 \in [-2, -1]$ and $\Delta \in [0.1, 1.1]$. In this regime we see that the σ_A^2 of $\langle A_1(t)\rangle_{|\psi\rangle}$ is largely independent of Δ in the tested regime. On the contrary, the decay rate σ_A of $\langle A_2(t)\rangle_{|\phi\rangle}$ varies quite strongly with respect to Δ, most likely due to its construction hindering spin flip dynamics early. Our third example sits in-between these two. While the timescales associated with $\langle A_2(t)\rangle_{|\psi'\rangle}$ vary weakly with respect to Δ, the effect is non-negligible. Unsurprisingly, the timescales are much more sensitive to J_1 since it directly controls the magnitude of interactions which do not commute with the observables studied. As we will see, we can associate this lack of dependence on certain Hamiltonian parameters with the coincidence of timescales that we explore.

III. FLUCTUATIONS: SREDNICKI'S CORRELATION FUNCTION

We now consider the correlation function $\mathcal{C}(t)$, first defined in [15], which quantifies the "correlations in time" of $\langle A(t)\rangle$, as [43]

$$\mathcal{C}(t) = \frac{\overline{\langle A(t+t')\rangle\langle A(t')\rangle}}{\overline{\langle A(t')\rangle^2}}, \tag{12}$$

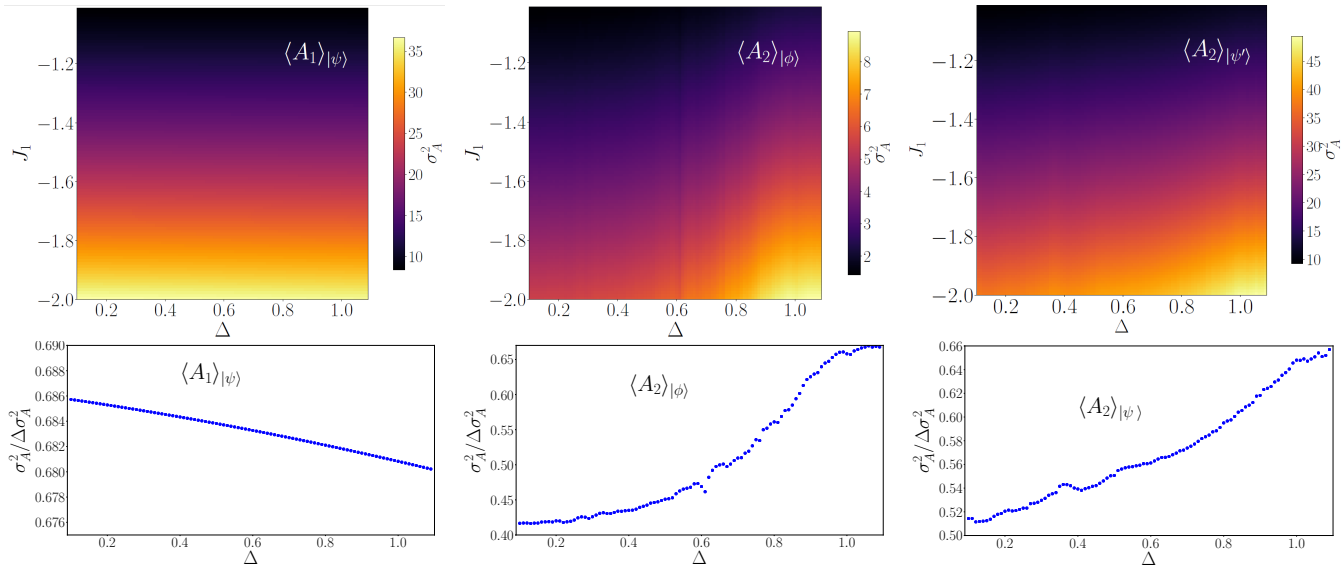

FIG. 2. The plots use the parameters of $(J_1, \gamma_1, J_2, \gamma_2) = (J_1, \frac{J_1\Delta}{2}, J_2, \frac{J_2\Delta}{2})$ with $J_2 = \frac{1}{2.7}J_1$ fixed. All data shown here has a system size of $L = 18$. (First row) Heat map of σ_A^2 as a function of J_1 and Δ for our three observable/state pairs. (Second row) We define $\Delta\sigma_A^2 = \max\sigma_A^2 - \min\sigma_A^2$, where the maximum and minimum are extracted from the data of the first row. To illustrate the individual variation of σ_A^2 with respect to Δ we cut the data from the first row by fixing $J_1 = -1.8$. Normalizing the σ_A^2 by dividing out $\Delta\sigma_A^2$ indicates how much change in the value is due to changes in Δ compared to J_1.

where $\overline{X(t')} \equiv \lim_{T\to\infty}\int_0^T \frac{\mathrm{d}t'}{T}X(t')$. It can also be written as

$$\mathcal{C}(t) = \frac{\sum_{j\neq k}|c_j|^2|c_k|^2|A_{jk}|^2 e^{-it(E_j-E_k)}}{\sum_{j\neq k}|c_j|^2|c_k|^2|A_{jk}|^2}. \tag{13}$$

The ETH and properties of the observable and the state imply that, for short times, this function decays as $\mathcal{C}(t) \simeq e^{-\frac{\sigma_G^2 t^2}{2}} \simeq 1 - \frac{\sigma_G^2 t^2}{2}$ (since it is at early times, the quadratic function is also a good approximation). This is discussed in more detail in Appendix A. Moreover, the initial decay rate is given by

$$\begin{aligned}\sigma_G^2 &= \frac{\sum_{j\neq k}|c_j|^2|c_k|^2|A_{jk}|^2(E_k-E_j)^2}{\sum_{j\neq k}|c_j|^2|c_k|^2|A_{jk}|^2} \\ &= \frac{\mathrm{Tr}\left[\mathcal{D}(|\Phi\rangle\langle\Phi|)[A,H]\mathcal{D}(|\Phi\rangle\langle\Phi|)[H,A]\right]}{\mathrm{Tr}\left[(\mathcal{D}(|\Phi\rangle\langle\Phi|)A)^2\right]},\end{aligned} \tag{14}$$

where $\mathcal{D}(|\Phi\rangle\langle\Phi|) \coloneqq \sum_k |c_k|^2|E_k\rangle\langle E_k|$ is the so-called *diagonal ensemble*. Note that $\langle A(\infty)\rangle = \mathrm{Tr}\left[\mathcal{D}(|\Phi\rangle\langle\Phi|)A\right] = 0$. This can be seen by expanding Eq. (13) to second order at short times. With this expression, σ_G could be calculated by more efficient methods than exact diagonalization, such as tensor networks [44].

It will be often the case that σ_G characterizes relaxation timescales beyond the short-time behaviour of $\mathcal{C}(t)$. We prove in Appendix B that the rate at which the correlation function changes is upper bounded by $\left|\frac{d\mathcal{C}(t)}{dt}\right| \leq \sigma_G$ at all times – a form of quantum speed limit on $\mathcal{C}(t)$. The main results of [45] also apply to this function. They show that σ_G characterizes not only the initial rate but also the timescales for $\mathcal{C}(t)$ to equilibrate to the steady state value in generic situations (see Appendix C).

Unlike the form of σ_A in Eq. (11), σ_G in Eq. (14) implies that the characteristic rate σ_G is independent of the terms in the Hamiltonian that commute with A. In our examples, both observables commute with the term $\gamma_1 S_j^Z S_{j+1}^Z$ and as such σ_G is independent of γ_1. We can now compare this conclusion to that of Fig. 2, where we see that σ_A is mostly independent of γ_1 only for $\langle A_1(t)\rangle_{|\psi\rangle}$. This already hints to situations where we expect $\sigma_A \sim \sigma_G$.

In [15], it was argued that $\mathcal{C}(t)$ exactly models the decay of $\langle A(t)\rangle$ after possible large out-of-equilibrium fluctuations that happen after the system has thermalized. We have not been able to numerically verify this claim, since it appears that the potential fluctuations that this correlation function models happen at late times (likely scaling quickly with system size). In any case, from the definition in Eq. (12), we can establish that $\mathcal{C}(t)$ quantifies the correlations in time of the fluctuations of $\langle A(t)\rangle$.

Notice that this function depends on the same initial conditions as $\langle A(t)\rangle$ (with the difference that it does not depend on the phases of $c_j c_k^* A_{jk}$). We may then expect what is one of our main points: that in some "generic" cases, e.g. in which the dependence with the phases is unimportant, its decay rate may be close to σ_A in Eq. (2). This is in fact the conclusion reached by slightly different arguments of previous works on relaxation timescales [27]. These suggests that, given ETH, the relevant decay timescale in which $\langle A(t)\rangle \to \langle A\rangle_\beta$ is close to precisely σ_G (see Eq. (15) of [27]).

We now explain why this can be expected. As dis-

cussed in e.g. [27], the initial relaxation rate can be understood as follows: for many-body systems, the expectation value of an observable

$$\langle A(t)\rangle = \sum_{jk} c_j c_k^* A_{jk} e^{-it(E_j - E_k)}, \tag{15}$$

at time time $t > 0$ is a sum over a dense set of complex numbers oscillating at different frequencies in the complex plane. If these complex numbers are spread evenly enough among the plane, they will typically collectively cancel. This will cause the oscillating part of $\langle A(t)\rangle$ to average to zero, leading to equilibration to a steady value. This will happen quickly in general, provided that there are not too many spurious correlations among the coefficients $c_j c_k^* A_{jk}$ and the energy gaps, that might make the spread uneven. We thus identify this spread and lack of correlations between the complex coefficients with the concept of "typicality". A similar picture is also provided in [28].

The conclusion stemming from this is that the relaxation or "dephasing" time is controlled by the variance of the energy gaps, as weighted by the absolute value of the coefficients in Eq. (15) [9, 27, 28]. This exactly coincides with the expression for σ_G in Eq. (14). This implies that the initial decay rate is the same as that of a correlation function $\mathcal{C}(t)$, which we already know to be σ_G from the discussion in Sec. (III), and so $\sigma_A \simeq \sigma_G$.

However, from this coarse argument it is not clear whether a conclusion as strong as $\sigma_A \simeq \sigma_G$ can hold in full generality — in fact, we will see that at times they are only within the same order of magnitude. Nevertheless, it suggests that this coincidence of timescales will be closer the more evenly spread the coefficients in Eq. (15) are in the complex plane, and the fewer spurious correlations there are between them. We explore this numerically in Sec. V below, and further explain it in Sec. VII.

IV. DISSIPATION: THE KUBO THERMAL RESPONSE FUNCTION

The Kubo correlation function models the dissipation of small perturbations away from thermal equilibrium [46]

$$\mathcal{C}_{\text{Kubo}}(t) \propto \sum_{j\neq k} \frac{e^{-\beta E_j} - e^{-\beta E_k}}{E_k - E_j} |A_{jk}|^2 e^{i(E_j - E_k)t}. \tag{16}$$

By a similar argument as that used for $\mathcal{C}(t)$ in Appendix A, this function has an initial Gaussian/quadratic decay

$$\mathcal{C}_{\text{Kubo}}(t) \simeq \mathcal{C}_{\text{Kubo}}(0) e^{-\sigma_K^2 t^2} \simeq \mathcal{C}_{\text{Kubo}}(0)\left(1 - \sigma_K^2 t^2\right), \tag{17}$$

with a characteristic decay rate given by

$$\sigma_K^2 = \sum_{j,k} \frac{e^{-\beta E_k} - e^{-\beta E_j}}{\mathcal{C}_{\text{Kubo}}(0)} |A_{jk}|^2 (E_k - E_j) \tag{18}$$

$$= \frac{1}{\mathcal{C}_{\text{Kubo}(0)}} \text{Tr}\left[\left[A, \frac{e^{-\beta H}}{Z}\right][A, H]\right]. \tag{19}$$

The initial decay rate σ_K also characterizes other aspects of the dynamics of the correlation function, as was the case for $\mathcal{C}(t)$. Theorem 5 in [45] shows that in some cases σ_K also governs the equilibration timescale of C_{Kubo}, and Appendix E shows that σ_K also upper bounds its rate of change.

Based on the ETH, the work of Srednicki [15] argues that $\mathcal{C}(t)$ behaves similarly to $\text{C}_{\text{Kubo}}(t)$. We reproduce the theoretical argument based on the ETH ansätz in Appendix D. The reason behind it is similar to that of the previous section: states that have a support uniformly spread over many energy eigenstates will behave in a more "thermal", or "typical" manner, so that both correlation functions evolve similarly by virtue of being largely independent of the coefficients of Eqs. (15) and (16). More specifically, if the function $f(\langle H\rangle, \omega)$ of the ETH ansätz [see Eq.(A1)] decays rapidly at frequencies $\omega > W$ and the initial state has variance λ, then

$$\mathcal{C}(t) \simeq \mathcal{C}_{\text{Kubo}}(t) + \mathcal{O}(\beta^2 W^2) + \mathcal{O}\left(\frac{W^2}{\lambda^2}\right). \tag{20}$$

The function $f(\langle H\rangle, \omega)$ has been thoroughly explored in numerical simulations [3, 16, 22, 47, 48], showing a relatively fast decay with frequency. This suggests that the two error terms in this equation are small, so that $\mathcal{C}(t) \simeq \mathcal{C}_{\text{Kubo}}(t)$ or that, at least, $\sigma_G \simeq \sigma_K$. We check this similarity for our examples in Sec. V below. This coincidence of the dynamics of $\mathcal{C}(t)$ and $\mathcal{C}_{\text{Kubo}}(t)$ has been previously identified as a quantum "fluctuation-dissipation" relation [16].

Note that the argument leading to Eq. (20) crucially relies on the coefficients c_j and A_{jk} being uniformly distributed (see Eq. (D1)). Thus, as we find, in the more "non-generic" situations, hidden correlations between these coefficients can make the argument fail. This also agrees with the fact that only some of the examples studied in [16] show that $\mathcal{C}(t) \sim \mathcal{C}_{\text{Kubo}}(t)$, which correspond to the quenches in which we expect typicality. That is, when the lack of structure or correlations between the coefficients $c_j, e^{-\beta E_j}$ and A_{jk}, is more prominent.

V. COMPARISON OF TIMESCALES

In the discussion above we have introduced three different rates: σ_A, σ_G and σ_K, defined respectively in Eqs. (11), (14) and (18), and speculated with the possibility that they may coincide in certain cases. We now numerically compute these quantities, and explore whether this coincidence indeed happens.

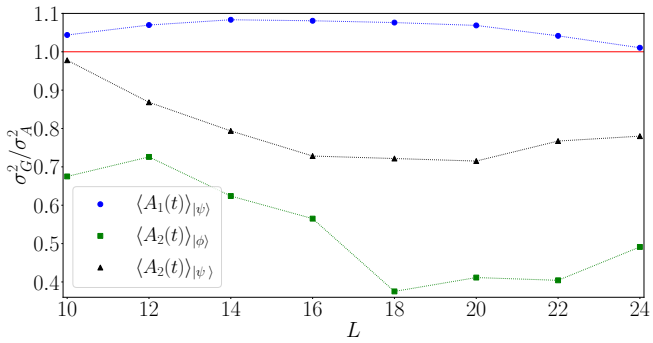

FIG. 3. Ratio between σ_G^2 defined in Eq. (14) and σ_A^2 defined in Eq. (2), as a function of system size. We see that in the case of $\langle A_1(t)\rangle_{|\psi\rangle}$ the ratio approaches 1 for larger L.

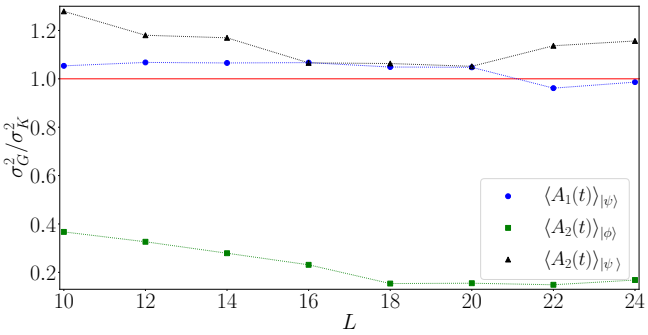

FIG. 4. Ratio between σ_G^2 defined in Eq. (14) and σ_K^2 defined in Eq. (17) as a function of system size. The thermal state was restricted to energy eigenstates with non-zero weight in the states defined in Eqs. (6) and (8)]. The value of β was determined so that the thermal state had identical energy to the initial pure state.

First, we compare the decay rates σ_A and σ_G in each of our three pairs of initial states and observables in Eqs. (9). The results are shown in Fig. 3, where we see that σ_A and σ_G are of the same order of magnitude, and that they converge in the case of the state-observable pair $\langle A_1(t)\rangle_{|\psi\rangle}$ in Eq. (9a) as the size of the system grows. At system size $L = 24$, we see the decay rates strongly coincide, with $\sigma_G^2/\sigma_A^2 \approx 1.0105$. This shows that, at least in the latter case, the two rates converge, which is consistent with our expectation from Fig. 2. Given our discussion above, we thus expect that $\langle A_1(t)\rangle_{|\psi\rangle}$ is the most "typical" scenario, with $\langle A_2(t)\rangle_{|\phi\rangle}$ being the least.

The case of $\langle A_2(t)\rangle_{|\phi\rangle}$ is the one for which σ_A and σ_G differ the most, and also the one for which σ_A is more sensitive to changes in γ_1 (see Fig. 2). A possible reason for this is that we expect that transport processes are relevant in the relaxation of state $|\phi\rangle$. These are generally associated with an "atypicality" of the dynamics, and a breakdown of random matrix theory features [36], which can potentially cause correlations between the coefficients of Eq. (15).

Additionally, Fig. 4 compares the rates σ_G and σ_K. We observe that the two timescales are similar for both state-observable pairs $\langle A_1(t)\rangle_\psi$ and $\langle A_2(t)\rangle_\phi$, with the former being the closest. Indeed, for $\langle A_1(t)\rangle_{|\psi\rangle}$ and the largest system size tested $L = 24$ we have that $\sigma_G^2/\sigma_K^2 \approx 0.9864$. This shows how in some cases the aforementioned "fluctuation-dissipation" relation can emerge in certain situations, as previously found in [16]. On the other hand, the rates σ_G and σ_K differ significantly for the third case of $\langle A_2(t)\rangle_{|\psi'\rangle}$ (although still within an order of magnitude).

Moreover, comparing Figs. 3 and 4 shows that the cases when $\sigma_K \sim \sigma_G$ coincide with those for which $\sigma_K \sim \sigma_A$. This is not surprising since, as per the discussions above, we expect that the most typical situations are the ones in which all these rates are similar. Here, the most typical case is $\langle A_1(t)\rangle_\psi$, with $\langle A_2(t)\rangle_{|\psi'\rangle}$ being somewhat far from it.

VI. RANDOM MATRIX THEORY ANALYSIS

We have seen how in the model of Eq. (3) the different timescales considered coincide for certain state-observable combinations. We now explore the conclusions of the previous sections in the paradigmatic model of "typicality", with a Hamiltonian diagonalized by a random unitary matrix [35].

This is a simpler model in which the characteristic relaxation rates can be analytically computed exactly. Let us define an arbitrary Hamiltonian in which the eigenbasis is chosen at random, as

$$H_U \equiv UHU^\dagger, \tag{21}$$

where U is drawn from the Haar measure over the unitary group [49]. This model, which has previously appeared in the study of equilibration of closed systems [6, 35, 50], is motivated by the fact that quantum non-integrable systems have highly entangled eigenstates, that highly resemble random states [3, 4, 51–53].

With it, we are able to give analytical expressions for the average squared decay rates $\langle\sigma_A^2\rangle_U$, $\langle\sigma_G^2\rangle_U$ and $\langle\sigma_K^2\rangle_U$, where $\langle\cdot\rangle_U$ indicates the average over the Haar measure. Given that the corresponding thermal state of this model is always the maximally mixed state, the thermal state corresponding to $\mathcal{D}(|\Phi\rangle\langle\Phi|)$ is always the infinite temperature state $\beta = 0$.

In Appendix F, we show that

$$\begin{aligned}\langle\sigma_G^2\rangle_U &\simeq \langle\sigma_A^2\rangle_U + \mathcal{O}\left(\frac{1}{d}\right) = \langle\sigma_K^2\rangle_U + \mathcal{O}\left(\frac{1}{d}\right) \\ &= 2\left(\langle H^2\rangle_{\mathrm{MC}} - \langle H\rangle_{\mathrm{MC}}^2\right) + \mathcal{O}\left(\frac{1}{d}\right),\end{aligned} \tag{22}$$

where $d = 2^L$ is the dimension of the total Hilbert space and $\langle B\rangle_{\mathrm{MC}} = \mathrm{Tr}\left[B\right]/d$. That is, the rates coincide with the energy variance at infinite temperature for $L \gg 1$.

The intuitive reason behind this is that the randomness in the eigenstates washes out any correlations between $\{A_{jk}\}$, $\{c_j, c_k\}$ and $E_j - E_k$, such that the relevant timescale does not depend on the observable nor the initial state but only on the spectrum. The " $\simeq$ " in Eq. (22) relies on the accuracy of the approximation $\langle f/g\rangle_U \approx \langle f\rangle_U/\langle g\rangle_U$, sometimes referred to as the "annealed approximation" [54–60], which we justify analytically in Appendix G.

To derive Eq. (22), we need to compute the average of certain correlation functions over the unitary group. These involve the fourth moment of the Haar measure, which results in cumbersome analytical expressions of hundreds of coefficients coming from the Weingarten calculus [49]. We deal with these analytically with the recently introduced RTNI package [61]. In contrast, the calculations with the same model of e.g., [7] only involve second moments, which can be done by hand.

The result in Eq. (22) supports the fact that, in typical instances of the dynamics where RMT is accurate, the timescales studied here coincide with a "universal" value. It is also consistent with previous studies of RMT models [7, 29], where such coincidence of timescales for different dynamical processes is already hinted at.

VII. TYPICALITY OF THE DYNAMICS AND THE EFFECTIVE DIMENSION

Here, we propose to quantify the typicality of the situations studied with two figures of merit, and connect them to the dynamics of the observables and correlation functions.

The dephasing argument in Sec. III suggests that the more "evenly spread" in frequency the coefficients $c_j c_k^* A_{jk}$ are, the more we expect the decay rates to coincide, $\sigma_A \sim \sigma_G$. On top of that, the result of the Sec. VI shows that, when these are fully random, the rates coincide for large Hilbert space dimension d. Motivated by these facts, we aim to understand our numerical findings from Sec. V in terms of two different measures of typicality of the initial conditions.

The first one contains information about the state and the Hamiltonian, and is the so-called *effective dimension*, also commonly referred to as the inverse participation ratio. The effective dimension D_Φ of a pure state $|\Phi\rangle$, defined by

$$D_\Phi^{-1} \equiv \mathrm{Tr}\left[\mathcal{D}(|\Phi\rangle\langle\Phi|)^2\right] = \left(\sum_j |c_j|^4\right), \qquad (23)$$

controls the long-time equilibration of isolated quantum systems [32, 62, 63]. Here, $|\overline{\Phi(t)}\rangle\langle\overline{\Phi(t)}| = \mathcal{D}(|\Phi\rangle\langle\Phi|)$ is the diagonal ensemble: the initial state dephased in the energy eigenbasis.

The effective dimension quantifies the number of eigenstates that participate in the process. A "typical" state thus has a large effective dimension. It is known to grow exponentially in system size under very general conditions on the eigenstates [64, 65] and to be close to the maximal value d if the initial state is chosen at random [66, 67]. Importantly, it bounds the size of late time fluctuations around equilibrium [32, 33].

A shortcoming of this measure is that it does not depend on the observable studied. To account for it, we consider a second measure of typicality $D_{\Phi,A}$ that incorporates information of the off-diagonal matrix elements of the observable, which play a role in dynamics. We refer to $D_{\Phi,A}$ as a *state-observable effective dimension*, and define it by [68]

$$D_{\Phi,A}^{-1} \equiv \sum_{j\neq k} |c_j|^2 |c_k^*|^2 |A_{jk}|^2. \qquad (24)$$

It holds that $D_{\Phi,A}^{-1} \leq ||A||^2 D_\Phi^{-1}$ [32, 33], where $||A||$ is the largest singular value of A. Comparing $D_{\Phi,A}^{-1}$ and D_Φ^{-1}, we can roughly think of $D_{\Phi,A}^{-1}$ as an inverse effective dimension that accounts for the observables off-diagonal elements. Notice that this expression only contains information about the off-diagonal terms which generate the dynamics, and not the diagonal ones.

The state-observable effective dimension is related to the fluctuations around equilibrium, as

$$D_{\Phi,A}^{-1} = \lim_{T\to\infty} \int_0^\infty |\langle A(t)\rangle - \mathrm{Tr}\left[\mathcal{D}\left(|\Phi\rangle\langle\Phi|\right) A\right]|^2 dt, \qquad (25)$$

where we have assumed non-degeneracy in the energy gaps.

The significance of these two measures for the dynamics at earlier times can be understood as follows: the larger the effective dimensions, the more off-diagonal terms A_{jk} can participate in the dynamics. This implies that the particular details and structure of individual off-diagonal matrix elements contribute less at an earlier time, making treatments akin to random-matrix theory, such as in [7, 11, 17, 69], more accurate. That is, we generally expect that the larger the effective dimensions D_Φ and $D_{\Phi,A}$, the more typical the dynamics is.

When that is the case, the initial state and the energy eigenbasis are closer to being "mutually unbiased" [70], which effectively means that the energy eigenbasis and a basis of low-entangled states including $|\Psi\rangle$ can be related by a random matrix. In [7], this was shown to imply that

$$\langle A(t)\rangle \propto \sum_{j,k} e^{-it(E_j - E_k)}, \qquad (26)$$

where the sum includes the set of energy gaps that participate in the dynamics. That is, $\langle A(t)\rangle$ resembles the *spectral form factor* of the Hamiltonian, and depends weakly on the details of the coefficients A_{jk} and c_j. This is consistent with the random matrix theory result of Section VI, which show that in a random-matrix model the timescales are set only by the Hamiltonian.

Another way to understand this is as follows: if we compute the coefficients c_j, A_{jk} with a random matrix

formalism, they will be all of similar weight, and close to maximally evenly distributed in the complex plane, leading on expectation to Eq. (26).

In contrast, in a local model with energy conservation, such as that of Eq. (3), the coefficients A_{jk} and c_j have non-trivial structure, and set the range of participating energy gaps to be those around the average energy (those for which $c_j c_k^* A_{jk}$ is not too small). Due to this, the decay rates σ_A can be significantly different from that of an actual form factor or the Loschmidt echo, which would correspond to the energy variance [71, 72] as we found in Eq. (22).

Exactly the same argument applies to $\mathcal{C}(t)$ and $\mathcal{C}_{\text{Kubo}}(t)$, and one can thus infer that they will behave similarly to $\langle A(t)\rangle$ on the basis of them also evolving like an spectral form factor $\sum_{j,k} e^{-it(E_j-E_k)}$ of the participating energy gaps. This idea is consistent with [73], which proposes that the coincidence of correlation functions and form factors is a key indicator of the validity of random matrix theory ansätze.

Given this discussion, we expect that the larger the effective dimensions D_Φ and $D_{\Phi,A}$, the closer the decay rates σ_A, σ_G and σ_{Kubo} shown in Fig. 3 of Sec. V become. We confirm this by calculating the effective dimensions as a function of system size for the three different initial states. The results are shown in Figs. 5 and 6, where we see an exponential decay in all cases. We also observe a noticeable difference between the different states, with $D_\psi > D_{\psi'} > D_\phi$, and with $D_{\psi,A_1} > D_{\psi',A_2} > D_{\phi,A_3}$ for sufficiently large systems with $L \geq 16$. This agrees with our expectations that the effective dimensions can serve to witness the situations in which the decay rates coincide. This is also consistent with the results of Sec. V and with Figs. 3 and 4. We find that $\langle A_1(t)\rangle$ is the most typical scenario, and the one in which the timescales $\sigma_A, \sigma_G, \sigma_K$ most resemble each other. In contrast, $\langle A_2(t)\rangle_{|\phi\rangle}$ is a more atypical scenario in which the decay rates differ the most.

These results suggest that the effective dimensions considered can serve as

- Figures of merit of the typicality of the dynamics, and of the validity of RMT frameworks.
- Indicators of the coincidence of the relaxation rate of the quench with correlation functions.

An interesting open problem is to make this connection more precise and quantitative, perhaps in the form of a bound similar to those for late-time fluctuations in [32, 33, 74].

VIII. CONCLUSIONS

We have analyzed the early time relaxation rate of observables with different initial conditions for a non-integrable quantum system. As a general conclusion, we observe a close link between the coincidence of different dynamical quantities and their initial relaxation rates with the typicality of the initial conditions. We quantify this typicality with two notions of "effective dimensions" that, in broad terms, quantify the number of frequencies involved in the evolution of an observable. This allows us to better understand how and when the complex relaxation behaviour of these quantum systems can be understood in simpler terms, either by linking it to correlation functions, or by having random matrix theory/typicality treatments to accurate describe dynamics.

We see that, in typical cases, the rate σ_A at which an observable initially decays is related to the rate σ_K, which dictates the approach to thermal equilibrium from perturbations, and to the rate σ_G, which dictates temporal fluctuations. This suggests a connection between (short-time) equilibration, fluctuation, and dissipation processes of an observable for typical states – a sort of *equilibration-fluctuation-dissipation* relation, formalized by $\sigma_A \simeq \sigma_K \simeq \sigma_G$, that goes beyond some previously studied fluctuation-dissipation relations [16].

A full theoretical characterization of relaxation dynamics and their timescales remains a largely open problem [10, 12, 75]. Our findings suggest that, while it may be possible to describe the dynamics of very generic situa-

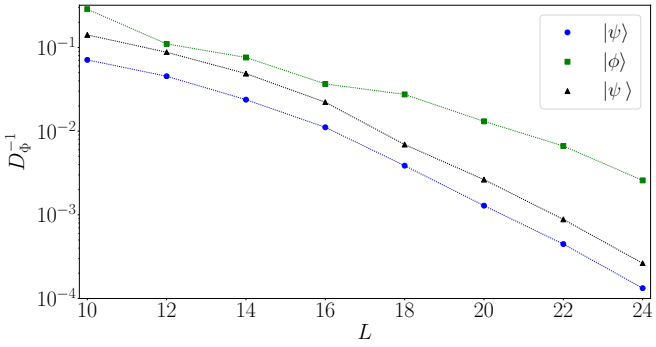

FIG. 5. $D_{\Phi,A}^{-1}$ as a function of system size, up to $L = 24$. We see clear exponential decay setting in at large system sizes at different rates.

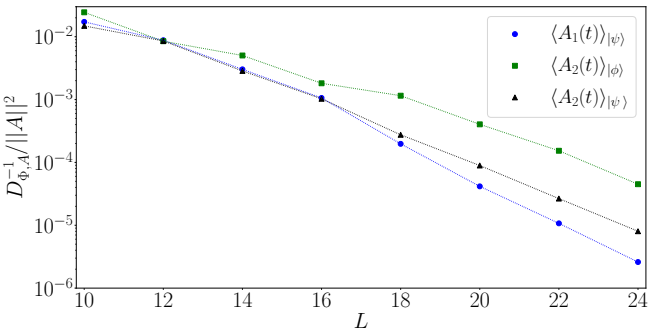

FIG. 6. Inverse effective dimension D_Φ^{-1} as a function of system size, up lo $L = 24$. We see a clear exponential decay, with different states decaying at diverging rates.

tions, the existence of "atypical" situations make general rigorous results challenging [76–78]. This impacts the regimes in which previous upper bounds on equilibration timescales correctly capture the dynamics of isolated systems [9, 27]. An important milestone could be to find more systematic ways of knowing when a particular dynamics can be considered typical, via the effective dimensions proposed here, or some related figure of merit.

The present results confirm the intuition provided by a large number of previous theoretical works that make similar connections through either typicality arguments [7, 62, 79] or random matrix theory ansätze [4, 17, 37, 50, 80]. They are also consistent with the picture that links typicality and the validity of different random matrix formalisms to the absence of macroscopic transport phenomena [36].

ACKNOWLEDGMENTS

AMA acknowledges support from the Alexander von Humboldt foundation. J.R acknowledges support from the Natural Sciences and Engineering Research Council of Canada (NSERC). J.R would also like to thank Steven Silber and Erik Sørensen for helpful discussions about exact diagonalization methods. LPGP acknowledges the DoE ASCR Accelerated Research in Quantum Computing program (award No. DE-SC0020312), DoE QSA, NSF QLCI, NSF PFCQC program, U.S. Department of Energy Award No. DE-SC0019449, DoE ASCR Quantum Testbed Pathfinder program (award No. DE-SC0019040), AFOSR, ARO MURI, AFOSR MURI, and DARPA SAVaNT ADVENT.

[1] A. Mitra, Annual Review of Condensed Matter Physics **9**, 245 (2018).
[2] C. Gogolin and J. Eisert, Rep. Prog. Phys. **79**, 056001 (2016).
[3] L. D'Alessio, Y. Kafri, A. Polkovnikov, and M. Rigol, Advances in Physics **65**, 239 (2016).
[4] J. M. Deutsch, Phys. Rev. A **43**, 2046 (1991).
[5] M. Srednicki, Phys. Rev. E **50**, 888 (1994).
[6] P. Reimann, New Journal of Physics **17**, 055025 (2015).
[7] P. Reimann, Nat. Commun. **7**, 1 (2016).
[8] A. J. Short and T. C. Farrelly, New. J. Phys. **14**, 013063 (2012).
[9] L. P. García-Pintos, N. Linden, A. S. L. Malabarba, A. J. Short, and A. Winter, Phys. Rev. X **7**, 031027 (2017).
[10] H. Wilming, T. R. de Oliveira, A. J. Short, and J. Eisert, Thermodynamics in the Quantum Regime , 435–455 (2018).
[11] J. Richter, J. Gemmer, and R. Steinigeweg, Phys. Rev. E **99**, 050104 (2019).
[12] R. Heveling, L. Knipschild, and J. Gemmer, Journal of Physics A: Mathematical and Theoretical **53**, 375303 (2020).
[13] R. Heveling, L. Knipschild, and J. Gemmer, Phys. Rev. X **10**, 028001 (2020).
[14] L. Dabelow and P. Reimann, Physical Review Letters **124** (2020), 10.1103/physrevlett.124.120602.
[15] M. Srednicki, Journal of Physics A: Mathematical and General **32**, 1163 (1999).
[16] E. Khatami, G. Pupillo, M. Srednicki, and M. Rigol, Phys. Rev. Lett. **111**, 050403 (2013).
[17] C. Nation and D. Porras, Phys. Rev. E **99** (2019), 10.1103/physreve.99.052139.
[18] J. D. Noh, T. Sagawa, and J. Yeo, Phys. Rev. Lett. **125** (2020), 10.1103/physrevlett.125.050603.
[19] B. Bertini, F. Heidrich-Meisner, C. Karrasch, T. Prosen, R. Steinigeweg, and M. ***Z***nidari***c***, Reviews of Modern Physics **93** (2021), 10.1103/revmodphys.93.025003.
[20] C. Schönle, D. Jansen, F. Heidrich-Meisner, and L. Vidmar, Phys. Rev. B **103**, 235137 (2021).
[21] A. Dymarsky, ArXiv e-prints (2018), arXiv:1804.08626 [cond-mat.stat-mech].
[22] R. Mondaini and M. Rigol, Physical Review E **96**, 012157 (2017).
[23] J. Richter, A. Dymarsky, R. Steinigeweg, and J. Gemmer, Phys. Rev. E **102** (2020), 10.1103/physreve.102.042127.
[24] M. Brenes, S. Pappalardi, M. T. Mitchison, J. Goold, and A. Silva, Physical Review E **104** (2021), 10.1103/physreve.104.034120.
[25] J. Lux, J. Müller, A. Mitra, and A. Rosch, Phys. Rev. A **89**, 053608 (2014).
[26] M. Blake, Phys. Rev. Lett. **117**, 091601 (2016).
[27] T. R. de Oliveira, C. Charalambous, D. Jonathan, M. Lewenstein, and A. Riera, New. J. Phys. **20**, 033032 (2018).
[28] H. Wilming, M. Goihl, C. Krumnow, and J. Eisert, arXiv e-prints , arXiv:1704.06291 (2017), arXiv:1704.06291 [quant-ph].
[29] C. Nation and D. Porras, Phys. Rev. E **99**, 052139 (2019).
[30] S. Pappalardi, L. Foini, and J. Kurchan, "Quantum bounds and fluctuation-dissipation relations," (2021), arXiv:2110.03497 [hep-th].
[31] J. Richter and R. Steinigeweg, Phys. Rev. E **99**, 012114 (2019).
[32] P. Reimann, Phys. Rev. Lett. **101**, 190403 (2008).
[33] A. J. Short, New. J. Phys. **13**, 053009 (2011).
[34] J. M. Deutsch, Phys. Rev. A **43**, 2046 (1991).
[35] S. Popescu, A. J. Short, and A. Winter, Nature Physics **2**, 754–758 (2006).
[36] P. Reimann, New. J. Phys. **21**, 053014 (2019).
[37] C. Nation and D. Porras, New. J. Phys. **20**, 103003 (2018).
[38] L. F. Santos and M. Rigol, Phys. Rev. E **81**, 036206 (2010).
[39] M. A. Cazalilla, R. Citro, T. Giamarchi, E. Orignac, and M. Rigol, Rev. Mod. Phys. **83**, 1405 (2011).
[40] P. Coleman, *Introduction to Many-Body Physics* (Cambridge University Press, 2015).
[41] C. Bartsch, R. Steinigeweg, and J. Gemmer, Phys. Rev. E **77** (2008), 10.1103/physreve.77.011119.
[42] K. Mallayya, M. Rigol, and W. De Roeck, Phys. Rev. X **9** (2019), 10.1103/physrevx.9.021027.

[43] Due to ETH, and the assumption that $\langle A(\infty)\rangle = 0$, one could equivalently write these sums including the terms with $j = k$.

[44] A. Çakan, J. I. Cirac, and M. C. Bañuls, Phys. Rev. B **103** (2021), 10.1103/physrevb.103.115113.

[45] Á. M. Alhambra, J. Riddell, and L. P. García-Pintos, Phys. Rev. Lett. **124**, 110605 (2020).

[46] R. Kubo, Journal of the Physical Society of Japan **12**, 570 (1957).

[47] W. Beugeling, R. Moessner, and M. Haque, Phys. Rev. E **91**, 012144 (2015).

[48] T. LeBlond, K. Mallayya, L. Vidmar, and M. Rigol, Phys. Rev. E **100**, 062134 (2019).

[49] B. Collins and P. Śniady, Communications in Mathematical Physics **264**, 773–795 (2006).

[50] F. G. S. L. Brandão, P. Ćwikliński, M. Horodecki, P. Horodecki, J. K. Korbicz, and M. Mozrzymas, Phys. Rev. E **86**, 031101 (2012).

[51] L. F. Santos, A. Polkovnikov, and M. Rigol, Physical Review E **86** (2012), 10.1103/physreve.86.010102.

[52] W. Beugeling, A. Andreanov, and M. Haque, Journal of Statistical Mechanics: Theory and Experiment **2015**, P02002 (2015).

[53] L. Vidmar and M. Rigol, Physical Review Letters **119** (2017), 10.1103/physrevlett.119.220603.

[54] R. Meir and N. Merhav, Machine Learning **19**, 241 (1995).

[55] T. Liu and R. Bundschuh, Phys. Rev. E **72**, 061905 (2005).

[56] J. S. Cotler, G. Gur-Ari, M. Hanada, J. Polchinski, P. Saad, S. H. Shenker, D. Stanford, A. Streicher, and M. Tezuka, Journal of High Energy Physics **2017**, 1 (2017).

[57] J. Cotler, N. Hunter-Jones, J. Liu, and B. Yoshida, Journal of High Energy Physics **2017** (2017), 10.1007/jhep11(2017)048.

[58] A. Chenu, J. Molina-Vilaplana, and A. del Campo, Quantum **3**, 127 (2019).

[59] Z. Xu, L. P. García-Pintos, A. Chenu, and A. del Campo, Phys. Rev. Lett. **122**, 014103 (2019).

[60] C. L. Baldwin and B. Swingle, Phys. Rev. X **10**, 031026 (2020).

[61] M. Fukuda, R. König, and I. Nechita, Journal of Physics A: Mathematical and Theoretical **52**, 425303 (2019).

[62] S. Popescu, A. J. Short, and A. Winter, Nat. Phys. **2**, 754 (2006).

[63] N. Linden, S. Popescu, A. J. Short, and A. Winter, Phys. Rev. E **79**, 061103 (2009).

[64] H. Wilming, M. Goihl, I. Roth, and J. Eisert, Phys. Rev. Lett. **123**, 200604 (2019).

[65] A. Rolandi and H. Wilming, "Extensive rényi entropies in matrix product states," (2020), arXiv:2008.11764 [quant-ph].

[66] Y. Huang and A. W. Harrow, "Instability of localization in translation-invariant systems," (2020), arXiv:1907.13392 [cond-mat.dis-nn].

[67] J. Haferkamp, C. Bertoni, I. Roth, and J. Eisert, PRX Quantum **2**, 040308 (2021).

[68] Notice that this quantity is very close $\mathrm{Tr}\left[A\mathcal{D}(|\Phi\rangle\langle\Phi|)A\mathcal{D}(|\Phi\rangle\langle\Phi|)\right]$ since they differ only by the $j = k$ terms.

[69] P. Reimann, New. J. Phys. **21**, 053014 (2019).

[70] F. Anza, C. Gogolin, and M. Huber, Phys. Rev. Lett. **120**, 150603 (2018).

[71] L. Campos Venuti and P. Zanardi, Phys. Rev. A **81** (2010), 10.1103/physreva.81.022113.

[72] A. M. Alhambra, A. Anshu, and H. Wilming, Phys. Rev. B **101** (2020), 10.1103/physrevb.101.205107.

[73] J. Cotler and N. Hunter-Jones, J. High Energy Phys. **2020**, 1 (2020).

[74] P. Reimann, New. J. Phys. **12**, 055027 (2010).

[75] L. Knipschild and J. Gemmer, Physical Review E **101** (2020), 10.1103/physreve.101.062205.

[76] S. Goldstein, T. Hara, and H. Tasaki, Phys. Rev. Lett. **111**, 140401 (2013), arXiv:1307.0572.

[77] A. S. L. Malabarba, L. P. García-Pintos, N. Linden, T. C. Farrelly, and A. J. Short, Phys. Rev. E **90**, 012121 (2014).

[78] H. Kim, M. C. Bañuls, J. I. Cirac, M. B. Hastings, and D. A. Huse, Phys. Rev. E **92**, 012128 (2015).

[79] J. Gemmer, M. Michel, and G. Mahler, *Quantum Thermodynamics*, Lecture Notes in Physics.

[80] L. Masanes, A. J. Roncaglia, and A. Acín, Phys. Rev. E **87**, 032137 (2013).

[81] C. Murthy and M. Srednicki, Phys. Rev. Lett. **123**, 230606 (2019).

[82] L. Foini and J. Kurchan, Phys. Rev. E **99**, 042139 (2019).

[83] M. Hartmann, G. Mahler, and O. Hess, Letters in Mathematical Physics **68**, 103 (2004).

[84] F. G. S. L. Brandao and M. Cramer, "Equivalence of statistical mechanical ensembles for non-critical quantum systems," (2015), arXiv:1502.03263 [quant-ph].

[85] I. Arad, T. Kuwahara, and Z. Landau, Journal of Statistical Mechanics: Theory and Experiment **2016**, 033301 (2016).

[86] On the other hand, this function is roughly constant for some range of small frequencies ω. This can be thought of as a consequence of the validity of random matrix theory at late times, after all transport phenomena have dissipated [21, 23, 24].

[87] A. Anshu, New. J. Phys. **18**, 083011 (2016).

[88] O. Shtanko, Y. A. Kharkov, L. P. García-Pintos, and A. V. Gorshkov, "Classical models of entanglement in monitored random circuits," (2020), arXiv:2004.06736 [cond-mat.dis-nn].

[89] G. W. Anderson, A. Guionnet, and O. Zeitouni, *An Introduction to Random Matrices*, Cambridge Studies in Advanced Mathematics (Cambridge University Press, 2009).

APPENDICES

Appendix A: Initial Gaussian decay

Here we explain why we expect $\mathcal{C}(t)$ to decay as a Gaussian for early times, which also implies that it is well approximated by a quadratic function. Similar results should also apply for $\mathcal{C}_{\text{Kubo}}$, as well as for the central quantity $\langle A(t)\rangle$. For the latter, however, the complex coefficients in the expansion Eq. (15) make that analysis far from straightforward.

We follow a method for estimating expectation values based on ETH that can be found in several references [3, 16, 81, 82], and that allows us to transform sums over energy gaps into integrals over frequencies. First, notice the dependence of Eq. (13) on the matrix elements A_{jk}. We can then make use of the ETH ansatz

$$\langle E_j|\, A\,|E_k\rangle \equiv A_{jk} = A(E)\delta_{jk} + e^{-S(E)/2} f(E, E_j - E_k) R_{jk}. \tag{A1}$$

Here, E_j, E_k are energies belonging to the same microcanonical ensemble with energy E. $S(E)$ is the microcanonical entropy of that ensemble, $f(E,\omega)$ is a function that decays monotonically with ω and R_{jk} are the coefficients of a random matrix.

The randomness in Eq. (A1), and the small level spacing in the thermodynamic limit, suggests that we can replace the sums $\sum_{k,j} |c_j|^2|c_k|^2$ in (13) with integrals over the energy sum and differences $\int\int \mathrm{d}E\mathrm{d}\omega e^{\beta_E S(E+\omega)} p(E-\omega/2)p(E+\omega/2)$ [3]. Here $e^{\beta_E S(E)}$ is the density of states at energy E, and β_E is the inverse temperature corresponding to average energy E. The integral is as follows

$$\mathcal{C}(t) - \mathcal{C}(\infty) \propto \int\int \mathrm{d}E\mathrm{d}\omega e^{\beta_E(S(E+\omega)-S(E))} p(E-\omega/2)p(E+\omega/2)|f(E,\omega)|^2 e^{i\omega t}, \tag{A2}$$

where $p(E)$ is the probability of being in energy E, the continuum limit of the coefficients $|c_j|^2$, and $\mathcal{C}(\infty) = \overline{\mathcal{C}}(t)$.

For physically relevant initial states, such as product or shortly-correlated states on lattices, this energy distribution is always close to a Gaussian (see [83, 84] for rigorous statements)

$$p(E) \simeq \frac{1}{\sqrt{2\pi\lambda}} e^{-\frac{(E-\langle H\rangle)^2}{2\lambda^2}}, \tag{A3}$$

where $\langle H\rangle = \langle\Phi|\, H\,|\Phi\rangle$ and $\lambda^2 = \langle\Phi|\, H^2\,|\Phi\rangle - (\langle\Phi|\, H\,|\Phi\rangle)^2$. Typically, $\lambda^2 \sim N$, so that the energy fluctuations are subextensive, and thus the energy density is essentially free of uncertainty. We can then write

$$p(E+\omega/2)p(E-\omega/2) \propto e^{-\frac{(E-\langle H\rangle)^2}{\lambda^2}} e^{-\frac{\omega^2}{2\lambda^2}}. \tag{A4}$$

This means that the energy is highly peaked around the average value, with small fluctuations around it. This fixes the "effective" temperature $\beta_E = \beta_{\langle H\rangle} \equiv \beta$. At the same time, $S(E+\omega)$ can only change significantly if ω changes by an extensive amount. As such, we can approximate $S(E+\omega) - S(E)$ to leading order in ω, obtaining

$$e^{\beta_E(S(E+\omega)-S(E))} \simeq e^{\beta_E \frac{\omega}{2}} = e^{\beta\frac{\omega}{2}}. \tag{A5}$$

Notice that the only dependence left on E is on the function $f(E,\omega)$, which again changes very slowly with E (it should be effectively constant within the same energy density). Putting everything together, we can write

$$\begin{aligned}\mathcal{C}(t) - \mathcal{C}(\infty) &\propto \int \mathrm{d}\omega e^{\beta\frac{\omega}{2}} |f(\langle H\rangle,\omega)|^2 e^{it\omega} e^{-\frac{\omega^2}{2\lambda^2}} \\ &\propto \int \mathrm{d}\omega |f(\langle H\rangle,\omega)|^2 e^{it\omega} e^{-(\frac{\omega}{\sqrt{2}\lambda} - \frac{\beta\lambda}{\sqrt{8}})^2}.\end{aligned} \tag{A6}$$

An extra constraint on the observable is imposed by its locality. This implies that $\mathrm{Tr}\left[\rho A^2\right]$ must be finite and $\mathcal{O}(1)$ for any ρ, and it was argued in [81] [Eq. (12)] that this implies that at large enough ω, f decays at least as fast as

$$f(\langle H\rangle,\omega) \sim e^{-\frac{\beta|\omega|}{4}}. \tag{A7}$$

This exponential decay at large frequencies has been numerically verified in at least [3, 16, 22, 47, 48] (see [27, 85] for mathematically rigorous but weaker statements). It further justifies the approximation in Eq. (A5), since the

integrand will be very suppressed at large ω [86]. Essentially, this means that if we are interested in short times t, for which the high frequencies matter more, we can assume that $f(E,\omega)$ decays like a simple exponential in $|\omega|$. We do not have an estimate for the cut-off frequency or time at which this argument starts to fail, but it is likely some timescale related to the transport processes in the system.

We see then that the integrand *at short times* is just a product of Gaussians and of decaying exponentials, with the Fourier factor $e^{i\omega t}$. We conclude that

$$\int \mathrm{d}\omega e^{-\frac{(\omega-\omega_0)^2}{2\sigma^2}} e^{it\omega} \propto e^{-\sigma^2(t-t_0)^2}, \tag{A8}$$

where ω_0 and σ depend on the details of the function f, and on the constants β and λ.

At the same time, we can see that if we Taylor-expand $\mathcal{C}(t)$ and write it as in Eq. (13), we have

$$\begin{aligned}\mathcal{C}(t) &= 1 - \frac{t^2}{2}\frac{\sum_{j,k}|c_j|^2|c_k|^2|A_{jk}|^2(E_k-E_j)^2}{\sum_{j,k}|c_j|^2|c_k|^2|A_{jk}|^2} + \mathcal{O}\left(t^3\right) \\ &= 1 - \frac{\sigma_G^2 t^2}{2} + \mathcal{O}\left(t^3\right),\end{aligned} \tag{A9}$$

where we have defined

$$\sigma_G^2 := \frac{\sum_{j,k}|c_j|^2|c_k|^2|A_{jk}|^2(E_k-E_j)^2}{\sum_{j,k}|c_j|^2|c_k|^2|A_{jk}|^2}. \tag{A10}$$

Given the form of (A8), this shows that the initial decay constant is $\sigma = \sigma_G$ and $t_0 = 0$, which is confirmed by our numerical examples.

A similar argument can be also done for the Gaussianity of the early-time decay of $\langle A(t)\rangle$ (e.g. see [28]), with the extra potential difficulty of the *relative phases* of the complex c_j, A_{jk}. Our numerical calculations support the conclusion that both $\mathcal{C}(t)$ and $\langle A(t)\rangle$ decay as Gaussians at early times.

Appendix B: Upper bound on the rate of change of $\mathcal{C}(t)$

From Eq. (13) in the main text we have that

$$\left|\frac{d\mathcal{C}(t)}{dt}\right| = \frac{1}{\sum_{jk}|c_j|^2|c_k|^2|A_{jk}|^2}\left|\sum_{j\neq k}|c_j|^2|c_k|^2|A_{jk}|^2 e^{it(E_j-E_k)}(E_j-E_k)\right|. \tag{B1}$$

Using the Cauchy-Schwarz inequality and Eq. (14) in the main text gives that

$$\begin{aligned}\left|\sum_{j\neq k}|c_j|^2|c_k|^2|A_{jk}|^2 e^{it(E_j-E_k)}(E_j-E_k)\right|^2 &\leq \sum_{j\neq k}|c_j|^2|c_k|^2|A_{jk}|^2 \sum_{j\neq k}|c_j|^2|c_k|^2|A_{jk}|^2(E_j-E_k)^2 \\ &\leq \left(\sum_{jk}|c_j|^2|c_k|^2|A_{jk}|^2\right)^2 \sigma_G^2.\end{aligned} \tag{B2}$$

Thus,

$$\left|\frac{d\mathcal{C}(t)}{dt}\right| \leq \sigma_G. \tag{B3}$$

This bounds the rate of change of $\mathcal{C}(t)$ by its short time decay rate σ_G, and this holds at all times t.

Appendix C: Upper bound on the equilibration timescale of $\mathcal{C}(t)$

Defining $\mathcal{C}(\infty) \coloneqq \overline{\mathcal{C}(t)} = \mathcal{D}(|\Phi\rangle\langle\Phi|)$, we have

$$\mathcal{C}(t) - \mathcal{C}(\infty) = \frac{\sum_{j\neq k} |c_j|^2|c_k|^2|A_{jk}|^2 e^{it(E_j-E_k)}}{\sum_{j,k} |c_j|^2|c_k|^2|A_{jk}|^2} \tag{C1}$$

$$= \frac{\sum_{j\neq k} |c_j|^2|c_k|^2|A_{jk}|^2 e^{it(E_j-E_k)}}{\mathrm{Tr}\left[\mathcal{D}(|\Phi\rangle\langle\Phi|)A\mathcal{D}(|\Phi\rangle\langle\Phi|)A\right]}. \tag{C2}$$

Let us denote the normalized distribution $q_\alpha \coloneqq \frac{1}{K}|c_j|^2|c_k|^2|A_{jk}|^2$, where $\alpha = (j,k)$ denotes pairs of energy levels and $K \coloneqq \mathrm{Tr}\left[\mathcal{D}(|\Phi\rangle\langle\Phi|)A^\dagger\mathcal{D}(|\Phi\rangle\langle\Phi|)A\right]$. Then, we can write

$$\langle|\mathcal{C}(t) - \mathcal{C}(\infty)|^2\rangle_T = \sum_{\alpha,\beta} q_\alpha q_\beta \left\langle e^{-it(G_\alpha - G_\beta)}\right\rangle_T, \tag{C3}$$

where $\langle f(t)\rangle_T \coloneqq \frac{1}{T}\int_0^T f(t)dt$ denotes time average.

Lemma 2 of [45] and Proposition 5 of [9] imply that

$$\langle|\mathcal{C}(t) - \mathcal{C}(\infty)|^2\rangle_T \leq 3\pi\left(\frac{a(\epsilon)}{\sigma_G T} + \delta(\epsilon)\right). \tag{C4}$$

Here, $a(\epsilon)$ and $\delta(\epsilon)$ are functions of energy gaps that depend on the form of the distribution q_α, and therefore depend on the observable, initial state, and Hamiltonian of the system. One can argue that, typically, one can find ϵ such that $a(\epsilon) \sim 1$ and $\delta(\epsilon) \ll 1$ for generic many-body systems (see [9, 45] for more details, and [12] for a discussion of cases when this condition may not hold).

The variance of the energy gaps G_α with respect to the distribution q_α is given by

$$\sigma_G^2 = \frac{1}{K}\sum_{jk} |c_j|^2|c_k|^2|A_{jk}|^2(E_j - E_k)^2 \tag{C5}$$

$$= \frac{\mathrm{Tr}\left[\mathcal{D}(|\Phi\rangle\langle\Phi|)[A,H]\mathcal{D}(|\Phi\rangle\langle\Phi|)[H,A]\right]}{\mathrm{Tr}\left[\mathcal{D}(|\Phi\rangle\langle\Phi|)A\mathcal{D}(|\Phi\rangle\langle\Phi|)A\right]}, \tag{C6}$$

and when $a(\epsilon) \sim 1$ it dominates the approach to equilibrium of $\mathcal{C}(t)$. Note that this matches the short-time decay rate (Eq. (14)) as well as the fastest rate of change of the correlation function (Eq. (B3)).

Appendix D: The Kubo function and $\mathcal{C}(t)$

Making use of the ETH ansatz as in Eq. (A2), we obtain that, for the Kubo function in Eq. (16),

$$\mathcal{C}_{\mathrm{Kubo}}(t) \propto \int \mathrm{d}E \int \mathrm{d}\omega e^{\beta_E S(E+\omega)} e^{-\beta_E S(E)} |f(E,\omega)|^2 e^{i\omega t} \frac{\sinh(\frac{\beta\omega}{2})}{\omega} e^{-\beta E}. \tag{D1}$$

The integrand is thus proportional to the Gibbs distribution $e^{-\beta E}$. In most situations, this is very peaked around the average energy $\langle H\rangle$ [87], in the same way as above for the initial pure states are (since both are states with short-range correlations). This means that the typical energy fluctuations are subextensive, and the system has a well defined energy density. As such, we can treat it in the same way as the diagonal distribution in Eq. (A3): effectively a Dirac δ function centered at the average energy $\langle H\rangle$. Moreover, as in Eq. (A5), we can approximate $e^{\beta_E(S(E+\omega)-S(E))} \simeq e^{\beta_E \frac{\omega}{2}}$ and write

$$\mathcal{C}_{\mathrm{Kubo}}(t) \propto \int \mathrm{d}\omega e^{\beta\frac{\omega}{2}} |f(\langle H\rangle,\omega)|^2 e^{i\omega t} \frac{\sinh(\frac{\beta\omega}{2})}{\omega}. \tag{D2}$$

Notice that the difference between Eq. (D2) and Eq. (A6) is only on the last factor, and that for small ω,

$$\frac{\sinh(\frac{\beta\omega}{2})}{\omega} \simeq 1 + \mathcal{O}(\beta^2\omega^2) \tag{D3}$$

$$e^{-\frac{\omega^2}{2\lambda^2}} \simeq 1 + \mathcal{O}\left(\frac{\omega^2}{\lambda^2}\right). \tag{D4}$$

Thus, if the function f decays quickly on an energy scale of $\omega \sim W$, we expect that

$$\mathcal{C}(t) \simeq \mathcal{C}_{\text{Kubo}}(t) + \mathcal{O}(\beta^2 W^2) + \mathcal{O}\left(\frac{W^2}{\lambda^2}\right). \tag{D5}$$

This is the conclusion of [15]. That this is the case, and that these two functions coincide, has been verified in at least [16, 22, 48]. There, it is shown that $f(E,\omega)$ is constant for some small interval around $\omega = 0$, and then quickly decays in an exponential fashion. We provide further evidence within our setting in Sec. V.

Appendix E: Upper bound on the rate of change of $\mathrm{C}_{\mathbf{Kubo}}(t)$

From Eq. (16) in the main text, we have that the rate of change of the Kubo correlation function satisfies

$$\left|\frac{d\,\mathcal{C}_{\text{Kubo}}(t)}{dt}\right| = \frac{1}{\mathcal{C}_{\text{Kubo}}(0)}\left|\sum_{j\neq k}\frac{e^{-\beta E_j}-e^{-\beta E_k}}{E_k-E_j}|A_{jk}|^2 e^{i(E_j-E_k)t}(E_j-E_k)\right|. \tag{E1}$$

The Cauchy-Schwarz inequality implies that

$$\begin{aligned}\left|\sum_{j\neq k}\frac{e^{-\beta E_j}-e^{-\beta E_k}}{E_k-E_j}|A_{jk}|^2 e^{i(E_j-E_k)t}(E_j-E_k)\right|^2 &\leq \left|\sum_{j\neq k}\frac{e^{-\beta E_j}-e^{-\beta E_k}}{E_k-E_j}|A_{jk}|^2\right|\left|\sum_{j\neq k}\frac{e^{-\beta E_j}-e^{-\beta E_k}}{E_k-E_j}|A_{jk}|^2(E_j-E_k)^2\right| \\ &= \mathcal{C}_{\text{Kubo}}(0)\left|\sum_{j\neq k}\left(e^{-\beta E_j}-e^{-\beta E_k}\right)|A_{jk}|^2(E_j-E_k)\right| \\ &= \mathcal{C}^2_{\text{Kubo}}(0)\,\sigma_K^2,\end{aligned} \tag{E2}$$

where we used the definition of σ_K, Eq. (17) in the main text.

Therefore,

$$\left|\frac{d\,\mathcal{C}_{\text{Kubo}}(t)}{dt}\right| \leq \sigma_K, \tag{E3}$$

as claimed in the main text.

Appendix F: Decay rates for random Hamiltonians

We focus on a model of a quantum system in which the eigenbasis of the Hamiltonian is chosen randomly as $H_U = UHU^\dagger$, where we average over U drawn from the Haar measure on the unitary group. We now calculate the rates analyzed in the main text, by performing analytical calculations consisting on those Haar averages, and show that for typical random Hamiltonians, the timescales coincide. These calculations are done with the Mathematica package RTNI [61].

For a given state $|\Psi\rangle$ and observable A, we can write the decay rates as

$$\sigma_A^2 = -\frac{\langle[H_U,[H_U,A]]\rangle}{\langle A(0)\rangle}, \tag{F1}$$

$$\sigma_G^2 = \frac{\mathrm{Tr}\left[\mathcal{D}_U(|\Phi\rangle\langle\Phi|)[A,H_U]\mathcal{D}_U(|\Phi\rangle\langle\Phi|)[H_U,A]\right]}{\mathrm{Tr}\left[(\mathcal{D}_U(|\Phi\rangle\langle\Phi|)A)^2\right]}, \tag{F2}$$

where if $H = \sum_j E_j\,|E_j\rangle\,\langle E_j|$, the dephasing in the random eigenbasis is defined as

$$\mathcal{D}_U(|\Phi\rangle\langle\Phi|) = \sum_j U\,|E_j\rangle\,\langle E_j|\,U^\dagger|\Phi\rangle\langle\Phi|U\,|E_j\rangle\,\langle E_j|\,U^\dagger. \tag{F3}$$

For the Kubo function, we consider the limit $\beta \to 0$, which is such that

$$\lim_{\beta\to 0}\frac{\mathcal{C}_{\text{Kubo}}(t)}{\mathcal{C}_{\text{Kubo}}(0)} = \frac{\mathrm{Tr}\left[A(t)A\right]}{\mathrm{Tr}\left[A^2\right]}, \tag{F4}$$

and thus in this model we have the corresponding rate

$$\sigma_K^2 = \frac{\mathrm{Tr}\left[[H_U, A][A, H_U]\right]}{\mathrm{Tr}\left[A^2\right]}. \tag{F5}$$

Denoting the Haar average $\int_{\mathrm{Haar}} \cdot \, \mathrm{d}U = \langle\cdot\rangle_U$, let us first calculate $\langle\sigma_A^2\rangle_U$.

$$\langle\sigma_A^2\rangle_U = -\left\langle \frac{\langle[H_U,[H_U,A]]\rangle}{\langle A(0)\rangle}\right\rangle_U \tag{F6}$$

$$= -\frac{1}{\langle A(0)\rangle}\Big(\Big\langle \mathrm{Tr}\left[|\Phi\rangle\langle\Phi|H_U^2 A\right] + \mathrm{Tr}\left[|\Phi\rangle\langle\Phi|AH_U^2\right] - 2\,\mathrm{Tr}\left[|\Phi\rangle\langle\Phi|H_U A H_U\right]\Big\rangle_U\Big). \tag{F7}$$

Since the Hamiltonian appears twice, this sum of expectation values is computed with the first and second moments of the Haar measure. The result, to leading order in the inverse of the system's dimension d^{-1}, is

$$\langle\sigma_A^2\rangle_U = 2\left(\langle H^2\rangle_{\mathrm{MC}} - \langle H\rangle_{\mathrm{MC}}^2\right)\frac{\left(\langle A(0)\rangle - \langle A\rangle_{\mathrm{MC}}\right)}{\langle A(0)\rangle} + \mathcal{O}\left(\frac{1}{d^2}\right), \tag{F8}$$

where $\langle A\rangle_{\mathrm{MC}} = \frac{\mathrm{Tr}[A]}{d}$ is the microcanonical average. Notice that our assumption of $\mathrm{Tr}\left[\mathcal{D}(|\Phi\rangle\langle\Phi|)A\right] = 0$ from the main text here translates to $\langle A\rangle_{\mathrm{MC}} = 0$.

Now we calculate the other rate, which is significantly more involved. It reads

$$\langle\sigma_G^2\rangle_U = \left\langle \frac{\mathrm{Tr}\left[\mathcal{D}_U(|\Phi\rangle\langle\Phi|)[A,H_U]\mathcal{D}_U(|\Phi\rangle\langle\Phi|)[H_U,A]\right]}{\mathrm{Tr}\left[(\mathcal{D}_U(|\Phi\rangle\langle\Phi|)A)^2\right]}\right\rangle_U. \tag{F9}$$

As a first simplification, we use the so-called "annealed approximation", which states that we can approximate the average of the ratio is similar to the ratio of the averages

$$\langle\sigma_G^2\rangle_U \simeq \frac{\langle\mathrm{Tr}\left[\mathcal{D}_U(|\Phi\rangle\langle\Phi|)[A,H_U]\mathcal{D}_U(|\Phi\rangle\langle\Phi|)[H_U,A]\right]\rangle_U}{\langle\mathrm{Tr}\left[(\mathcal{D}_U(|\Phi\rangle\langle\Phi|)A)^2\right]\rangle_U}. \tag{F10}$$

As explained in Appendix G below, this approximation can be made rigorous through concentration arguments and Levy's lemma. Let us now calculate the numerator and denominator separately. If we decompose the dephased states as in Eq. (F3), and define $U|E_j\rangle\langle E_j|U^\dagger \equiv P_U^j$, the numerator of Eq. (F10) is

$$\sum_{j,k} 2\left\langle \mathrm{Tr}\left[P_U^j|\Phi\rangle\langle\Phi|P_U^j A H_U P_U^k|\Phi\rangle\langle\Phi|P_U^k H_U A\right]\right\rangle_U \tag{F11}$$

$$-\left\langle \mathrm{Tr}\left[P_U^j|\Phi\rangle\langle\Phi|P_U^j H_U A P_U^k|\Phi\rangle\langle\Phi|P_U^k H_U A\right]\right\rangle_U \tag{F12}$$

$$-\left\langle \mathrm{Tr}\left[P_U^j|\Phi\rangle\langle\Phi|P_U^j A H_U P_U^k|\Phi\rangle\langle\Phi|P_U^k A H_U\right]\right\rangle_U. \tag{F13}$$

Due to cancellations of some of the unitaries, these three correlators involve at most four pairs $\{U, U^\dagger\}$, and can thus be calculated with the fourth moment of the Haar measure. Because of this, it is an analytical expression with $3\times 4!^2 = 1728$ terms, for which then the sum over j,k has to be taken. This sum can then be simplified to

$$2\frac{\left(\langle H^2\rangle_{\mathrm{MC}} - \langle H\rangle_{\mathrm{MC}}^2\right)}{(d-1)(d+1)(d+2)(d+3)}\times \tag{F14}$$

$$\Big(2\left(d^2-1\right)\langle A(0)^2\rangle + \langle A(0)\rangle^2\left(d^2+d+2\right) - 2\langle A(0)\rangle\langle A\rangle_{\mathrm{MC}} d(3d+1) + d\left((d+1)^2\langle A^2\rangle_{\mathrm{MC}} - \langle A\rangle_{\mathrm{MC}}^2(d-1)d\right)\Big).$$

The denominator on the other hand consists of a single correlator, which can be written as

$$\sum_{j,k}\mathrm{Tr}\left[P_U^j|\Phi\rangle\langle\Phi|P_U^j A P_U^k|\Phi\rangle\langle\Phi|P_U^k A\right]. \tag{F15}$$

This still requires the 4th moment of the Haar measure, and involves $4!^2 = 576$ terms. With the sums over j,k, they simplify to the expression

$$\frac{1}{d(d+1)(d+2)(d+3)}\Big(d\left(\langle A\rangle_{\mathrm{MC}}^2 d(d+1) + d(d+4)\langle A\rangle_{\mathrm{MC}}^2 + 2(d+4)\langle A(0)^2\rangle + \langle A\rangle_{\mathrm{MC}}^2\right) \tag{F16}$$

$$+\langle A(0)\rangle^2(d(d+5)+2) + 2\langle A(0)\rangle\langle A\rangle_{\mathrm{MC}}(d-1)d + -2\langle A(0)^2\rangle\Big).$$

Now, with the denominator and numerator, their ratio to leading order yields the average rate

$$\langle \sigma_G^2 \rangle_U \simeq 2\left(\langle H^2\rangle_{\rm MC} - \langle H\rangle^2_{\rm MC}\right)\frac{\langle A(0)\rangle - \langle A\rangle_{\rm MC}}{\langle A(0)\rangle} + \mathcal{O}\left(\frac{1}{d}\right). \tag{F17}$$

We end with the computation of the Kubo decay rate

$$\langle \sigma_K^2 \rangle_U = \frac{2}{{\rm Tr}\left[A^2\right]}\left(\langle {\rm Tr}\left[H_U A H_U A - A^2 H_U^2\right]\rangle_U\right). \tag{F18}$$

This again only requires the second moment of the Haar measure, from which it follows that

$$\langle \sigma_K^2 \rangle_U = 2d^2\frac{(\langle A^2\rangle_{\rm MC} - \langle A\rangle^2_{\rm MC})(\langle H^2\rangle_{\rm MC} - \langle H\rangle^2_{\rm MC})}{(d^2-1)\langle A^2\rangle_{\rm MC}} \tag{F19}$$

$$= 2\left(1 - \frac{\langle A\rangle^2_{\rm MC}}{\langle A^2\rangle_{\rm MC}}\right)\left(\langle H^2\rangle_{\rm MC} - \langle H\rangle^2_{\rm MC}\right) + \mathcal{O}\left(\frac{1}{d^2}\right). \tag{F20}$$

We can now compare Eq. (F8), Eq. (F17) and Eq. (F19). We see that when we set the thermal or long-time value to zero $\langle A\rangle_{\rm MC} = 0$ (as discussed in the main text, this is necessary to compare them given the definition of the correlation functions), the three timescales coincide up to leading order

$$\langle \sigma_G^2 \rangle_U \simeq \langle \sigma_A^2 \rangle_U + \mathcal{O}\left(\frac{1}{d}\right) = \langle \sigma_K^2 \rangle_U + \mathcal{O}\left(\frac{1}{d}\right) = 2\Big(\langle H^2\rangle_{\rm MC} - \langle H\rangle^2_{\rm MC}\Big) + \mathcal{O}\left(\frac{1}{d}\right). \tag{F21}$$

This is the energy variance in the microcanonical distribution of the Hamiltonian H.

Appendix G: The annealed approximation

In Eq. (F10) we assumed that the average of the ratio of the correlators is approximately equal to the ratio of their averages. This has been previously referred to in the literature as the "annealed" approximation [54–60, 88]. Its general form is as follows. Given two functions two functions $f, g : U(d) \to \mathcal{R}$, such that $g(U) > 0$, then

$$\left\langle \frac{f}{g} \right\rangle_U \simeq \frac{\langle f\rangle_U}{\langle g\rangle_U} \tag{G1}$$

We now show why concentration bounds imply that this approximation is very often accurate. For the two functions f, g, let us write

$$\langle f\rangle_U = \int_{\rm Haar} {\rm d}U f(U) = \int_{\rm Haar} {\rm d}U \frac{f(U)}{g(U)} g(U). \tag{G2}$$

Defining the deviation $g(U) = \langle g\rangle_U + \delta_U$, we write

$$\langle f\rangle_U = \int_{\rm Haar} {\rm d}U \frac{f(U)}{g(U)} g(U) = \left\langle \frac{f}{g} \right\rangle_U \langle g\rangle_U + \int_{\rm Haar} {\rm d}U \frac{f(U)}{g(U)} \delta_U. \tag{G3}$$

We thus need to show that the second term is small. To do so, let us define the following quantities

$$K_1 \equiv \max_U \left|\frac{f(U)}{g(U)}\right|, \tag{G4}$$

$$K_2 \equiv \frac{\max_U g(U)}{\langle g\rangle_U}, \tag{G5}$$

$$K_3 \equiv \min\left\{K : \forall U, V \ \frac{|g(U) - g(V)|}{\langle g\rangle_U} \leq K||U - V||_2\right\}. \tag{G6}$$

The first two are the results of optimizations, and the last is the Lipschitz constant of $g(U)/\langle g\rangle_U$. We now divide the Haar average into two and bound

$$\left|\int_{\rm Haar} {\rm d}U \frac{f(U)}{g(U)}\delta_U\right| \leq \left|\int_{|\delta_U|\leq\varepsilon} {\rm d}U \frac{f(U)}{g(U)}\delta_U\right| + \left|\int_{|\delta_U|>\varepsilon} {\rm d}U \frac{f(U)}{g(U)}\delta_U\right| \tag{G7}$$

$$\leq \varepsilon K_1 + K_1 K_2 \langle g\rangle_U \times {\rm Prob}(|\delta_U| > \varepsilon). \tag{G8}$$

The second term can be upper bounded with Levy's lemma for the Haar distribution [89], which states that

$$\mathrm{Prob}(|\delta_U| > \varepsilon) \leq \exp\left(-\frac{d\varepsilon^2}{4\langle g\rangle_U K_3}\right). \tag{G9}$$

This finally allows us to write, from Eq. (G3),

$$\left\langle \frac{f}{g} \right\rangle_U = \frac{\langle f\rangle_U}{\langle g\rangle_U} + \varepsilon', \tag{G10}$$

where $|\varepsilon'| \leq K_1\left(\frac{\varepsilon}{\langle g\rangle_U} + K_2 \exp\left(-\frac{d\varepsilon^2}{4K_3}\right)\right)$. For instance, under the assumption that $K_1, K_2, K_3 \leq \mathcal{O}(\mathrm{polylog}(d))$, choosing $\varepsilon = \langle g\rangle_U d^{-1/2} \times \mathrm{polylog}(d)$ yields the bound $\varepsilon' \leq \mathrm{poly}(d^{-1})$.

In our case, we have

$$f(U) = \mathrm{Tr}\left[\mathcal{D}_U(|\Phi\rangle\langle\Phi|)[A, H_U]\mathcal{D}_U(|\Phi\rangle\langle\Phi|)[H_U, A]\right] \tag{G11}$$

$$g(U) = \mathrm{Tr}\left[(\mathcal{D}_U(|\Phi\rangle\langle\Phi|)A)^2\right]. \tag{G12}$$

The assumption that $g(U) > 0$ holds here since $g(U)$ it is a trace of two positive matrices $\mathcal{D}_U(|\Phi\rangle\langle\Phi|)$ and $A\mathcal{D}_U(|\Phi\rangle\langle\Phi|)A$. To prove a more explicit bound on the error of the annealed approximation, one needs to give upper bounds on the constants K_i, which can in principle be obtained from the explicit expressions of $f(U)$ and $g(U)$. The assumption that $K_i \leq \mathcal{O}(\mathrm{polylog}(d))$ is likely to be satisfied in this case, since it requires that those constants grow at most polynomially in the system size.

Chapter 4

Concentration of quantum equilibration and an estimate of the recurrence time

Concentration of quantum equilibration and an estimate of the recurrence time

Jonathon Riddell,[1,2,*] Nathan J. Pagliaroli,[3,†] and Álvaro M. Alhambra[4,‡]

[1] *Department of Physics & Astronomy, McMaster University, 1280 Main St. W., Hamilton ON L8S 4M1, Canada.*
[2] *Perimeter Institute for Theoretical Physics, Waterloo, ON N2L 2Y5, Canada*
[3] *Department of Mathematics, Western University, 1151 Richmond St, London ON N6A 3K7, Canada*
[4] *Max-Planck-Institut für Quantenoptik, Hans-Kopfermann-Straße 1, D-85748 Garching, Germany*

(Dated: June 27, 2022)

We show that the dynamics of generic quantum systems concentrate around their equilibrium value when measuring at arbitrary times. This means that the probability of finding such values away from that equilibrium is exponentially suppressed, with a decay rate given by the effective dimension. Our result allows us to place a lower bound on the recurrence time of quantum systems, since recurrences corresponds to the rare events of finding a state away from equilibrium. In many-body systems, this bound is doubly exponential in system size. We also show corresponding results for free fermions, which display a weaker concentration and earlier recurrences.

I. INTRODUCTION

Closed quantum systems obey the Schrödinger equation, so that their dynamics are both unitary and reversible. Most large systems seem to quickly evolve towards a steady state for long times, with only very small out-of-equilibrium fluctuations around it. This process is usually called *equilibration*, and is associated with the emergence of statistical physics [1, 2]. The equilibrated or average expectation value of an observable A is

$$\langle A(\infty)\rangle = \lim_{T\to\infty}\int_0^T \frac{\mathrm{d}t}{T}\langle A(t)\rangle, \tag{1}$$

where $\langle A(t)\rangle = \langle\Psi| e^{-iHt}Ae^{iHt}|\Psi\rangle$ for some initial state Ψ and Hamiltonian H.

If a system equilibrates, it is because the probability of finding $\langle A(t)\rangle$ very close to $\langle A(\infty)\rangle$ at any given time is overwhelmingly large. We show that this is indeed the case: the dynamics of quantum systems with a *generic* spectrum concentrate highly around the steady-state value $\langle A(\infty)\rangle$.

More specifically, we show that when sampling times at random $t \in [0,\infty)$ the probability of finding the system away from equilibrium is exponentially suppressed. The decay rate of that exponential is given by the *effective dimension* or *inverse participation ratio*. This is defined as $\mathrm{Tr}\left[\omega^2\right]^{-1}$, where ω is the diagonal ensemble

$$\omega = \lim_{T\to\infty}\int_0^T \frac{\mathrm{d}t}{T}e^{-iHt}|\Psi\rangle\langle\Psi|e^{iHt}, \tag{2}$$

which is such that $\mathrm{Tr}\left[A\omega\right] = \langle A(\infty)\rangle$.

That this equilibration happens, leaving little or no memory from the initial conditions, seems to conflict with the unitarity and reversibility of the dynamics. This conflict can be seen by considering the Poincaré recurrence theorem in quantum mechanics [3–7], which states that any closed quantum evolution eventually returns arbitrarily close to its initial state.

The solution to this problem is that even if the initial state is eventually recovered to an arbitrarily good approximation, this only happens at extremely long times. These recurrences constitute large out-of-equilibrium fluctuations, that can be understood as the rare events of finding a system far from its equilibrated state.

Based on this idea, we show how a lower bound on the average spacing between recurrences follows from our concentration results, as the inverse of the tail bound. We find that recurrences occur at time intervals that are at least exponential in the effective dimension. This gives, for the first time, a mathematically rigorous scaling on the average recurrence time, that matches the scaling of previous estimates [8, 9]. See [10, 11] for other results.

We also show equivalent results for free fermion Hamiltonians with generic single-particle modes. We find that under the assumption of extensivity in the single particle eigenstates a similar concentration bound and recurrence time result hold, but with a slower exponential scaling on the lattice size. This shows the markedly different behaviour with respect to generic models. See Table I for a summary.

Our results constitute a qualitative improvement over previous bounds on out-of-equilibrium fluctuations [12–14] for systems with a generic spectrum. These only focused on the variance induced by the probability measure $\lim_{T\to\infty}\int_0^T \frac{\mathrm{d}t}{T}$, while we are able to analyze arbitrarily high moments thereof. The improvement is exponential in the same sense in which the Chernoff-Hoeffding bound is exponentially better than Chebyshev's inequality.

* riddeljp@mcmaster.ca
† npagliar@uwo.ca
‡ alvaro.alhambra@mpq.mpg.de

	$\langle A(t)\rangle$	$\lvert\langle\Psi\rvert e^{-itH}\lvert\Psi\rangle\rvert^2$
Generic	$e^{\Omega\left(\mathrm{Tr}[\omega^2]^{-1/2}\right)}$	$e^{\Omega\left(\mathrm{Tr}[\omega^2]^{-1}\right)}$
Free	$e^{\Omega(\sqrt{L})}$	$e^{\Omega(L)}$

TABLE I. Lower bounds on the recurrence time for different dynamical quantities. $\mathrm{Tr}\left[\omega^2\right]^{-1}$ is the effective dimension of a generic system and L is the number of sites in a fermionic lattice. In the free case, the observable and initial state are restricted to specific forms. See Sec. IV for the precise statements.

II. THE CONCENTRATION BOUND

We consider functions of time $f(t)$ that track some physical property of interest. In the cases here, $f(t) = \langle A(t)\rangle$ is the expectation value of a time-evolved operator $A(t)$. This allows us to define the moments of a probability distribution

$$f(\infty) \equiv \lim_{T\to\infty}\int_0^T \frac{\mathrm{d}t}{T} f(t), \tag{3}$$

$$\kappa_q \equiv \lim_{T\to\infty}\int_0^T \frac{\mathrm{d}t}{T}\left(f(t)-f(\infty)\right)^q. \tag{4}$$

These moments are bounded for arbitrary q as $\kappa_q \leq (2||A||)^q$. This means that they uniquely determine a characteristic function with an infinite radius of convergence

$$\phi(\lambda) = \sum_q \frac{k_q \lambda}{q!}. \tag{5}$$

This function defines a probability distribution, which we can write formally as

$$P(x) = \lim_{T\to\infty}\int_0^T \frac{\mathrm{d}t}{T}\delta(x-f(t)). \tag{6}$$

Here $P(x)$ should be understood as the probability that, if we pick a random time $t \in [0,\infty)$, the value of $f(t)$ is exactly x (see also [15] and [16] for an overview of previous results). Note that in order to compute $\int x^q P(x)dx$ the limit in T is swapped with the integral in x. For justification of this see Appendix A. An example of $P(x)$ forming for $f(t) = \langle A(t)\rangle$ is given in Fig. 1.

Below we prove that the moments κ_q are bounded by

$$\kappa_q \leq (qg)^q, \tag{7}$$

where g is some small quantity, decreasing quickly as the size of the system grows and such that $g \to 0$ in the thermodynamic limit. A bound of this form implies that the distribution concentrates highly around the average, as per the following elementary lemma.

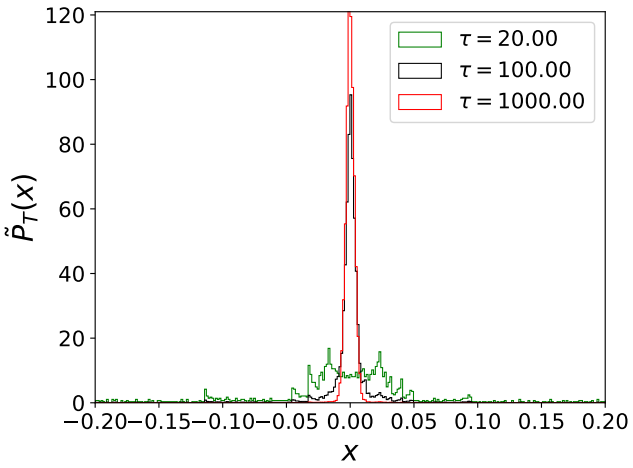

FIG. 1. Convergence of $P_T(x)$ to $P(x)$ where $P_T(x) = \int_0^T \frac{\mathrm{d}t}{T}\delta(x-\langle A(t)\rangle)$ and $P(x)$ is recovered as $T\to\infty$. $\tilde{P}_T(x)$ represents the approximation of $P_T(x)$ by binning samples and constructing a histogram. 1000 bins were used to create this histogram. Numerics were performed on a spin 1/2 chain with 22 sites. The data is normalized such that $\int_{-\infty}^{\infty}\tilde{P}_T(x)dx = 1$. The Hamiltonian is a Heisenberg type model with nearest and next nearest neighbour interactions. Further details can be found in Appendix D.

Lemma 1. *Let $|\kappa_q| \leq (qg)^q$ for q even. Then,*

$$\Pr\left[\left|f(t)-f(\infty)\right| \geq \delta\right] \leq 2e \times \exp\left(-\frac{\delta}{eg}\right). \tag{8}$$

Proof. Let us set $f(\infty) = 0$ for simplicity, and focus on the case $x \geq \delta$. We have that

$$\Pr\left[\langle A(t)\rangle \geq \delta\right] = \int_{x\geq\delta} P(x)\mathrm{d}x \tag{9}$$

$$\leq \frac{1}{\delta^q}\int_{x\geq\delta} x^q P(x)\mathrm{d}x \tag{10}$$

$$\leq \frac{\kappa_q}{\delta^q} \tag{11}$$

$$\leq \left(\frac{qg}{\delta}\right)^q. \tag{12}$$

A similar inequality holds for $x \leq -\delta$, so that $\Pr\left[\left|f(t)\right| \geq \delta\right] \leq 2\left(\frac{qg}{\delta}\right)^q$. The bound is obtained by choosing $q = \lfloor\frac{\delta}{eg}\rfloor$. □

We now simply need to find the corresponding g for the concentration bound to hold, which we do for various physical problems.

III. MODELS AND THEIR MOMENTS

A. Generic models

First we consider models governed by a Hamiltonian $H = \sum_{m=1}^{D} E_m|E_m\rangle\langle E_m|$, which we assume to have a

discrete and *generic* spectrum.

Definition 1. *Let H be a Hamiltonian with spectrum $H = \sum_j E_j |E_j\rangle\langle E_j|$, and let Λ_q, Λ'_q be two arbitrary sets of q energy levels $\{E_j\}$. H is generic if for all $q \in \mathbb{N}$ and all Λ_q, Λ'_q, the equality*

$$\sum_{j\in\Lambda_q} E_j = \sum_{j\in\Lambda'_q} E_j \tag{13}$$

implies that $\Lambda_q = \Lambda'_q$.

This condition is expected to hold in non-integrable and chaotic models, such as those with Wigner-Dyson level statistics [17]. It is an extension of the well-known non-degenerate gaps condition, which is the $q = 2$ case [1]. Notably, the probability of uniformly choosing a non-generic Hamiltonian is zero, as seen in the following lemma.

Lemma 2. *For any positive integer $d \geq 2$, the set of $d \times d$ complex Hermitian matrices that are not generic has Lebesgue measure zero.*

The proof is a straightforward generalization of the $q = 2$ case in [18] and can be found in Appendix B.

Consider $f(t) = \langle\psi|A(t)|\psi\rangle$ to be the pure state time evolution of some observable A. The first concentration result is as follows.

Theorem 1. *Let H be a generic non-integrable Hamiltonian, ω the diagonal ensemble, and $||A||$ the largest singular value of A. The moments in Eq. 1 are such that*

$$\kappa_q \leq \left(q||A||\sqrt{\mathrm{Tr}[\omega^2]}\right)^q. \tag{14}$$

We thus have the bound

$$\begin{aligned}&\Pr\left[\left|\langle A(t)\rangle - \langle A(\infty)\rangle\right| \geq \delta\right] \\ &\leq 2e \times \exp\left(-\frac{\delta}{e||A||\sqrt{\mathrm{Tr}[\omega^2]}}\right).\end{aligned} \tag{15}$$

This states that the probability of finding $\langle A(t)\rangle$ away from $\langle A(\infty)\rangle$ even by a small amount is exponentially suppressed in $\sqrt{\mathrm{Tr}[\omega^2]}$. Previous results [12, 19] only yield the bound

$$\Pr\left[\left|\langle A(t)\rangle - \langle A(\infty)\rangle\right| \geq \delta\right] \leq \frac{||A||^2\mathrm{Tr}[\omega^2]}{\delta^2}. \tag{16}$$

A particular observable of interest is the initial state itself, $A = |\Psi\rangle\langle\Psi|$. In this case, the quantity at hand is the fidelity with the initial state

$$F(t) = \langle\Psi| e^{-itH} |\Psi\rangle \langle\Psi| e^{itH} |\Psi\rangle. \tag{17}$$

Theorem 2. *Let H be generic and let $A = |\Psi\rangle\langle\Psi|$, then*

$$\kappa_q \leq \left(q\,\mathrm{Tr}\left[\omega^2\right]\right)^q. \tag{18}$$

Notably, assuming a generic Hamiltonian, the average fidelity is $F(\infty) = \mathrm{Tr}\left[\omega^2\right]$, so that we have the concentration bound

$$\Pr\left[\left|F(t) - \mathrm{Tr}[\omega^2]\right| \geq \delta\right] \leq 2e \times \exp\left(-\frac{\delta}{e\mathrm{Tr}[\omega^2]}\right). \tag{19}$$

This improves on Eq. (15) by a factor of $\sqrt{\mathrm{Tr}\left[\omega^2\right]}$ when substituted into $A = |\Psi\rangle\langle\Psi|$ and $||A|| = 1$. Eq. (18) appeared previously in [20].

It is well known that $\mathrm{Tr}\left[\omega^2\right]$ is exponentially suppressed in system size for generic models for sufficiently well behaved initial conditions. As an example, see figure 2, which shows a clear exponential decay of $\mathrm{Tr}\left[\omega^2\right]$ with system size L.

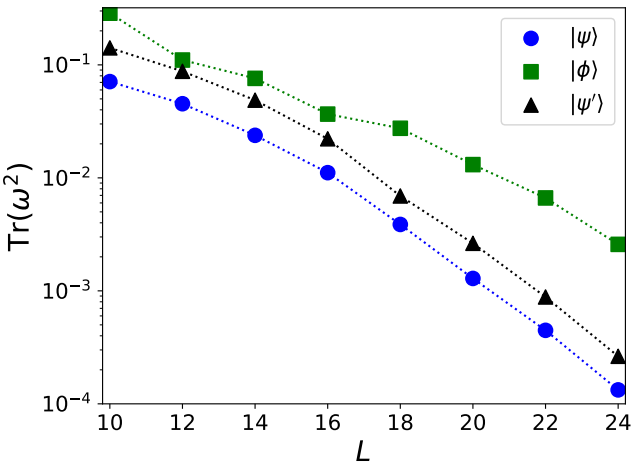

FIG. 2. $\mathrm{Tr}\left[\omega^2\right]$ for a variety of system sizes and states. Numerics were done with the same model as Fig. 1. More details on the states and the model can be found in App. D.

B. Generic extended free fermions

The second class that we consider are generic extended free fermionic models

$$H = \sum_{m,n=1}^{L} M_{m,n} f_m^\dagger f_n, \tag{20}$$

where f_n is a fermionic annihilation operator for the lattice site n. The fermionic operators obey the standard canonical anti-commutation relations $\{f_m, f_n\} = \{f_m^\dagger, f_n^\dagger\} = 0$, $\{f_m^\dagger, f_n\} = \delta_{m,n}$. We assume M is real symmetric, so it is diagonalized with a real orthogonal matrix O such that $M = ODO^T$. D is a diagonal matrix with entries $D_{k,k} = \epsilon_k$, which allows us to rewrite the Hamiltonian as

$$H = \sum_{k=1}^{L} \epsilon_k d_k^\dagger d_k, \tag{21}$$

where ϵ_k are the single particle energy eigenmodes, and we have new fermionic operators in eigenmode space defined in terms of the real space fermionic operators: $d_k = \sum_{j=1}^{L} O_{j,k} f_j$. This class of models notably does not obey Def. 1. However, we can instead give the following definition.

Definition 2. *Let $H = \sum_{k=1}^{L} \epsilon_k d_k^\dagger d_k$ be a free Hamiltonian. Let Λ_q, Λ_q' be two arbitrary sets of q eigenmodes $\{\epsilon_j\}$. Then H is a generic extended free fermionic model if, for all $q \in \mathbb{N}$ and all Λ_q, Λ_q', the equality*

$$\sum_{j \in \Lambda_q} \epsilon_j = \sum_{j \in \Lambda_q'} \epsilon_j \tag{22}$$

implies that $\Lambda_q = \Lambda_q'$ and the entries of O are such that

$$O_{j,k} = \frac{c_{j,k}}{\sqrt{L}}, \tag{23}$$

with $c_{j,k} = \mathcal{O}(1)$.

The equivalent of Lemma 2 also holds here by applying it to the matrix M and the energy eigenmodes. This definition crucially excludes localized models, which have entries of the form, $O_{m,k} \sim e^{-|k-m|/\xi}$, with ξ the localization length. The bound on the moments is as follows.

Theorem 3. *Let H be a generic extended free fermionic Hamiltonian and let $A = f_m^\dagger f_n$. Then, for even q,*

$$\kappa_q \leq \left(q c^2 \sqrt{\frac{\nu}{L}} \right)^q, \tag{24}$$

where $\nu = \frac{N}{L}$ is the filling factor of the fermions on the lattice and $c = \sqrt{L} \max_{k_j} \{O_{m,k_j}, O_{n,k_j}\}$.

The corresponding concentration bound is

$$\begin{aligned} &\Pr\left[\left| \langle f_m^\dagger f_n(t) \rangle - \langle f_m^\dagger f_n(\infty) \rangle \right| \geq \delta \right] \\ &\leq 2e \times \exp\left(-\frac{\delta}{e c^2} \sqrt{\frac{L}{\nu}} \right). \end{aligned} \tag{25}$$

Theorem 3 can be contrasted with the bound found in [21] for the second moment. The authors consider a potentially extensive observable and do not limit the analysis to extensive models, recovering $\kappa_2 \leq ||a||^2 \nu L$ for an observable $A = \sum_{m,n} f_m^\dagger a_{m,n} f_n$.

The last quantity of interest is the single particle propagator

$$\{f_m^\dagger(t), f_n\} = a_{m,n}(t). \tag{26}$$

For example, if we initialize our state as $|\Psi\rangle = f_m^\dagger |0\rangle$, then the fidelity is

$$F(t) = |a_{m,m}(t)|^2. \tag{27}$$

The more general $|a_{m,n}(t)|^2$ is also studied in the context of out of time ordered correlators [22–25]. Consider

$$|a_{m,n}(t)|^2 = \sum_{k,l} O_{m,k} O_{n,k} O_{m,l} O_{n,l} e^{i(\epsilon_k - \epsilon_l)t}. \tag{28}$$

The infinite time average of this quantity is taken as

$$\omega_{m,n} = \sum_k O_{m,k}^2 O_{n,k}^2. \tag{29}$$

For extended models with non-degenerate frequencies this quantity decays to zero since $\omega_{m,n} \sim \frac{1}{L}$ and $\kappa_2 \leq \frac{c}{L^2}$, where c is weakly dependent on system size and is $\mathcal{O}(1)$ in the thermodynamic limit [23]. We can bound the moments for the single particle propagator as follows.

Theorem 4. *Let H be a generic free fermionic Hamiltonian, and let our dynamical function $f(t) = |a_{m,n}(t)|^2$ be the squared single particle propagator, then we can bound the moments by*

$$\kappa_q \leq \left(\frac{q c^4}{L} \right)^q, \tag{30}$$

where $c = \sqrt{L} \max_{k_j} \{O_{m,k_j}, O_{n,k_j}\}$.

Finally, the corresponding concentration bound is

$$\Pr\left[\left| |a_{m,n}(t)|^2 - \omega_{m,n} \right| \geq \delta \right] \leq 2e \times \exp\left(-\frac{\delta L}{e c^4} \right). \tag{31}$$

IV. RECURRENCE TIME

All the quantities analyzed above always come back arbitrarily close to their initial values at $t = 0$. For large systems, however, such recurrences only happen at astronomically large timescales, inaccessible to both experiments and numerical studies. We now put a lower bound on those timescales through a suitably defined notion of *average recurrence time*, both for observables and also the whole state.

Definition 3. *A (u, Δ, A)-recurrence occurs at a time interval $\mathcal{C}_\Delta = [t_\Delta, t_\Delta + \Delta]$ if, for all $t \in \mathcal{C}_\Delta$,*

$$|\langle A(t) \rangle - \langle A(0) \rangle| \leq u ||A||. \tag{32}$$

Similarly, a (u, Δ)-recurrence occurs if, for all $t \in \mathcal{C}_\Delta$,

$$1 - F(t) \leq u. \tag{33}$$

Notice that an (u, Δ)-recurrence implies an (u, Δ, A)-recurrence for all A, and that conversely an (u, Δ, A)-recurrence for all A implies an (u, Δ)-recurrence. However, individual observables may have additional earlier recurrences.

Let us also define $t_\Delta^n(A)$ as the time for the n-th (u, Δ, A)-recurrence, so that $t_\Delta^n(A) < t_\Delta^{n+1}(A)$, and analogously, t_Δ^n for the fidelity. This motivates the following definition, inspired by that in [9].

Definition 4. *The average (u, Δ, A)-recurrence time is*

$$T(u, \Delta, A) \equiv \lim_{n\to\infty} \frac{t^n_\Delta(A)}{n}, \tag{34}$$

with $T(u, \Delta)$ analogously defined.

These quantities can be easily bounded with the concentration bounds above. First, for $T(u, \Delta, A)$.

Corollary 1. *Let H be generic, and let w.l.o.g. $\langle A(0)\rangle - \langle A(\infty)\rangle = c_A||A|| \geq 0$. Then, for $u \leq c_A$,*

$$\frac{\Delta}{2e}\exp\left(\frac{c_A - u}{e\sqrt{\mathrm{Tr}[\omega^2]}}\right) \leq T(u, \Delta, A). \tag{35}$$

Proof. From the definition of the distribution $P(x)$ in Eq. (6) and Eq. (15) we have that

$$\begin{aligned}\lim_{n\to\infty} \frac{\Delta n}{t^n_\Delta(A) + \Delta} &\leq \Pr\left[|\langle A(t)\rangle - \langle A(0)\rangle| \leq u||A||\right] \\ &\leq \Pr\left[|\langle A(t)\rangle - \langle A(\infty)\rangle| \geq (c_A - u)||A||\right] \\ &\leq 2e \times \exp\left(\frac{u - c_A}{e\sqrt{\mathrm{Tr}\left[\omega^2\right]}}\right).\end{aligned} \tag{36}$$

Notice that $\lim_{n\to\infty} \frac{\Delta n}{t^n_\Delta(A)+\Delta} = \Delta/T(u, \Delta, A)$. Solving for $T(u, \Delta, A)$ yields the result. □

With typical out-of-equilibrium initial conditions, we have that $c_A = \mathcal{O}(1)$. The larger recurrences should have a duration comparable to that of the initial equilibration time T^A_{eq}, which we can define as the time it takes for $\langle A(t)\rangle$ to settle around the steady value $\langle A(\infty)\rangle$. The recurrences with $u = \mathcal{O}(1)$ are then on average spaced by a time

$$T \gtrsim T^A_{\mathrm{eq}} e^{\Omega\left(\mathrm{Tr}\left[\omega^2\right]^{-1/2}\right)}. \tag{37}$$

Note that for local Hamiltonians and observables, T^A_{eq} is believed to generally scale as a low-degree polynomial in system size [26].

For the fidelity, the bound on the recurrence follows exactly the proof of Corollary 1 but using Eq. (19) instead.

Corollary 2. *Let H be generic. Then,*

$$\frac{\Delta}{2e^2}\exp\left(\frac{1 - u}{e\mathrm{Tr}[\omega^2]}\right) \leq T(u, \Delta). \tag{38}$$

Proof. Again from Eq. (6) and Eq. (19) we have that

$$\begin{aligned}\lim_{n\to\infty} \frac{\Delta n}{t^n_\Delta + \Delta} &\leq \Pr\left[F(t) \geq 1 - u\right] \\ &\leq \Pr\left[|F(t) - \mathrm{Tr}[\omega^2]| \geq 1 - u - \mathrm{Tr}[\omega^2]\right] \\ &\leq 2e \times \exp\left(-\frac{1 - u - \mathrm{Tr}[\omega^2]}{e\mathrm{Tr}[\omega^2]}\right) \\ &\leq 2e^2 \times \exp\left(-\frac{1 - u}{e\mathrm{Tr}[\omega^2]}\right).\end{aligned} \tag{39}$$

Also, $\lim_{n\to\infty} \frac{\Delta n}{t^n_\Delta + \Delta} = \Delta/T(u, \Delta)$, and solving for $T(u, \Delta)$ yields the result. □

In many-body systems, the fidelity initially decays as $F(t) = e^{-\sigma^2 t^2/2}$ where $\sigma^2 = \langle\Phi| H^2 |\Phi\rangle - \langle\Phi| H |\Phi\rangle^2$ is the energy variance [27–29]. Recurrences with $u = \mathcal{O}(1)$ likely decay in a similar fashion, with $\Delta \sim \sigma^{-1}$, so that on average they are spaced by a time

$$T \gtrsim \sigma^{-1} e^{\Omega\left(\mathrm{Tr}\left[\omega^2\right]^{-1}\right)}. \tag{40}$$

This closely matches the behaviour found in [9], which gives an exact calculation of the average recurrence time assuming a Gaussian wavefunction. It also matches the scaling of other previous estimates [8], so Eq. (38) should be close to optimal.

Finally, we also have corresponding bounds for fermions.

Corollary 3. *Let H be a generic free fermionic Hamiltonian, and let w.l.o.g. $\langle f^\dagger_m f_n(0)\rangle - \langle f^\dagger_m f_n(\infty)\rangle = c_f \geq 0$. Then, for $u \leq c_f$,*

$$\frac{\Delta}{2e}\exp\left(\frac{c_f - u}{ec^2}\sqrt{\frac{L}{\nu}}\right) \leq T(u, \Delta, f^\dagger_m f_n), \tag{41}$$

as well as for the fidelity in Eq. (27).

Corollary 4. *Let H be a generic free fermionic Hamiltonian. Then,*

$$\frac{\Delta}{2e}\exp\left(\frac{(1 - u)L}{ec^4}\right) \leq T(u, \Delta). \tag{42}$$

The analogue of Eq. (37) and Eq. (40) also holds following the same considerations. These bounds however scale as $e^{\Omega\left(\sqrt{L}\right)}$ and $e^{\Omega(L)}$ respectively, which are exponential in the number of sites L. This is a fast scaling, but still exponentially slower than that from Corollaries 1 and 2. Even shorter recurrence times are also found in specific instances of Bose gases [30–32], which can even be experimentally tested [33] with cold atoms.

V. CONCLUSION

We have shown how in generic systems both observables and the fidelity with the initial state equilibrate around their time-averaged values, with out-of-equilibrium fluctuations suppressed exponentially in the effective dimension $\mathrm{Tr}\left[\omega^2\right]^{-1}$. This number scales exponentially under very general conditions on the state and the Hamiltonian [18, 34–36], so in generic systems fluctuations are most often doubly exponentially suppressed. Since partial or full recurrences are far from equilibrium fluctuations, our bounds yield an estimate of their occurrence, with a scaling that we believe is almost optimal. Equivalent results with a slower scaling also hold for free fermions.

Previous works [18, 34, 36–39] start with the bound on the second moment in [12, 13] to obtain results on equilibration, so the present findings naturally strengthen them. Also, Theorem 2 in [40] extends [12, 13] to two-point correlation functions, and the corresponding concentration bound is straightforward.

Our bounds on the recurrence time apply to individual states. A given Hamiltonian should also have other later state-independent recurrences. For instance, the recent result for random circuits [41] suggests that a recurrence in complexity of e^{-itH} might still doubly exponential, but with a larger exponent that Eq. (40).

ACKNOWLEDGMENTS

AMA acknowledges support from the Alexander von Humboldt foundation. J.R. and N.J.P. acknowledges support from the Natural Sciences and Engineering Research Council of Canada (NSERC).

[1] C. Gogolin and J. Eisert, Rep. Prog. Phys. **79**, 056001 (2016).
[2] M. Ueda, Nature Reviews Physics **2**, 669 (2020).
[3] P. Bocchieri and A. Loinger, Phys. Rev. **107**, 337 (1957).
[4] I. C. Percival, Journal of Mathematical Physics **2**, 235 (1961), https://doi.org/10.1063/1.1703705.
[5] T. Hogg and B. A. Huberman, Phys. Rev. Lett. **48**, 711 (1982).
[6] R. Duvenhage, International Journal of Theoretical Physics **41**, 45 (2002).
[7] D. Wallace, Journal of Mathematical Physics **56**, 022105 (2015), https://doi.org/10.1063/1.4907384.
[8] K. Bhattacharyya and D. Mukherjee, The Journal of Chemical Physics **84**, 3212 (1986), https://doi.org/10.1063/1.450251.
[9] L. C. Venuti, "The recurrence time in quantum mechanics," (2015).
[10] T. Hogg and B. A. Huberman, Phys. Rev. A **28**, 22 (1983).
[11] A. Peres, Phys. Rev. Lett. **49**, 1118 (1982).
[12] P. Reimann, Phys. Rev. Lett. **101**, 190403 (2008).
[13] N. Linden, S. Popescu, A. J. Short, and A. Winter, Phys. Rev. E **79**, 061103 (2009).
[14] P. Reimann and M. Kastner, New Journal of Physics **14**, 043020 (2012).
[15] L. C. Venuti and P. Zanardi, Physical Review A **81** (2010), 10.1103/physreva.81.032113.
[16] L. C. Venuti, in *Quantum Criticality in Condensed Matter* (WORLD SCIENTIFIC, 2015).
[17] A possible stronger condition, that implies Def. 1, is that of rational independence of the energy levels [20].
[18] Y. Huang and A. W. Harrow, "Instability of localization in translation-invariant systems," (2020), arXiv:1907.13392 [cond-mat.dis-nn].
[19] A. J. Short, New. J. Phys. **13**, 053009 (2011).
[20] L. Campos Venuti and P. Zanardi, Phys. Rev. A **81** (2010), 10.1103/physreva.81.022113.
[21] L. C. Venuti and P. Zanardi, Phys. Rev. E **87**, 012106 (2013).
[22] J. Riddell and E. S. Sørensen, Phys. Rev. B **99**, 054205 (2019).
[23] J. Riddell and E. S. Sørensen, Phys. Rev. B **101**, 024202 (2020).
[24] S. Xu and B. Swingle, Nature Physics **16**, 199 (2020).
[25] V. Khemani, D. A. Huse, and A. Nahum, Phys. Rev. B **98**, 144304 (2018).
[26] L. D'Alessio, Y. Kafri, A. Polkovnikov, and M. Rigol, Advances in Physics **65**, 239 (2016).
[27] E. J. Torres-Herrera and L. F. Santos, Physical Review A **89** (2014), 10.1103/physreva.89.043620.
[28] E. J. Torres-Herrera, M. Vyas, and L. F. Santos, New Journal of Physics **16**, 063010 (2014).
[29] A. M. Alhambra, A. Anshu, and H. Wilming, Phys. Rev. B **101** (2020), 10.1103/physrevb.101.205107.
[30] E. Kaminishi, J. Sato, and T. Deguchi, Journal of the Physical Society of Japan **84**, 064002 (2015), https://doi.org/10.7566/JPSJ.84.064002.
[31] E. Solano-Carrillo, Phys. Rev. E **92**, 042164 (2015).
[32] E. Kaminishi and T. Mori, Phys. Rev. A **100**, 013606 (2019).
[33] B. Rauer, S. Erne, T. Schweigler, F. Cataldini, M. Tajik, and J. Schmiedmayer, Science **360**, 307 (2018), https://www.science.org/doi/pdf/10.1126/science.aan7938.
[34] H. Wilming, M. Goihl, I. Roth, and J. Eisert, Phys. Rev. Lett. **123**, 200604 (2019).
[35] A. Rolandi and H. Wilming, "Extensive rényi entropies in matrix product states," (2020), arXiv:2008.11764 [quant-ph].
[36] J. Haferkamp, C. Bertoni, I. Roth, and J. Eisert, PRX Quantum **2** (2021), 10.1103/prxquantum.2.040308.
[37] N. Linden, S. Popescu, A. J. Short, and A. Winter, New Journal of Physics **12**, 055021 (2010).
[38] M. Friesdorf, A. H. Werner, M. Goihl, J. Eisert, and W. Brown, New Journal of Physics **17**, 113054 (2015).
[39] T. Farrelly, F. G. Brandão, and M. Cramer, Phys. Rev. Lett. **118**, 140601 (2017).
[40] Á. M. Alhambra, J. Riddell, and L. P. García-Pintos, Phys. Rev. Lett. **124**, 110605 (2020).
[41] M. Oszmaniec, M. Horodecki, and N. Hunter-Jones, "Saturation and recurrence of quantum complexity in random quantum circuits," (2022).

Appendix A: Defining moments

The average value of $\langle A(t)\rangle$ in Eq. (1) motivates the formal definition of the following probability distribution

$$P(x) = \lim_{T\to\infty} \int_0^T \frac{\mathrm{d}t}{T} \delta(x - \langle A(t)\rangle).$$

We would like to compute the moments as

$$\kappa_q \equiv \lim_{T\to\infty} \int_0^T \frac{\mathrm{d}t}{T} \left(\langle A(t)\rangle - \langle A(\infty)\rangle\right)^q .$$

This requires swapping the integral over x and limit in T and can be justified using the dominated convergence theorem. To use this famous result we must prove that the absolute value of the integrand is bounded by an integrable function. Consider

$$\kappa_q = \int x^q \lim_{T\to\infty} P_T(x) dx.$$

For book-keeping purposes let $g(t) = (\langle A(t)\rangle - \langle A(\infty)\rangle)$. We may bound the integrand inside the limit

$$|x^q P_T(x)| = |\frac{x^q}{T} \int_0^T \mathrm{d}t \delta(x - g(t))| \leq \frac{|x|^q}{T} \int_0^T \mathrm{d}t \delta(x - g(t)).$$

Integrating the absolute value of the right-hand side and applying Fubini's theorem we find

$$\int \left| \frac{|x|^q}{T} \int_0^T \mathrm{d}t \delta(x - g(t)) \right| dx \leq \int \frac{|x|^q}{T} \left| \int_0^T \mathrm{d}t \delta(x - g(t)) \right| dx \leq \int \frac{|x|^q}{T} \int_0^T \mathrm{d}t \delta(x - g(t)) dx$$

$$\leq \frac{1}{T} \int_0^T \mathrm{d}t |g(t)|^q.$$

The function $g(t)$ is continuous and therefore bounded on the interval $[0, T]$, so the integral is finite, therefore its positive and negative components are as well, thus the q-th absolute moment is bounded. We may therefore conclude that the absolute value of the integrand is bounded by an integrable function, so by the dominated convergence theorem we may swap the integral and limit.

Note that equivalently, one may define the moments for finite T and then take the limit.

Appendix B: Generic spectra

Lemma 1. *The set of generic Hermitian matrices in $M_d(\mathbb{C})$ has full Lebesgue measure.*

Proof. Note that this proof is similar to the proof that the set of non-diagonalizable matrices has Lebesgue measure zero. Let H be some Hermitian $d \times d$ matrix. We start by defining the function

$$F(H) = \prod_{\substack{n_1, m_1, \ldots, n_q, m_q \\ n_i \neq m_i}} \left(\sum_{i=1}^{q} E_{n_i} - E_{m_i} \right).$$

This function is zero precisely when the spectrum is not generic. Clearly swapping eigenvalues does not change the function F, i.e. F is a symmetric polynomial of the eigenvalues. By the fundamental theorem of symmetric (real) polynomials F can be written uniquely as a polynomial in the elementary symmetric polynomials in E_i's, which are precisely trace powers of H.

Recall that H can be expressed in some basis. For example some generalized Pauli basis, or even the standard basis. This is conceptually equivalent to saying that the vector space of all possible H can be parameterized by the coefficients of the basis elements in the expansion. Thus, we may expand H in this basis and then take trace powers, showing us that F is a real polynomial in the space of these coefficients.

It is a well known fact from measure theory that the zero set of a multivariate polynomial has Lebesgue measure zero. □

Appendix C: Bounding the moments

1. Proof for generic models

Theorem 1. *Let H be a generic non-integrable Hamiltonian, ω the diagonal ensemble, and $||A||$ the largest singular value of A. The moments in Eq. 1 are such that*

$$\kappa_q \leq \left(q||A||\sqrt{\mathrm{Tr}[\omega^2]}\right)^q. \tag{C1}$$

Proof. First we prove the following inequality:

$$|\,\mathrm{Tr}\left[(A\omega)^q\right]\,| \leq \left(||A||\sqrt{\mathrm{Tr}\left[\omega^2\right]}\right)^q. \tag{C2}$$

To realize this, consider the matrix $A\omega$, which is not Hermitian and therefore may have complex eigenvalues and may potentially not be diagonalizable. This, however, does not prevent us from finding a complete set of eigenvalues such that their multiplicity summed is the dimension of $A\omega$. The matrix is always similar to its Jordan form, and we can in general always write

$$\mathrm{Tr}\left[A\omega\right] = \sum_i \lambda_i, \tag{C3}$$

where λ_i is the i-th (potentially complex) eigenvalue of $A\omega$. More generally, we can always write

$$\mathrm{Tr}\left[(A\omega)^q\right] = \sum_i \lambda_i^q. \tag{C4}$$

From here we can bound the following:

$$\begin{aligned}
|\,\mathrm{Tr}\left[(A\omega)^q\right]\,| &= |\sum_i \lambda_i^q| && \text{(C5)}\\
&\leq \sum_i |\lambda_i^q| && \text{(C6)}\\
&= ||\lambda||_q^q && \text{(C7)}\\
&\leq ||\lambda||_2^q = \left(\sum_i |\lambda_i|^2\right)^{q/2} && \text{(C8)}
\end{aligned}$$

where we used the triangle inequality in (C6), and in (C8) we use the property $||x||_{p+a} \leq ||x||_p$ for any vector x and real numbers $p \geq 1$ and $a \geq 0$. Note that, using the Shur decomposition, we may write $A\omega = QUQ^\dagger$, where Q is a unitary matrix, and U is upper triangular with the same spectrum on the diagonal as $A\omega$. Using this, we have that

$$\mathrm{Tr}\left[(A\omega)(A\omega)^\dagger\right] = \mathrm{Tr}\left[QUQ^\dagger(QUQ^\dagger)^\dagger\right] = \mathrm{Tr}\left[UU^\dagger\right] = \sum_i |\lambda_i|^2 + \text{other non-negative terms.}$$

Thus,

$$\sum_i |\lambda_i|^2 \leq \mathrm{Tr}\left[A\omega\omega^\dagger A^\dagger\right] \leq ||AA^\dagger||\,\mathrm{Tr}\left[\omega\omega^\dagger\right] \leq ||A||^2\,\mathrm{Tr}\left[\omega\omega^\dagger\right] = ||A||^2\,\mathrm{Tr}\left[\omega^2\right].$$

This gives us our desired inequality.

Moving on, let us derive a general bound for the q-th moment of models satisfying Definition 1. For simplicity, and w.l.o.g., let us assume that $\langle A(\infty)\rangle = 0$. Expanding the definition of the moments we arrive at

$$\kappa_q = \lim_{\tau\to\infty}\frac{1}{\tau}\int_0^\tau dt \sum_{m_1,n_1,\ldots,m_q,n_q}\prod_{i=1}^q \left(A_{m_i,n_i}\bar{c}_{m_i}c_{n_i}\right)e^{i(E_{m_i}-E_{n_i})t}. \tag{C9}$$

The assumption that the Hamiltonian is generic means that only certain terms in the sum survive after averaging over all time: those for which the sets of $\{m_i\}$ and $\{n_i\}$ coincide up to permutations, which we denote with $\{\sigma(i)\}$. Due to the equilibrium expectation value being zero, we can also eliminate all terms for which $i = \sigma(i)$ for $1 \leq i \leq q$. Thus, we want all permutations on q elements except those that have a fixed point. Such permutations are called derangements. The number of distinct derangements is denoted by $!q$, the subfactorial of q, and has no explicit formula. However, it may be computed recursively, the first few being $0, 1, 2, 9, 44, 265$. Let D_q denote the set of derangements on $\{1, 2, .., q\}$. Eq. (C9) becomes

$$\kappa_q = \sum_{m_1,...,m_q} \prod_{i=1}^{q} |c_{m_i}|^2 \sum_{\sigma \in D_q} \prod_{i=1}^{q} A_{m_i,\sigma(m_i)}. \tag{C10}$$

Given a derangement σ, it can be decomposed as the product of cycles $\sigma_1, \sigma_2, ..., \sigma_r$ with lengths $\ell_1, \ell_2, ..., \ell_r$, respectively, such that $\sum_{j=1}^{r} l_j = q$. In each term of the inner summation we can collect terms of the same cycle. For example for $q = 6$ and $\sigma = \sigma_1\sigma_2 = (m_1, m_2)(m_3, m_4, m_5, m_6)$ the term can be written as

$$(A_{m_1,m_2} A_{m2,m_1})(A_{m_3,m_4} A_{m_4,m_5} A_{m_5,m_6} A_{m_6,m_3}).$$

Summing over $m_1, m_2, m_3, m_4, m_5, m_6$ we have that this term is precisely

$$\operatorname{Tr}\left[(A\omega)^2\right] \operatorname{Tr}\left[(A\omega)^4\right].$$

In general, each cycle of a term will correspond to a product of trace powers i.e. $\sigma = \sigma_1, \sigma_2, ..., \sigma_r$ corresponds to

$$\operatorname{Tr}\left[(A\omega)^{\ell_1}\right] \operatorname{Tr}\left[(A\omega)^{\ell_2}\right] ... \operatorname{Tr}\left[(A\omega)^{\ell_r}\right].$$

We may apply Eq. (C2) term-wise to get

$$\operatorname{Tr}\left[(A\omega)^{\ell_1}\right] \operatorname{Tr}\left[(A\omega)^{\ell_2}\right] ... \operatorname{Tr}\left[(A\omega)^{\ell_r}\right] \leq \left(||A||\sqrt{\operatorname{Tr}\left[\omega^2\right]}\right)^{\ell_1+\ell_2+...+\ell_r} = \left(||A||\sqrt{\operatorname{Tr}\left[\omega^2\right]}\right)^{q}.$$

In each moment's inner summation there are precisely $!q$ terms of this form because there are $!q$ derangements, thus

$$\kappa_q \leq !q \left(||A||\sqrt{\operatorname{Tr}\left[\omega^2\right]}\right)^{q} \leq \left(q||A||\sqrt{\operatorname{Tr}\left[\omega^2\right]}\right)^{q}. \tag{C11}$$

□

The $q = 2$ case can be found in [19].

Theorem 2. *Let H be generic and let $A = |\Psi\rangle\langle\Psi|$, then*

$$\kappa_q \leq \left(q \operatorname{Tr}\left[\omega^2\right]\right)^{q}. \tag{C12}$$

Proof. The moments defined for the fidelity are defined as

$$\kappa_q = \lim_{\tau\to\infty} \frac{1}{\tau} \int_0^{\tau} dt \prod_{i=1}^{q} \sum_{m_i \neq n_i} |c_{m_i}|^2 |c_{n_i}|^2 e^{i(E_{m_i} - E_{n_i})t}, \tag{C13}$$

$$= \sum_{m_1,...m_q} \prod_{i=1}^{q} |c_{m_i}|^2 \prod_{\sigma \in D_q} |c_{\sigma(m_i)}|^2. \tag{C14}$$

In the above expression we can note that there are $!q$ possible derangements using genericity given in Definition 1. Each m_i will have one pair given to us from $\sigma(m_i)$, implying each individual term in the sum is $\operatorname{Tr}\left[\omega^2\right]^q$, so our final expression is

$$\kappa_q = !q \operatorname{Tr}\left[\omega^2\right]^q \leq \left(q \operatorname{Tr}\left[\omega^2\right]\right)^{q}. \tag{C15}$$

□

2. Generic free models

This class of models conserves total particle number, which we will denote as

$$N = \sum_{j=1}^{L} \langle f_j^\dagger f_j \rangle = \sum_{k=1}^{L} \langle d_k^\dagger d_k \rangle. \tag{C16}$$

Theorem 3. *Let H be a generic extended free fermionic Hamiltonian and let $A = f_m^\dagger f_n$. Then, the even moments are bounded above by*

$$\kappa_q \leq \left(q c^2 \sqrt{\frac{\nu}{L}} \right)^q, \tag{C17}$$

where $\nu = \frac{N}{L}$ is the filling factor of the fermions on the lattice and $c = \sqrt{L} \max_{k_j} \{O_{m,k_j}, O_{n,k_j}\}$.

Proof. Consider

$$\kappa_{2n} = \lim_{T\to\infty} \frac{1}{T} \int_0^\infty dt \prod_{j=1}^{n} \sum_{k_j \neq l_j} O_{m,k_j} O_{n,l_j} \langle d_{k_j}^\dagger d_{l_j} \rangle e^{i(\epsilon_{k_j} - \epsilon_{l_j})t} \sum_{p_j \neq q_j} O_{m,p_j} O_{n,q_j} \langle d_{q_j}^\dagger d_{p_j} \rangle e^{i(\epsilon_{q_j} - \epsilon_{p_j})t}. \tag{C18}$$

Let us define the tensor (note the j dependence)

$$B_{k_j,l_j} = \begin{cases} O_{m,k_j} O_{n,l_j} \langle d_{k_j}^\dagger d_{l_j} \rangle & j \text{ odd} \\ O_{m,l_j} O_{n,k_j} \langle d_{k_j}^\dagger d_{l_j} \rangle & j \text{ even} \\ 0 & k_j = l_j \end{cases}. \tag{C19}$$

This allows us to rewrite our equation as

$$\kappa_{2n} = \lim_{T\to\infty} \frac{1}{T} \int_0^\infty dt \prod_{j=1}^{2n} \sum_{k_j,l_j} B_{k_j,l_j} e^{i(\epsilon_{k_j} - \epsilon_{l_j})t}. \tag{C20}$$

This can likewise be rewritten as

$$\kappa_{2n} = \lim_{T\to\infty} \frac{1}{T} \int_0^\infty dt \sum_{k_1,l_1,\ldots k_{2n},l_{2n}} \prod_{j=1}^{2n} B_{k_j,l_j} e^{i(\epsilon_{k_j} - \epsilon_{l_j})t}. \tag{C21}$$

Assuming a generic single-particle spectrum, this means we have the following surviving terms:

$$\kappa_{2n} = \sum_{k_1,\ldots k_{2n}} \sum_{\sigma \in S_{2n}} \prod_{j=1}^{2n} B_{k_j,\sigma(k_j)} \tag{C22}$$

where S_{2n} denotes the symmetric group on $1, 2 \ldots 2n$. We can then enforce the fact that these terms are zero if $k_j = \sigma(k_j)$ for $1 \leq j \leq 2n$. So denoting the derangements as D_{2n} as earlier, we arrive at

$$\kappa_{2n} = \sum_{k_1,\ldots k_{2n}} \sum_{\sigma \in D_{2n}} \prod_{j=1}^{2n} B_{k_j,\sigma(k_j)}. \tag{C23}$$

Next, recognizing that each definition of B contains two extensive terms multiplied, let $c = \sqrt{L} \max_{k_j} \{O_{m,k_j}, O_{n,k_j}\}$,

$$\kappa_{2n} \leq \frac{c^{4n}}{L^{2n}} \sum_{k_1,\dots k_{2n}} \sum_{\sigma \in D_{2n}} \prod_{j=1}^{2n} \langle d_{k_j}^\dagger d_{\sigma(k_j)} \rangle \tag{C24}$$

As in Theorem 1, each term will be a trace of powers of Λ, and there can be at most n products of traces of Λ. Since $0 \leq \Lambda \leq \mathbb{I}$, each trace of Λ can further be bounded by $\mathrm{Tr}\left[\Lambda^p\right] \leq \mathrm{Tr}\left[\Lambda\right] = N = \nu L$, which means we can bound κ_{2n} by

$$\kappa_{2n} \leq !(2n) \frac{c^{4n}\nu^n}{L^{2n-n}} \leq \left(\frac{4n^2c^4\nu}{L}\right)^n, \tag{C25}$$

where c' is weakly dependent on system size and $0 \leq \nu \leq 1$. Choosing $q = 2n$ and reorganizing gives the desired result. □

Theorem 4. *Let H be a generic free fermionic Hamiltonian, and let our dynamical function $f(t) = |a_{m,n}(t)|^2$ be the squared single particle propagator, then we can bound the moments by*

$$\kappa_q \leq \left(\frac{qc^4}{L}\right)^q, \tag{C26}$$

where $c = \sqrt{L}\max_{k_j}\{O_{m,k_j}, O_{n,k_j}\}$.

Proof. The q-th moment can be written as

$$\kappa_q = \lim_{T\to\infty} \frac{1}{T} \int_0^\infty dt \prod_{i=1}^{q} \sum_{k_i \neq l_i} O_{m,k_i} O_{n,k_i} O_{m,l_i} O_{n,l_i} e^{i(\epsilon_{k_i} - \epsilon_{l_i})t}, \tag{C27}$$

through the usual procedure and using definition 2 we recover

$$\kappa_q = \sum_{k_1,\dots k_q} \prod_{i=1}^{q} O_{m,k_i} O_{n,k_i} \prod_{\sigma \in D_q} O_{m,\sigma(k_i)} O_{n,\sigma(k_i)}, \tag{C28}$$

defining $c = \sqrt{L}\max_{k_j}\{O_{m,k_j}, O_{n,k_j}\}$, we factor out four of these, and sum up the indices, giving us

$$\kappa_q \leq \frac{!qc^{4q}}{L^q} \leq \left(\frac{qc^4}{L}\right)^q. \tag{C29}$$

□

Appendix D: Numerics

The numerics for the figures in the main body were carried out on the spin 1/2 Hamiltonian,

$$H = \sum_{j=1}^{L} J_1 \left(S_j^+ S_{j+1}^- + \text{h.c}\right) + \gamma_1 S_j^Z S_{j+1}^Z + J_2 \left(S_j^+ S_{j+2}^- + \text{h.c}\right) + \gamma_2 S_j^Z S_{j+2}^Z,$$

where $(J_1, \gamma_1, J_2, \gamma_2) = (-1, 1, -0.2, 0.5)$ giving us a non-integrable model. We perform exact diagonalization exploiting total spin conservation and translation invariance. We choose pure states that allow us to further exploit the Z_2 spin flip symmetry and the spatial reflection symmetry. In Fig. 1 we see the approximated probability distribution function $\tilde{P}_T(x)$ as a histogram. The observable is $A = \sigma_1^Z$, the Pauli-z matrix on the first lattice site. The initial state is a Néel type state:

$$|\psi\rangle = |\uparrow\downarrow\dots\rangle. \tag{D1}$$

In Fig. 2 we calculate the purity of the diagonal ensemble Tr $\left[\omega^2\right]$ for three states. The states featured are

$$|\psi\rangle \coloneqq |\uparrow\downarrow\uparrow\downarrow \ldots..\rangle, \tag{D2}$$

$$|\psi'\rangle \coloneqq \frac{1}{\sqrt{2}}\left(|\uparrow\downarrow\uparrow\downarrow \ldots..\rangle + |\downarrow\uparrow\downarrow\uparrow \ldots..\rangle\right), \tag{D3}$$

$$|\phi\rangle \coloneqq \frac{1}{\sqrt{L}} \sum_{r=0}^{L-1} \hat{T}^r |\uparrow\uparrow \ldots \uparrow\downarrow \ldots \downarrow\downarrow\rangle. \tag{D4}$$

Chapter 5

Scaling at the OTOC Wavefront: Integrable versus chaotic models

Scaling at the OTOC Wavefront: Integrable versus chaotic models

Jonathon Riddell,[1] Wyatt Kirkby,[1] D. H. J. O'Dell,[1] and Erik S. Sørensen[1]

[1]*Department of Physics & Astronomy, McMaster University 1280 Main St. W., Hamilton ON L8S 4M1, Canada.*

(Dated: November 11, 2021)

Out of time ordered correlators (OTOCs) are useful tools for investigating foundational questions such as thermalization in closed quantum systems because they can potentially distinguish between integrable and non-integrable dynamics. Here we discuss the properties of wavefronts of OTOCs by focusing on the region around the main wavefront at $x = v_B t$, where v_B is the butterfly velocity. Using a Heisenberg spin model as an example, we find that a propagating Gaussian with the argument $-m(x)\left(x - v_B t\right)^2 + b(x)t$ gives an excellent fit for both the integrable case and the chaotic case. However, the scaling in these two regimes is very different: in the integrable case the coefficients $m(x)$ and $b(x)$ have an inverse power law dependence on x whereas in the chaotic case they decay exponentially. In fact, the wavefront in the integrable case is a rainbow caustic and catastrophe theory can be invoked to assert that power law scaling holds rigorously in that case. Thus, we conjecture that exponential scaling at the OTOC wavefront is a robust signature of a nonintegrable dynamics.

Introduction: The hallmark of chaos in classical dynamics is an exponential sensitivity to small changes in initial conditions (butterfly effect). This is at odds with quantum mechanics where unitary time evolution means that the overlap between two states is constant in time. Although quantum systems do not display chaos, there are qualitative differences in behavior depending upon whether their classical limit is integrable or nonintegrable (chaotic) [1]. In the latter case we have 'quantum chaos' which is well studied in single-particle quantum mechanics, including in experiments [2–12]. On the theoretical side, the main approach has traditionally been through spectral statistics [13, 14]. These have universal properties that depend only on the symmetries of the Hamiltonian and show close agreement with the predictions of random matrix theory (RMT)[15–18]. More recently, attention has shifted to many body quantum chaos and particularly its role in foundational issues such as thermalization in closed quantum systems. One limitation of RMT is that it does not describe thermodynamic quantities like temperature and energy that are needed for such analyses [19]. This is remedied by the eigenstate thermalization hypothesis (ETH) [20–24] which has been numerically verified in a range of generic models [25–28] but is violated in integrable and localized systems [29–38], as expected. The ETH generalizes RMT and gives identical predictions if one focuses on a small enough region of the spectrum. Any diagnostic of quantum chaos should therefore clearly differentiate between the integrable and ETH cases. While the ETH does give rise to the notion of chaotic eigenstates, it is a time independent statement and does not resemble classical chaos. In fact, aside from the weak ETH (eigenstate typicality) [39–41], it has no classical counterpart.

The out-of-time-ordered correlator (OTOC) has risen to prominence as a dynamical diagnostic for quantum many body chaos [42–52]. It takes the form

$$C(x,t) = \langle [\hat{A}(t), \hat{B}]^\dagger [\hat{A}(t), \hat{B}] \rangle, \tag{1}$$

where $\hat{A}$ and $\hat{B}$ are operators that at $t = 0$ only have local support (act on different individual lattice sites) and hence commute. The average is usually taken over an ensemble diagonal in the energy basis, but some studies have considered pure states as well [53–55]. As $\hat{A}$ evolves in time it picks up weight throughout the lattice, becoming non-local and causing $C(x,t)$ to become non-zero. This, in effect, tracks the tendency of dynamics to smear information across the system, and it becomes impossible to determine the initial conditions from local data alone. In this respect the OTOC resembles classical chaos where incomplete information leads to exponential inaccuracy. Indeed, the late time value of the OTOC in local spin models does appear to be an indicator of chaos [43, 53–65]. In the classical limit commutators become Poisson brackets which are a diagnostic for classical chaos, and the general expectation is therefore that OTOCs in nonintegrable models experience exponential growth [52],

$$C(0,t) \sim e^{\lambda_L t}\,, \tag{2}$$

where λ_L is the quantum Lyapunov exponent and obeys [52],

$$\lambda_L \leq 2\pi k_B T/\hbar\,. \tag{3}$$

Models that approach the bound are known as fast scramblers. However, doubt has been cast upon whether exponential growth of the OTOC really is unique to chaotic systems because integrable systems near unstable points behave similarly [66–71].

An OTOC should also display spatial dependence as information propagates across the system. A new conjecture gives the *early time* growth of the OTOC wavefront as [72–74]

$$C(x,t) \sim \exp\left[-\lambda_L \frac{(x/v_B - t)^{1+p}}{t^p}\right]\,. \tag{4}$$

This has been verified in several cases and used to study the many body localization transition [72–83]. For interacting models Eq. (4) is usually fitted in regimes where $C(x,t) \ll 1$ [73, 79], corresponding to early times *significantly before* the arrival of the main front. When the broadening coefficient takes the value $p = 0$, it reduces to the simple "Lyapunov-like" exponential growth of Eq. (2), but for quantum spin models expected to obey ETH it is believed that in general $p > 0$ [74]. However, broadening is not necessarily a general

indicator of how close one is to a chaotic model in the sense of ETH [84, 85], and puzzles remain concerning the value of p in this early growth regime. For example, in two dimensions the values of p coincide in chaotic and integrable models, so the broadening coefficient is inadequate for distinguishing them [74], while some studies [72, 74, 86–89] differ on whether the distinction between values of p even exists in either regime.

The aim of this Letter is to show that the main wavefront (region around $x = v_B t$ which is the edge of the OTOC "light cone") carries information on integrability. While there can be signatures of chaos in OTOCs at late times, including long-time oscillations [74, 85, 90–92], it is preferable to examine the main front rather than the signal either at early times (exponentially small) or late times (more contamination from the environment or numerical errors). Recent numerical work in free models has shown that the OTOC in this region is well-fitted by a propagating Gaussian of the form [54, 93],

$$C_G(x,t) \sim e^{-m(x)(x-v_B t)^2 + b(x)t}, \tag{5}$$

where $m(x)$ and $b(x)$ are well behaved functions of x. A Gaussian also occurs in random circuit models [84] and wavefront results suggest it would also be found in the critical Ising model [60]. Here we will employ rigorous arguments from catastrophe theory to show that in many models that can be mapped to free fermions the wavefront takes on a universal Airy function form that can be locally described by Eq. (5). This allows us to extract the scaling of $m(x), b(x)$ analytically, verifying the findings of [54, 93]. For the chaotic case, we numerically verify the Gaussian wave form of Eq. (5) and show that the scaling of $m(x), b(x)$ is very different from the free model. In locally interacting models the Gaussian wave form Eq. (5) therefore carries signatures of whether the model is free or ETH-obeying.

Model: We consider a Heisenberg spin Hamiltonian with nearest and next nearest interactions:

$$\begin{aligned}\hat{H} = &\sum_{j=1}^{L-1} J_1 \left(\hat{S}_j^+ S_{j+1}^- + \text{h.c}\right) + \Delta \hat{S}_j^Z \hat{S}_{j+1}^Z \\ &+ \sum_{j=1}^{L-2} J_2 \left(\hat{S}_j^+ S_{j+2}^- + \text{h.c}\right) + \gamma \hat{S}_j^Z \hat{S}_{j+2}^Z \,,\end{aligned} \tag{6}$$

and open boundary conditions. This model has both free and non-integrable regimes. In particular, we consider two choices of the coefficient vector $\vec{c} = (J_1, \Delta, J_2, \gamma)$. The first one, $\vec{c}_f = (-1, 0, 0, 0)$ is the XX chain and is free while the second, $\vec{c}_{\text{ETH}} = (-0.5, 1, -0.2, 0.5)$ has all parameters non-zero which has been verified to obey the ETH with periodic boundary conditions [25]. In the supplementary materials (SM) [94] we demonstrate that an alternative choice of parameters for $\vec{c}_{\text{ETH}}$ leads to the same basic results. Suitable operators for $\hat{A}(t)$ and $\hat{B}$ must be chosen for the OTOC in Eq. (1). In the ETH regime we use spin operators $\hat{A}(t) = \sigma_1^Z$, and $\hat{B} = \sigma_m^Z$, where x is the distance between sites 1 and m, and the average $\langle \ldots \rangle$ is taken over the thermal ensemble restricted to eigenstates with zero magnetization, $m_z = \sum_{j=1}^{L} \langle \hat{S}_j^Z \rangle = 0$. In the integrable case we perform a Jordan-Wigner transformation from spins to fermions and for simplicity the OTOC we use in this case is

$$C(x,t) = |a_{m,n}(t)|^2 \tag{7}$$

where $a_{m,n}(t) = \{\hat{f}_m^\dagger(t), \hat{f}_n\}$. Here, $\hat{f}_m$ is the annihilation operator for a fermion on site m. Note that if instead of Eq. (7) we use Eq. (1) with operators σ_m^z, then in the case of a pure Gaussian state or a thermal ensemble the dominant dynamical term is in fact $|a_{m,n}(t)|^2$, see Refs. [54, 93] for further details.

Airy light cones in free systems: In 1972 Lieb and Robinson [95] showed that quantum correlations in spin systems propagate at finite speeds and spread out in a light cone-like fashion. Pioneering experiments with ultracold atoms and trapped ions [96–101], where a sudden quench leads to a nonequilibrium state, have confirmed this behavior. In particular, the wavefront for interacting bosonic atoms in an optical lattice was measured to have an Airy function profile [96] in qualitative agreement with theoretical calculations which can be done analytically in certain limits [102]. The associated problem of domain wall propagation [103–110] also yields Airy functions or related kernels for the wavefront. The Airy function shape implies a dynamical scaling behavior, such as a $t^{1/3}$ broadening of the magnetization domain wall in an XX chain [103]. This body of results has led to the notion of an *Airy universality class* for free systems [111–113].

A more general understanding of light cones can be gained by realizing that they are caustics [114]. These are singularities of the ray description of a wave, where in the present case the rays are trajectories of quasiparticles excited by the quench. Caustics are regions where rays coalesce, leading to a diverging probability density in the classical limit. Significantly, only certain morphologies of caustic are structurally stable and hence occur generically in nature; these form a hierarchy described by catastrophe theory where each catastrophe forms an equivalence class with its own scaling properties similar to universality classes for phase transitions [115, 116]. The simplest catastrophe is the fold which occurs where rays coalesce in pairs and an everyday example of this is the rainbow, and another is a ship's wake [117, 118].

In the wave theory each caustic is dressed by a characteristic wavefunction, and in the case of the fold it is the Airy function [119]. To see how this works, consider the case where the quench excites a Bogoliubov fermion on the site at $x = 0$, say. The resulting wavefunction is

$$\begin{aligned}\Psi(x,t) = \langle x_b | \mathrm{e}^{-\mathrm{i}\hat{H}t} \hat{b}_{x=0}^\dagger |0_b\rangle &= \langle x_b | \sum_k \mathrm{e}^{-\mathrm{i}\epsilon(k)t} |k\rangle \\ &\approx \frac{\sqrt{a}}{2\pi} \int_{-\frac{\pi}{a}}^{\frac{\pi}{a}} \mathrm{d}k \, \mathrm{e}^{\mathrm{i}[kx - \epsilon(k)t]}\end{aligned} \tag{8}$$

where a is the lattice constant. The operators $\hat{b}_x$ are the linear combinations of $\hat{f}_m$ and $\hat{f}_m^\dagger$ that diagonalize the Hamiltonian via a Bogoliubov transformation and $\epsilon(k)$ is the Bogoliubov dispersion relation [for the XX chain $\epsilon(k) = J_1 \cos ka$].

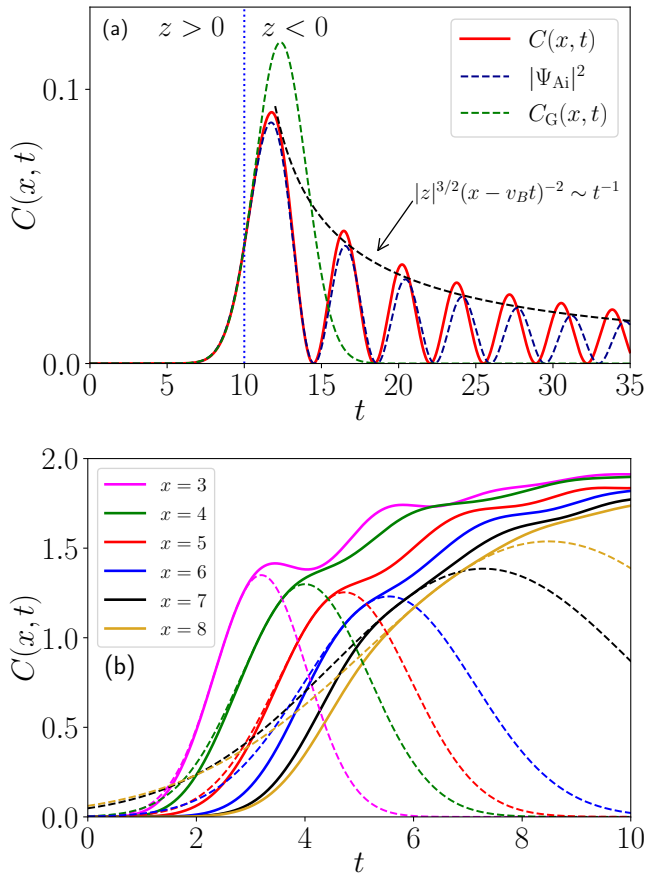

Figure 1. Wavefronts of $C(x,t)$. **(a)** The integrable case, $\vec{c}_f$. Here $x = 10$. Exact numerical results (solid red) along with a fit to the Gaussian form Eq. (5) (green), and the Airy result from Eq. (9) (blue). The expected t^{-1} decay in the amplitude is also shown (black). **(b)** ETH case, $\vec{c}_{\rm ETH}$, at different positions x. Solid lines indicate the OTOC data, and dashed lines are fits to Eq. (5) centered at $x = v_B t$.

Defining $\Phi(k,x,t) = kx - \epsilon(k)t$, a caustic occurs at quasi-momentum k_c, where two conditions are satisfied [119]: $(\partial\Phi/\partial k)_{k_c} = 0$ and $(\partial^2\Phi/\partial k^2)_{k_c} = 0$. The first condition is Fermat's principle that gives classical rays as saddles of the action $k\dot{x} - \epsilon(k)$ and the second defines the caustic as the place where saddles coalesce. These conditions correspond exactly to the Lieb-Robinson (LR) bound for a light cone as being determined by the maximum value of the group velocity $d\epsilon/dk$ of the fermions [114, 120, 121], $v_{\rm LR} = \max_k |d\epsilon/dk|$.

The fact that light cones are caustics allows a number of powerful results from catastrophe theory to be applied: *i*) The only structurally stable catastrophes in two dimensions (the space-time formed by x and t) are fold lines that meet at cusp points, as anyone who has ironed a shirt knows. For a light cone the only place a cusp could occur is at the origin where the two edges meet. However, in the present case of the XX model the dispersion relation is so simple that only two rays can coalesce and no cusp occurs, just two pure fold lines that meet at $x = t = 0$. This result is special and if a symmetry breaking term is added the two folds will instead generically meet at a cusp (coalescence of three rays) and the back-to-back Airy functions are locally replaced by a Pearcey function [114]; *ii*) The defining feature of a fold catastrophe is that the phase $\Phi(k,x,t)$ is cubic in k. This is why the Airy function is the universal wavefunction at a fold because $\mathrm{Ai}(z) = (1/2\pi)\int_{-\infty}^{\infty} \mathrm{d}s\ \exp[\mathrm{i}(zs + s^3/3)]$; *iii*) There exists a diffeomorphism from the physical variables (k,x,t) to the canonical Airy cubic form (s,z). Therefore, a Taylor expansion truncated at precisely third order about the caustic gives the exact semiclassical description in the neighborhood of that point. Performing the transformation of variables, $s^3 = 2(k-k_c)^3/[t\partial_k^3\epsilon(k_c)]$ gives [72, 74, 94]

$$\Psi_{\rm Ai}(x,t) \sim \sqrt{a}\left(\frac{-2}{\partial_k^3\epsilon(k_c)t}\right)^{1/3} \mathrm{e}^{\mathrm{i}\Phi(k_c,x,t)}\ \mathrm{Ai}(z)\ , \qquad (9)$$

$$\text{where} \quad z = (x - v_B t)\left|t\partial_k^3\epsilon(k_c)/2\right|^{-1/3}\ . \qquad (10)$$

In Fig. 1(a), we plot $|\Psi_{\rm Ai}(x,t)|^2$ alongside the numerical result at the point $x = 10$, with the caustic ($z = 0$) marked by the vertical dotted line. The Airy wavefunction gradually goes out of phase at longer times because the Taylor expansion was made at a single point, but the range could be extended via a uniform mapping [122]. From the asymptotics of the Airy function as $z \to -\infty$ it follows that the amplitude of the OTOC wavefront decays as $|z|^{3/2}/(x-vt)^2 \sim 1/t$ (in agreement with Refs. [60, 61]), and the fringe spacing becomes *constant*. In this way one also finds that the amplitude along the wavefront $x/t = v_B$ decays as $x^{-2/3}$ [94]. Furthermore, Eq. (9) also correctly predicts the early time growth. Keeping just the first term of the $z \to \infty$ asymptotic series for the Airy function [94] gives the universal $p = 1/2$ form of the OTOC in Eq. (4) [72–74].

While an Airy function has been derived for OTOCs before [72, 74, 113], the point we emphasize here is that catastrophe theory guarantees that this result is rigorously true and robust to perturbations. Hence, deviations from it imply some qualitative change to the dynamics. One possibility is the presence of a symmetry breaking term which gives one of the higher catastrophes [114] (such as a cusp in the XY model which has a double cone). Another possibility is nonintegrable dynamics, and it is to that case we now turn.

Profile of the wavefront in the ETH case: In Fig. 1(b) we plot the exact results for the OTOC for $\vec{c}_{\rm ETH}$. Fringes are partially visible at smaller x but the Airy nodes have disappeared. Although structural stability implies that catastrophes are stable against weak chaos, $\vec{c}_{\rm ETH}$ corresponds to strong chaos which disrupts the rays and their interference significantly. At $x = 3$ the wavefront has quite a sharp slope, indicating that the process of scrambling (the increase in non-locality of the observable) is still in full swing. By $x = 8$, the slope of the OTOC at the wavefront has significantly decreased. The Gaussian waveform of Eq. (5) provides an excellent local fit to the wavefront in both the integrable [54, 93] and chaotic regimes, as seen from the dashed curves in Fig. 1(a) and 1(b), respectively. The fit is performed over the range $t = \frac{x}{v_B} \pm \Delta$

where $\Delta \approx 0.5$ gives a reasonably large window to describe the shape of $C(x,t)$. Within the fitting window, for a fixed x, the parameters $m(x)$ and $b(x)$ in Eq. (5) can be determined with very high precision with errors on each term of the order of 10^{-7} to 10^{-9}. A crucial ingredient to identify the parameters in the ETH case is to first determine the butterfly velocity v_B, which can be done using velocity-dependent Lyapunov exponents [74, 123], as demonstrated in the SM [94]. We find that the velocity for the ETH model characterized by $\vec{c}_{\rm ETH}$ is roughly $v_B \approx 1.28$ (in contrast to $v_B = 1$ for $\vec{c}_f$). Although the integrable and ETH wavefronts both display flattening, the scaling properties of $m(x)$ and $b(x)$ are fundamentally different in the two regimes as we now show.

Scaling in Free Models: By expanding the Airy wavefunction given in Eq. (9) about the caustic at $z = 0$ we obtain

$$m(x) = \frac{c_m}{x^{\frac{2}{3}}}\,, \quad b(x) = \frac{c_b}{x^{\frac{1}{3}}}\,, \tag{11}$$

where c_m and c_b are constants that depend explicitly on the dispersion relation (see the SM [94] for details). Due to the universality of the Airy wavefunction, this scaling is expected to hold for many models which can be written in terms of freely propagating quasiparticles. Furthermore, corrections beyond quadratic order in $x - v_B t$ can be obtained. However, the cubic term in the exponent falls off rapidly (at least as x^{-1}), and so it is reasonable, even at moderate distances, to keep only the Gaussian approximation. We have numerically verified Eq. (11) and the results are shown in Fig. 2(a). Fitting the scaling of each parameter for distances $0 < x \leq 650$ we find,

$$m(x) \propto \frac{1}{x^{a_m}}\,, \quad b(x) \propto \frac{1}{x^{a_b}}\,, \tag{12}$$

with $a_m = 0.68857 \pm 0.00008$, and $a_b = 0.33043 \pm 0.00002$, indicating good agreement with the expected values. We also note that because $m(x) \propto b(x)^2$, $m(x)$ falls off significantly quicker than $b(x)$. This may point to an intermediate regime in x where the OTOC is well described by $C(x,t) \sim e^{b(x)t}$.

Scaling in ETH regime: In Fig. 2(b) we show a plot of the data for the $\vec{c}_{\rm ETH}$ case. A linear trend emerges, implying that the spatial dependence on $m(x)$ and $b(x)$ in the ETH regime exhibits exponential rather than power-law decay,

$$b(x) \sim e^{-cx}, \;\; m(x) \sim e^{-wx}, \tag{13}$$

where $c, w > 0$ are constants. We find that $c = 0.38 \pm 0.02$ and $w = 0.66 \pm 0.05$. Like the free case, $m(x) \propto b(x)^2$, however, as shown in the SM [94], this is not generally the case.

The exponentially decaying behavior of $m(x)$ and $b(x)$ is clearly distinct from the free fermion case. This indicates that the Gaussian waveform can distinguish ETH-obeying from free dynamics. In both Figs. 2(a) and (b) $m(x), b(x)$ decay by upwards of two orders of magnitude as a function of position, however the exponential decay in the ETH regime ensures that this occurs over a short distance of $x \approx 10$ while in the free model it takes a distance of $x \approx 600$. Thus, the general flattening of the OTOC at the wavefront (see e.g. Fig. 1) occurs *much* faster in thermalizing models.

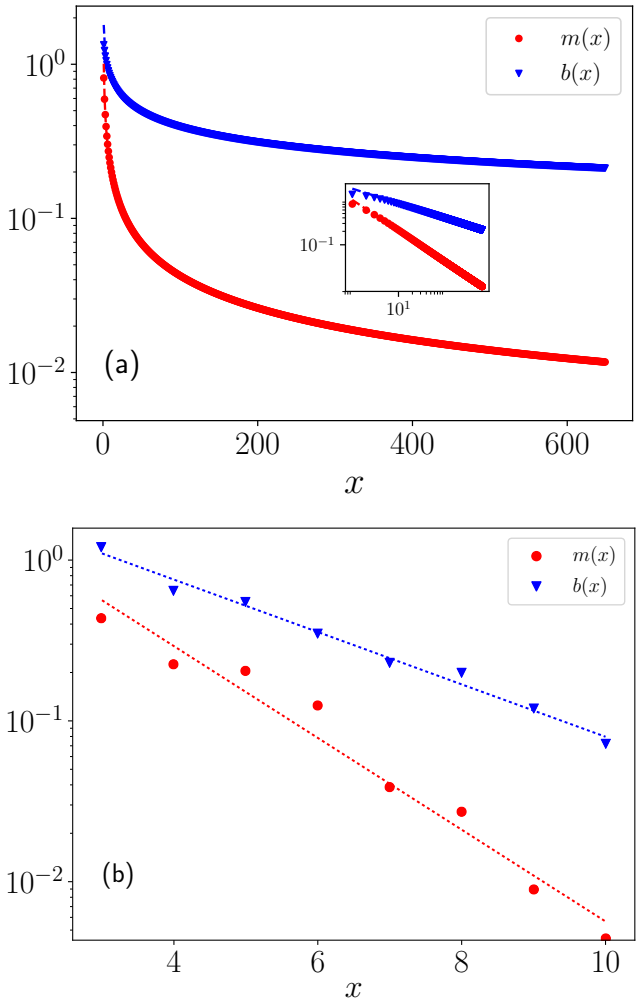

Figure 2. Log-linear plots for the Gaussian parameters $m(x)$ (red) and $b(x)$ [blue]. **(a)** The free Hamiltonian, $\vec{c}_f$. Dashed lines are fits to Eq. 12. Inset is a log-log plot of the same data. **(b)** The ETH Hamiltonian, $\vec{c}_{\rm ETH}$, using the same data as in Fig. 1(b) indicating exponential decay of $m(x), b(x)$.

Conclusions: Close to the wavefront, integrable and ETH models can be distinguished by the difference in scaling of the parameters $m(x)$, $b(x)$ in Eq. (5). The ability of modern experiments to measure quantum light cone profiles [96–101] and OTOCs [124–129] holds out the possibility that this prediction can be tested in the laboratory. A remaining open question concerns the transition from integrable to ETH dynamics [130–132] and the degree to which structural stability protects the Airy wavefront. A resolution of this question would constitute a quantum version of the celebrated KAM theorem [133].

This research was supported by NSERC (Canada). Computations were performed in part by support provided by

SHARCNET (www.sharcnet.ca) and Compute/Calcul Canada (www.computecanada.ca).

[1] M. V. Berry, Quantum chaology (The Bakerian Lecture), Proc. R. Soc. A **413**, 183 (1987).

[2] R. A. Jalabert, H. U. Baranger, and A. D. Stone, Conductance fluctuations in the ballistic regime: A probe of quantum chaos?, Phys. Rev. Lett. **65**, 2442 (1990).

[3] C. M. Marcus, A. J. Rimberg, R. M. Westervelt, P. F. Hopkins, and A. C. Gossard, Conductance fluctuations and chaotic scattering in ballistic microstructures, Phys. Rev. Lett. **69**, 506 (1992).

[4] V. Milner, J. L. Hanssen, W. C. Campbell, and M. G. Raizen, Optical billiards for atoms, Phys. Rev. Lett. **86**, 1514 (2001).

[5] N. Friedman, A. Kaplan, D. Carasso, and N. Davidson, Observation of chaotic and regular dynamics in atom-optics billiards, Phys. Rev. Lett. **86**, 1518 (2001).

[6] H. J. Stockmann and J. Stein, "Quantum" chaos in billiards studied by microwave absorption, Phys. Rev. Lett. **64**, 2215 (1990).

[7] S. Sridhar, Experimental observation of scarred eigenfunctions of chaotic microwave cavities, Phys. Rev. Lett. **67**, 785 (1991).

[8] F. L. Moore, J. C. Robinson, C. Bharucha, P. E. Williams, and M. G. Raizen, Observation of dynamical localization in atomic momentum transfer: A new testing ground for quantum chaos, Phys. Rev. Lett. **73**, 2974 (1994).

[9] D. A. Steck, W. H. Oskay, and M. G. Raizen, Observation of chaos-assisted tunneling between islands of stability, Science **293**, 274 (2001).

[10] W. K. Hensinger, H. Häffner, A. Browaeys, N. R. Heckenberg, K. Helmerson, C. McKenzie, G. J. Milburn, W. D. Phillips, S. L. Rolston, H. Rubinsztein-Dunlop, and B. Upcroft, Dynamical tunnelling of ultracold atoms, Nature **412**, 52 (2001).

[11] S. Chaudhury, A. Smith, B. E. Anderson, S. Ghose, and P. S. Jessen, Quantum signatures of chaos in a kicked top, Nature **461**, 768 (2009).

[12] Y. S. Weinstein, S. Lloyd, J. Emerson, and D. G. Cory, Experimental implementation of the quantum baker's map, Phys. Rev. Lett. **89**, 157902 (2002).

[13] M. C. Gutzwiller, Periodic orbits and classical quantization conditions, J. Math. Phys. **12**, 343 (1971).

[14] M. V. Berry and M. Tabor, Closed orbits and the regular bound spectrum, Proc. R. Soc. A **349**, 101 (1976).

[15] E. P. Wigner, On the statistical distribution of the widths and spacings of nuclear resonance levels, Proc. Cambridge Philos. Soc. **47**, 790 (1951).

[16] C. E. Porter, *Statistical theories of spectra: fluctuations* (Academic Press, New York, 1965).

[17] M. V. Berry and M. Tabor, Level clustering in the regular spectrum, Proc. R. Soc. A **356**, 375 (1977).

[18] O. Bohigas, M. J. Giannoni, and C. Schmit, Characterization of chaotic quantum spectra and universality of level fluctuation laws, Phys. Rev. Lett. **52**, 1 (1984).

[19] L. D'Alessio, Y. Kafri, A. Polkovnikov, and M. Rigol, From quantum chaos and eigenstate thermalization to statistical mechanics and thermodynamics, Advances in Physics **65**, 239 (2016), https://doi.org/10.1080/00018732.2016.1198134.

[20] J. M. Deutsch, Quantum statistical mechanics in a closed system, Phys. Rev. A **43**, 2046 (1991).

[21] M. Srednicki, Chaos and quantum thermalization, Phys. Rev. E **50**, 888 (1994).

[22] M. Srednicki, The approach to thermal equilibrium in quantized chaotic systems, Journal of Physics A: Mathematical and General **32**, 1163 (1999).

[23] M. Rigol, V. Dunjko, and M. Olshanii, Thermalization and its mechanism for generic isolated quantum systems, Nature **452**, 854 (2008).

[24] G. De Palma, A. Serafini, V. Giovannetti, and M. Cramer, Necessity of eigenstate thermalization, Phys. Rev. Lett. **115**, 220401 (2015).

[25] T. LeBlond, K. Mallayya, L. Vidmar, and M. Rigol, Entanglement and matrix elements of observables in interacting integrable systems, Phys. Rev. E **100**, 062134 (2019).

[26] H. Kim, T. N. Ikeda, and D. A. Huse, Testing whether all eigenstates obey the eigenstate thermalization hypothesis, Phys. Rev. E **90**, 052105 (2014).

[27] R. Mondaini, K. R. Fratus, M. Srednicki, and M. Rigol, Eigenstate thermalization in the two-dimensional transverse field Ising model, Phys. Rev. E **93**, 032104 (2016).

[28] K. Kaneko, E. Iyoda, and T. Sagawa, Work extraction from a single energy eigenstate, Phys. Rev. E **99**, 032128 (2019).

[29] G. Biroli, C. Kollath, and A. M. Läuchli, Effect of rare fluctuations on the thermalization of isolated quantum systems, Phys. Rev. Lett. **105**, 250401 (2010).

[30] H.-H. Lai and K. Yang, Entanglement entropy scaling laws and eigenstate typicality in free fermion systems, Phys. Rev. B **91**, 081110(R) (2015).

[31] J. Riddell and M. P. Müller, Generalized eigenstate typicality in translation-invariant quasifree fermionic models, Phys. Rev. B **97**, 035129 (2018).

[32] P. Ribeiro, M. Haque, and A. Lazarides, Strongly interacting bosons in multichromatic potentials supporting mobility edges: Localization, quasi-condensation, and expansion dynamics, Phys. Rev. A **87**, 043635 (2013).

[33] L. Vidmar and M. Rigol, Generalized Gibbs ensemble in integrable lattice models, Journal of Statistical Mechanics: Theory and Experiment **2016**, 064007 (2016).

[34] R. Nandkishore and D. A. Huse, Many-body localization and thermalization in quantum statistical mechanics, Annual Review of Condensed Matter Physics **6**, 15 (2015).

[35] S. Iyer, V. Oganesyan, G. Refael, and D. A. Huse, Many-body localization in a quasiperiodic system, Phys. Rev. B **87**, 134202 (2013).

[36] M. Schreiber, S. S. Hodgman, P. Bordia, H. P. Lüschen, M. H. Fischer, R. Vosk, E. Altman, U. Schneider, and I. Bloch, Observation of many-body localization of interacting fermions in a quasirandom optical lattice, Science **349**, 842 (2015).

[37] H. P. Lüschen, P. Bordia, S. S. Hodgman, M. Schreiber, S. Sarkar, A. J. Daley, M. H. Fischer, E. Altman, I. Bloch, and U. Schneider, Signatures of Many-Body Localization in a Controlled Open Quantum System, Phys. Rev. X **7**, 011034 (2017).

[38] H. P. Lüschen, P. Bordia, S. Scherg, F. Alet, E. Altman, U. Schneider, and I. Bloch, Observation of Slow Dynamics near the Many-Body Localization Transition in One-Dimensional Quasiperiodic Systems, Physical Review Letters **119**, 260401 (2017).

[39] T. Mori, Weak eigenstate thermalization with large deviation bound (2016), arXiv:1609.09776.

[40] F. G. S. L. Brandão, E. Crosson, M. B. Şahinoğlu, and J. Bowen, Quantum error correcting codes in eigenstates of translation-invariant spin chains, Phys. Rev. Lett. **123**, 110502 (2019).

[41] A. M. Alhambra, J. Riddell, and L. P. García-Pintos, Time evolution of correlation functions in quantum many-body systems, Phys. Rev. Lett. **124**, 110605 (2020).

[42] B. Yoshida, Firewalls vs. scrambling, Journal of High Energy Physics **10**, 132 (2019).

[43] B. Swingle and D. Chowdhury, Slow scrambling in disordered quantum systems, Phys. Rev. B **95**, 060201(R) (2017).

[44] J. R. González Alonso, N. Yunger Halpern, and J. Dressel, Out-of-time-ordered-correlator quasiprobabilities robustly witness scrambling, Phys. Rev. Lett. **122**, 040404 (2019).

[45] B. Yan, L. Cincio, and W. H. Zurek, Information scrambling and Loschmidt echo, Phys. Rev. Lett. **124**, 160603 (2020).

[46] J. Tuziemski, Out-of-time-ordered correlation functions in open systems: A Feynman-Vernon influence functional approach, Phys. Rev. A **100**, 062106 (2019).

[47] D. Mao, D. Chowdhury, and T. Senthil, Slow scrambling and hidden integrability in a random rotor model, Phys. Rev. B **102**, 094306 (2020).

[48] R. J. Lewis-Swan, A. Safavi-Naini, J. J. Bollinger, and A. M. Rey, Unifying scrambling, thermalization and entanglement through measurement of fidelity out-of-time-order correlators in the Dicke model, Nature Communications **10**, 1581 (2019).

[49] S. Nakamura, E. Iyoda, T. Deguchi, and T. Sagawa, Universal scrambling in gapless quantum spin chains (2019), arXiv:1904.09778.

[50] Y. Gu and A. Kitaev, On the relation between the magnitude and exponent of OTOCs, Journal of High Energy Physics **2019**, 75 (2019).

[51] R. Belyansky, P. Bienias, Y. A. Kharkov, A. V. Gorshkov, and B. Swingle, Minimal model for fast scrambling, Phys. Rev. Lett. **125**, 130601 (2020).

[52] J. Maldacena, S. H. Shenker, and D. Stanford, A bound on chaos, Journal of High Energy Physics **2016**, 106 (2016).

[53] J. Lee, D. Kim, and D.-H. Kim, Typical growth behavior of the out-of-time-ordered commutator in many-body localized systems, Phys. Rev. B **99**, 184202 (2019).

[54] J. Riddell and E. S. Sørensen, Out-of-time ordered correlators and entanglement growth in the random-field XX spin chain, Phys. Rev. B **99**, 054205 (2019).

[55] X. Chen, T. Zhou, D. A. Huse, and E. Fradkin, Out-of-time-order correlations in many-body localized and thermal phases, Annalen der Physik **529**, 1600332 (2017).

[56] Y. Huang, Y.-L. Zhang, and X. Chen, Out-of-time-ordered correlators in many-body localized systems, Annalen der Physik **529**, 1600318 (2017).

[57] R. Fan, P. Zhang, H. Shen, and H. Zhai, Out-of-time-order correlation for many-body localization, Science Bulletin **62**, 707 (2017).

[58] Y. Chen, Universal logarithmic scrambling in many body localization (2016), arXiv:1608.02765.

[59] R.-Q. He and Z.-Y. Lu, Characterizing many-body localization by out-of-time-ordered correlation, Phys. Rev. B **95**, 054201 (2017).

[60] C.-J. Lin and O. I. Motrunich, Out-of-time-ordered correlators in a quantum Ising chain, Phys. Rev. B **97**, 144304 (2018).

[61] J. Bao and C. Zhang, Out-of-time-order correlators in one-dimensional XY model (2019), arXiv:1901.09327.

[62] D. A. Roberts and B. Yoshida, Chaos and complexity by design, Journal of High Energy Physics **2017**, 121 (2017).

[63] Y. Huang, F. G. S. L. Brandão, and Y.-L. Zhang, Finite-size scaling of out-of-time-ordered correlators at late times, Phys. Rev. Lett. **123**, 010601 (2019).

[64] Y. Chen, Universal logarithmic scrambling in many body localization (2016), arXiv:1608.02765.

[65] J. K. Max McGinley, Andreas Nunnenkamp, Slow growth of entanglement and out-of-time-order correlators in integrable disordered systems (2018), arXiv:1807.06039.

[66] S. Pappalardi, A. Russomanno, B. B. Žunkovic, F. Iemini, A. Silva, and R. Fazio, Scrambling and entanglement spreading in long-range spin chains, Phys. Rev. B **98**, 134303 (2018).

[67] Q. Hummel, B. Geiger, J. D. Urbina, and K. Richter, Reversible quantum information spreading in many-body systems near criticality, Phys. Rev. Lett. **123**, 160401 (2019).

[68] K. Hashimoto, K.-B. Huh, K.-Y. Kim, and R. Watanabe, Exponential growth of out-of-time-order correlator without chaos: inverted harmonic oscillator, Journal of High Energy Physics **2020**, 68 (2020).

[69] S. Pilatowsky-Cameo, J. Chávez-Carlos, M. A. Bastarrachea-Magnani, P. Stránský, S. Lerma-Hernández, L. F. Santos, and J. G. Hirsch, Positive quantum Lyapunov exponents in experimental systems with a regular classical limit, Phys. Rev. E **101**, 010202(R) (2020).

[70] T. Xu, T. Scaffidi, and X. Cao, Does scrambling equal chaos?, Phys. Rev. Lett. **124**, 140602 (2020).

[71] W. Kirkby, D. H. J. O'Dell, and J. Mumford, False signals of chaos from quantum probes, Phys. Rev. A **104**, 043308 (2021).

[72] S. Xu and B. Swingle, Accessing scrambling using matrix product operators, Nature Physics **16**, 199–204 (2019).

[73] S. Xu and B. Swingle, Locality, quantum fluctuations, and scrambling, Physical Review X **9**, 031048 (2019).

[74] V. Khemani, D. A. Huse, and A. Nahum, Velocity-dependent Lyapunov exponents in many-body quantum, semiclassical, and classical chaos, Phys. Rev. B **98**, 144304 (2018).

[75] A. Nahum, S. Vijay, and J. Haah, Operator spreading in random unitary circuits, Phys. Rev. X **8**, 021014 (2018).

[76] C. W. von Keyserlingk, T. Rakovszky, F. Pollmann, and S. L. Sondhi, Operator hydrodynamics, OTOCs, and entanglement growth in systems without conservation laws, Phys. Rev. X **8**, 021013 (2018).

[77] S.-K. Jian and H. Yao, Universal properties of many-body quantum chaos at Gross-Neveu criticality (2018), arXiv:1805.12299.

[78] Y. Gu, X.-L. Qi, and D. Stanford, Local criticality, diffusion and chaos in generalized Sachdev-Ye-Kitaev models, Journal of High Energy Physics **2017**, 125 (2017).

[79] S. Sahu, S. Xu, and B. Swingle, Scrambling dynamics across a thermalization-localization quantum phase transition, Phys. Rev. Lett. **123**, 165902 (2019).

[80] T. Rakovszky, F. Pollmann, and C. W. von Keyserlingk, Diffusive hydrodynamics of out-of-time-ordered correlators with charge conservation, Phys. Rev. X **8**, 031058 (2018).

[81] S. H. Shenker and D. Stanford, Black holes and the butterfly effect, Journal of High Energy Physics **2014**, 67 (2014).

[82] A. A. Patel, D. Chowdhury, S. Sachdev, and B. Swingle, Quantum butterfly effect in weakly interacting diffusive metals, Phys. Rev. X **7**, 031047 (2017).

[83] D. Chowdhury and B. Swingle, Onset of many-body chaos in the $O(N)$ model, Phys. Rev. D **96**, 065005 (2017).

[84] V. Khemani, A. Vishwanath, and D. A. Huse, Operator Spreading and the Emergence of Dissipative Hydrodynamics under Unitary Evolution with Conservation Laws, Physical Review X **8**, 031057 (2018).

[85] N. Anand, G. Styliaris, M. Kumari, and P. Zanardi, Quantum coherence as a signature of chaos (2020), arXiv:2009.02760.

[86] S. Gopalakrishnan, D. A. Huse, V. Khemani, and R. Vasseur, Hydrodynamics of operator spreading and quasiparticle diffusion in interacting integrable systems, Phys. Rev. B **98**, 220303(R) (2018).

[87] P. L. Doussal, S. N. Majumdar, and G. Schehr, Large deviations for the height in 1D Kardar-Parisi-Zhang growth at late times, EPL (Europhysics Letters) **113**, 60004 (2016).

[88] C. Monthus and T. Garel, Probing the tails of the ground-state energy distribution for the directed polymer in a random medium of dimension $d = 1, 2, 3$ via a Monte Carlo procedure in the disorder, Phys. Rev. E **74**, 051109 (2006).

[89] I. V. Kolokolov and S. E. Korshunov, Universal and nonuniversal tails of distribution functions in the directed polymer and Kardar-Parisi-Zhang problems, Phys. Rev. B **78**, 024206 (2008).

[90] E. M. Fortes, I. García-Mata, R. A. Jalabert, and D. A. Wisniacki, Gauging classical and quantum integrability through out-of-time-ordered correlators, Phys. Rev. E **100**, 042201 (2019).

[91] E. M. Fortes, I. García-Mata, R. A. Jalabert, and D. A. Wisniacki, Signatures of quantum chaos transition in short spin chains, EPL (Europhysics Letters) **130**, 60001 (2020).

[92] J. Wang, G. Benenti, G. Casati, and W. Wang, Quantum chaos and the correspondence principle (2020), arXiv:2010.10360.

[93] J. Riddell and E. S. Sørensen, Out-of-time-order correlations in the quasiperiodic Aubry-André model, Phys. Rev. B **101**, 024202 (2020).

[94] J. Riddell, W. Kirkby, D. H. J. O'Dell, and E. S. Sørensen, Supplementary material (2021).

[95] E. H. Lieb and D. W. Robinson, The finite group velocity of quantum spin systems, Commun. Math. Phys. **28**, 251 (1972).

[96] M. Cheneau, P. Barmettler, D. Poletti, M. Endres, P. Schauß, T. Fukuhara, C. Gross, I. Bloch, C. Kollath, and S. Kuhr, Light-cone-like spreading of correlations in a quantum many-body system, Nature **481**, 484–487 (2012).

[97] T. Fukuhara, P. Schauß, M. Endres, S. Hild, M. Cheneau, I. Bloch, and C. Gross, Microscopic observation of magnon bound states and their dynamics, Nature **502**, 76–79 (2013).

[98] T. Langen, R. Geiger, M. Kuhnert, B. Rauer, and J. Schmiedmayer, Local emergence of thermal correlations in an isolated quantum many-body system, Nat. Phys. **9**, 643 (2013).

[99] P. Jurcevic, B. P. Lanyon, P. Hauke, C. Hempel, P. Zoller, R. Blatt, and C. F. Roos, Quasiparticle engineering and entanglement propagation in a quantum many-body system, Nature **511**, 202–205 (2014).

[100] P. M. Preiss, R. Ma, M. E. Tai, A. Lukin, M. Rispoli, P. Zupancic, Y. Lahini, R. Islam, and M. Greiner, Strongly correlated quantum walks in optical lattices, Science **347**, 1229 (2015).

[101] Y. Takasu, T. Yagami, H. Asaka, Y. Fukushima, K. Nagao, S. Goto, I. Danshita, and Y. Takahashi, Energy redistribution and spatiotemporal evolution of correlations after a sudden quench of the Bose-Hubbard model, Sci. Adv. **6**, eaba9255 (2020).

[102] P. Barmettler, D. Poletti, M. Cheneau, and C. Kollath, Propagation front of correlations in an interacting Bose gas, Phys. Rev. A **85**, 053625 (2012).

[103] V. Hunyadi, Z. Rácz, and L. Sasvári, Dynamic scaling of fronts in the quantum XX chain, Phys. Rev. E **69**, 066103 (2004).

[104] V. Eisler and Z. Rácz, Full counting statistics in a propagating quantum front and random matrix spectra, Phys. Rev. Lett. **110**, 060602 (2013).

[105] V. Eisler and F. Maislinger, Hydrodynamical phase transition for domain-wall melting in the XY chain, Phys. Rev. B **98**, 161117(R) (2018).

[106] V. Eisler and F. Maislinger, Front dynamics in the XY chain after local excitations, SciPost Physics **8**, 10.21468/scipostphys.8.3.037 (2020).

[107] M. Kormos, Inhomogeneous quenches in the transverse field Ising chain: scaling and front dynamics, SciPost Physics **3**, 10.21468/scipostphys.3.3.020 (2017).

[108] V. B. Bulchandani and C. Karrasch, Subdiffusive front scaling in interacting integrable models, Physical Review B **99**, 121410(R) (2019).

[109] J. Viti, J.-M. Stéphan, J. Dubail, and M. Haque, Inhomogeneous quenches in a free fermionic chain: Exact results, EPL (Europhysics Letters) **115**, 40011 (2016).

[110] G. Perfetto and A. Gambassi, Ballistic front dynamics after joining two semi-infinite quantum Ising chains, Physical Review E **96**, 012138 (2017).

[111] J.-M. Stéphan, Free fermions at the edge of interacting systems, SciPost Physics **6**, 10.21468/scipostphys.6.5.057 (2019).

[112] M. Fagotti, Higher-order generalized hydrodynamics in one dimension: The noninteracting test, Physical Review B **96**, 220302(R) (2017).

[113] S. Bhanu Kiran, D. A. Huse, and M. Kulkarni, Spatiotemporal spread of perturbations in power-law models at low temperatures: Exact results for OTOC (2020), arXiv:arXiv:2011.09320.

[114] W. Kirkby, J. Mumford, and D. H. J. O'Dell, Quantum caustics and the hierarchy of light cones in quenched spin chains, Phys. Rev. Research **1**, 033135 (2019).

[115] R. Thom, *Structural Stability and Morphogenesis* (Benjamin, Reading MA, 1975).

[116] V. I. Arnol'd, Critical points of smooth functions and their normal forms, Russ. Math. Survs. **30**, 1 (1975).

[117] L. Kelvin, Deep water ship-waves, Philos. Mag. **9**, 733 (1905).

[118] F. Ursell, *Ship Hydrodynamics, Water Waves and Asymptotics. Collected works of F. Ursell, 1946–1992*, Vol. 2 (World Scientific, Singapore, 1994).

[119] M. V. Berry, Singularities in waves and rays, in *Physics of Defects (1980)*, Vol. XXXV, edited by R. Balian and et al. (North-Holland Publishing, Amsterdam, 1981).

[120] J.-M. Stéphan and J. Dubail, Local quantum quenches in critical one-dimensional systems: entanglement, the Loschmidt echo, and light-cone effects, J. Stat. Mech. , P08019 (2011).

[121] P. Calabrese, F. H. L. Essler, and M. Fagotti, Quantum quench in the transverse field Ising chain: I. time evolution of order parameter correlators, J. Stat. Mech. , P07016 (2012).

[122] M. V. Berry and K. E. Mount, Semiclassical approximations in wave mechanics, Rep. Prog. Phys. **35**, 315 (1972).

[123] Y.-L. Zhang and V. Khemani, Asymmetric butterfly velocities in 2-local hamiltonians, SciPost Phys. **9**, 24 (2020).

[124] J. Li, R. Fan, H. Wang, B. Ye, B. Zeng, H. Zhai, X. Peng, and J. Du, Measuring out-of-time-order correlators on a nuclear magnetic resonance quantum simulator, Phys. Rev. X **7**, 031011 (2017).

[125] M. Gärttner, J. G. Bohnet, A. Safavi-Naini, M. L. Wall, J. J. Bollinger, and A. M. Rey, Measuring out-of-time-order correlations and multiple quantum spectra in a trapped-ion quantum magnet, Nat. Phys. **13**, 781 (2017).

[126] K. X. Wei, C. Ramanathan, and P. Cappellaro, Exploring localization in nuclear spin chains, Phys. Rev. Lett. **120**, 070501 (2018).

[127] K. A. Landsman, C. Figgatt, T. Schuster, N. M. Linke, B. Yoshida, N. Y. Yao, and C. Monroe, Verified quantum information scrambling, Nature **567**, 61 (2019).

[128] E. J. Meier, J. Ang'ong'a, F. A. An, , and B. Gadway, Exploring quantum signatures of chaos on a Floquet synthetic lattice, Phys. Rev. A **100**, 013623 (2019).

[129] M. Niknam, L. F. Santos, and D. G. Cory, Sensitivity of quantum information to environment perturbations measured with a nonlocal out-of-time-order correlation function, Phys. Rev.

Research **2**, 013200 (2020).
[130] M. Gring, M. Kuhnert, T. Langen, T. Kitagawa, B. Rauer, M. Schreitl, I. Mazets, D. Adu Smith, E. Demler, and J. Schmiedmayer, Relaxation and pre-thermalization in an isolated quantum system, Science **337**, 1318 (2012).
[131] F. H. L. Essler, S. Kehrein, S. R. Manmana, and N. J. Robinson, Quench dynamics in a model with tuneable integrability breaking, .
[132] B. Bertini and M. Fagotti, Pre-relaxation in weakly interacting models, J. Stat. Mech. , P07012 (2015).
[133] G. Brandino, J.-S. Caux, and R. Konik, Glimmers of a quantum KAM theorem: Insights from quantum quenches in one-dimensional Bose gases, Phys. Rev. X **5**, 041043 (2015).

Supplementary Material for "Scaling of wavefronts of out-of-time-ordered-correlators: integrable versus chaotic systems"

Jonathon Riddell,[1] Wyatt Kirkby,[1] D. H. J. O'Dell,[1] and Erik S. Sørensen[1]

[1]*Department of Physics & Astronomy, McMaster University 1280 Main St. W., Hamilton ON L8S 4M1, Canada.*

(Dated: November 11, 2021)

In these supplementary materials we give the details of the Airy function and its asymptotics, the calculation of OTOC wavefront in terms of the Airy function, the extraction of the butterfly velocity from the OTOC and also provide some alternative examples to those presented in the main text.

I. THE AIRY FUNCTION

The Airy function was constructed by the astronomer G. B. Airy in 1838 in order to describe the interference of light at a rainbow which is the simplest example of a caustic [1]. It has the integral representation

$$\mathrm{Ai}(z) = \frac{1}{2\pi}\int_{-\infty}^{\infty} \mathrm{d}s\ \mathrm{e}^{\mathrm{i}(zs+\frac{1}{3}s^3)}\ , \tag{SM1}$$

which can be interpreted as an elementary path integral where the paths being summed are labeled by s [2]. The key feature is that the phase is cubic in s; this means that it has a maximum of two stationary points (corresponding to two rays according to Fermat's principle) that merge at the point $z = 0$ which is the location of the caustic. Thus, the Airy function describes the interference between two waves when $z < 0$ (the interference fringes are the supernumerary arcs which can sometimes be observed inside the main bow) and one single evanescent wave when $z > 0$. For the calculation of the profile at very early times (far from the wavefront) we can use the $z \to \infty$ asymptotics of the Airy function which are given by [3],

$$\mathrm{Ai}(z) \sim \frac{\mathrm{e}^{-\frac{2}{3}z^{3/2}}}{2\sqrt{\pi}z^{1/4}}\sum_{n=0}^{\infty}(-1)^n\frac{u_n}{(\frac{2}{3})^n z^{3n/2}}\ , \tag{SM2}$$

where $u_n = (2n+1)(2n+3)...(6n-1)/(216^n n!)$. Truncating this series at $n = 0$ gives the universal $p = 1/2$ form of the OTOC in Eq. (4) in the main text for early entanglement growth in free systems. However, this asymptotic expansion is not valid close to the wavefront and that case is dealt with in the next section.

II. DERIVATION OF GAUSSIAN IN FREE MODELS

For models which can be mapped onto free-fermions, the Hamiltonian is,

$$\hat{H} = \sum_k \epsilon(k)\left(\tilde{b}_k^\dagger \tilde{b}_k - \frac{1}{2}\right) \tag{SM3}$$

where $\epsilon(k)$ is the dispersion relation. Starting with a single Bogoliubov localized Fermion,

$$\langle x_b|\mathrm{e}^{-\mathrm{i}\hat{H}t}\hat{b}^\dagger_{x=0}|0_b\rangle = \langle x_b|\sum_k \mathrm{e}^{-\mathrm{i}\epsilon(k)t}\,|k\rangle = \frac{1}{N}\sum_{k=-\frac{\pi}{a}}^{\frac{\pi}{a}-\frac{2\pi}{Na}}\mathrm{e}^{\mathrm{i}(kx-\epsilon(k)t)} \approx \frac{\sqrt{a}}{2\pi}\int_{-\frac{\pi}{a}}^{\frac{\pi}{a}}\mathrm{d}k\ \mathrm{e}^{\mathrm{i}(kx-\epsilon(k)t)}\ . \tag{SM4}$$

Now, we want to calculate the local form of the light cone via the focusing of trajectories. Using $\Phi = kx - \epsilon(k)t$, we require the conditions

$$\left.\frac{\partial\Phi}{\partial k}\right|_{k_c} = \left.\frac{\partial^2\Phi}{\partial k^2}\right|_{k_c} = 0\ , \tag{SM5}$$

to define the k_c. Hence, near the coalescing saddles of Φ,

$$\Phi \approx k_c x - \epsilon(k_c)t + (x - v_B t)(k-k_c) - \frac{1}{6}t\partial_k^3\epsilon(k_c)(k-k_c)^3 + \mathcal{O}(k^4)\ , \tag{SM6}$$

where $v_B = \partial_k \epsilon(k_c)$ is the butterfly velocity, and the second-order term vanishes since $\partial_k^2 \Phi(k_c) = \partial_k^2 \epsilon(k_c) = 0$. Assuming that the dispersion $\epsilon(k)$ only has two coalescing saddles, catastrophe theory indicates that the cubic form (a fold) is sufficient to qualitatively describe the local form of Φ. When a larger number of saddles coalesce one obtains one of the higher catastrophes (sometimes called generalized Airy functions), which we will not discuss here but an introduction in the context of spin chains can be found in Ref. [2]. Now, letting,

$$s^3 \equiv \frac{-t}{2} \partial_k^3 \epsilon(k_c)(k - k_c)^3 \tag{SM7}$$

and

$$z \equiv (x - v_B t) \left(\frac{-2}{\partial_k^3 \epsilon(k_c) t} \right)^{1/3} \tag{SM8}$$

Thus,

$$\Psi(x,t) \approx \frac{\sqrt{a}}{2\pi} \left(\frac{-2}{\partial_k^3 \epsilon(k_c) t} \right)^{1/3} \mathrm{e}^{\mathrm{i}(k_c x - \epsilon(k_c) t)} \int_{s_-}^{s_+} \mathrm{d}s \; \mathrm{e}^{\mathrm{i}(zs + \frac{1}{3}s^3)} \; , \tag{SM9}$$

where,

$$s_\pm = \left(\frac{-t}{2} \partial_k^3 \epsilon(k_c) \right)^{1/3} \left(\pm \frac{\pi}{a} - k_c \right) \; . \tag{SM10}$$

At sufficiently long times, these limits approach infinity and we recover the Airy function, which was defined in Eq. (SM1). $\mathrm{Ai}[z]$ can be approximated near $z = 0$ by making use of,

$$\ln\left(\mathrm{Ai}[z]\right) \approx -\frac{2}{3}\ln 3 - \ln(\Gamma[\frac{2}{3}]) - 3^{1/3}\frac{\Gamma[\frac{2}{3}]}{\Gamma[\frac{1}{3}]} z - \frac{1}{2}\left(3^{1/3}\frac{\Gamma[\frac{2}{3}]}{\Gamma[\frac{1}{3}]}\right)^2 z^2 + \frac{1}{3}\left(\frac{1}{2} - \frac{3\Gamma\left(\frac{2}{3}\right)^3}{\Gamma\left(\frac{1}{3}\right)^3}\right) z^3 + \mathcal{O}(z^4) \tag{SM11}$$

Thus, we expect the above wavefunctions to locally take the form,

$$\Psi(x,t) \approx \tilde{A} e^{-\tilde{m}(x - v_B t)^2} e^{-\tilde{b}(x - v_B t)} e^{-\zeta(x - v_B t)^3} ..., \tag{SM12}$$

where,

$$\tilde{A} = \frac{\sqrt{a}}{\pi \Gamma[\frac{2}{3}]} \left(\frac{-1}{36 \partial_k^3 \epsilon(k_c) t} \right)^{1/3} \mathrm{e}^{\mathrm{i}(k_c x - \epsilon(k_c) t)} \tag{SM13}$$

$$\tilde{m} = \frac{1}{2} \left(\frac{-6}{\partial_k^3 \epsilon(k_c)} \right)^{2/3} \left(\frac{\Gamma[\frac{2}{3}]}{\Gamma[\frac{1}{3}]} \right)^2 t^{-2/3} \tag{SM14}$$

$$\tilde{b} = \frac{\Gamma[\frac{2}{3}]}{\Gamma[\frac{1}{3}]} \left(\frac{-6}{\partial_k^3 \epsilon(k_c)} \right)^{1/3} t^{-1/3} \tag{SM15}$$

$$\zeta = -\frac{2}{3\partial_k^3 \epsilon(k_c)} \left(\frac{1}{2} - \frac{3\Gamma\left(\frac{2}{3}\right)^3}{\Gamma\left(\frac{1}{3}\right)^3} \right) t^{-1} \tag{SM16}$$

Each term in the exponential contains factors of the form $\frac{(x - v_B t)^n}{t^{n/3}}$ for integer n. Assuming close proximity to the light cone relative to the distance from the origin, such that $\delta x \equiv x - v_B t$, with $\delta x / x \ll 1$, then,

$$\frac{\delta x}{t^{1/3}} \approx \left(\frac{v_B}{x} \right)^{1/3} \delta x + \frac{1}{3} \left(\frac{v_B}{x^4} \right)^{1/3} \delta x^2 + \frac{2}{9} \left(\frac{v_B}{x^7} \right)^{1/3} \delta x^3 + ... \tag{SM17}$$

$$\frac{\delta x^2}{t^{2/3}} \approx \frac{1}{3} \left(\frac{v_B^2}{x^2} \right)^{1/3} \delta x^2 + \frac{2}{3} \left(\frac{v_B^2}{x^5} \right)^{1/3} \delta x^3 + \frac{5}{9} \left(\frac{v_B^2}{x^8} \right)^{1/3} \delta x^4 + ... \tag{SM18}$$

$$\frac{\delta x^3}{t} \approx \left(\frac{v_B}{x} \right) \delta x^3 + \left(\frac{v_B}{x} \right) \delta x^4 + \left(\frac{v_B}{x} \right) \delta x^5 + ... \tag{SM19}$$

Keeping terms of order lower than $\mathcal{O}(\delta x / x)$, amounts to replacing each factor of t with x / v_B. Note that the second-order term in Eq. (SM17) is suppressed by a factor of $x^{-2/3} v_B^{-1/3}$ when compared to the lowest-order term of Eq. (SM18), and so at

large x there is no need to consider both, although including them will provide lowest-order corrections to $\tilde{m}$ and $\tilde{b}$ at fixed x. Furthermore, all the terms in Eq. (SM19) can be neglected since any term of cubic order or above in δx will not only be small, but also further suppressed by at least x^{-1}. Therefore our Gaussian approximation remains valid, and we can then rewrite Eq. (SM12) by replacing $t \to x/v_B$ in Eqs. (SM13)-(SM16). Thus we define the Gaussian form,

$$\Psi_G(x,t) \equiv Ae^{-m(x-v_Bt)^2}e^{-b(x-v_Bt)} \tag{SM20}$$

such that $C_G(x,t) = |\Psi_G(x,t)|^2$ approximates the OTOC near the wavefront according to Eq. (5) of the main text, now with,

$$A = \frac{\sqrt{a}}{\pi\Gamma[\frac{2}{3}]}\left(\frac{-v_B}{36\partial_k^3\epsilon(k_c)x}\right)^{1/3} \mathrm{e}^{\mathrm{i}(k_cx-\epsilon(k_c)t)} \tag{SM21}$$

$$m = \frac{1}{2}\left(\frac{-6v_B}{\partial_k^3\epsilon(k_c)}\right)^{2/3}\left(\frac{\Gamma[\frac{2}{3}]}{\Gamma[\frac{1}{3}]}\right)^2 x^{-2/3} \tag{SM22}$$

$$b = \frac{\Gamma[\frac{2}{3}]}{\Gamma[\frac{1}{3}]}\left(\frac{-6v_B}{\partial_k^3\epsilon(k_c)}\right)^{1/3} x^{-1/3} \tag{SM23}$$

from which Eq. (11) of the main text follows directly.

From Eq. (SM20), and $C_G(x,t) = |\Psi_G(x,t)|^2$, it follows that exactly along the wavefront, there is a scaling $C(x = v_Bt, t) \sim x^{-2/3}$. This was verified numerically for the XX model in Fig. SM1, for $1 \leq x \leq 100$, giving an approximate amplitude scaling of $C(x = v_Bt, t) \sim x^{-0.664}$ at less than 0.5% error.

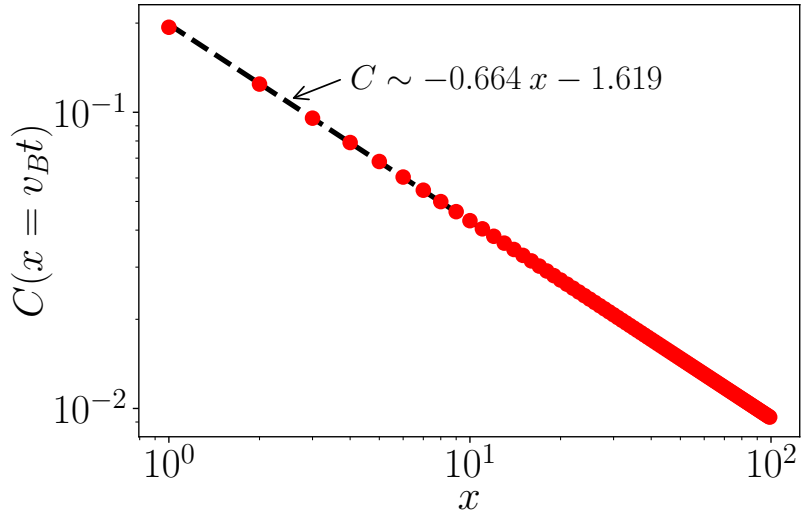

Figure SM1. OTOC amplitude scaling at the wavefront. Red circles indicate the amplitude of C evaluated along the light cone ($x = v_Bt$) as a function of the site number. A linear fit to the log-log data is shown as a black-dashed line.

III. VELOCITY

In this section we follow [4, 5] and extract the butterfly velocity from the OTOC using velocity dependent Lyapunov exponents. This method supposes that,

$$C(x,t) \sim e^{\lambda(v)t}, \tag{SM24}$$

such that,

$$\lambda(v) \sim -(v - v_B)^\alpha. \tag{SM25}$$

We can therefore find the butterfly velocities by looking for constant rays in the OTOC data such that $\lambda(v) = 0$. In this study however we do not limit ourselves to rays $x = vt$ for a set of velocities, we instead allow the rays to have a constant shift in

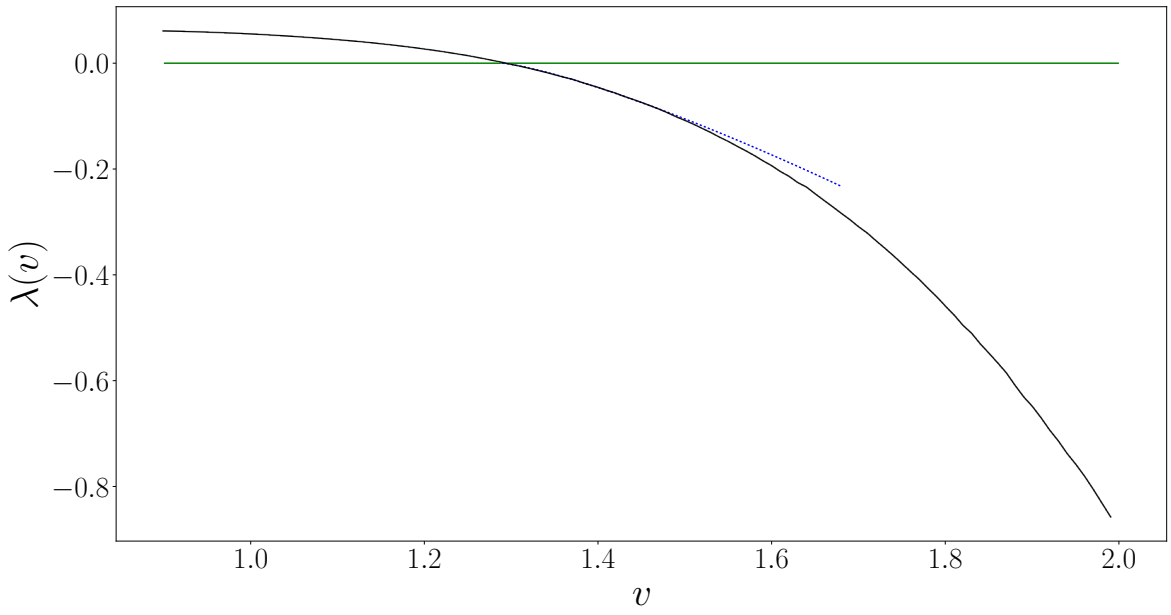

Figure SM2. Velocity dependent Lyapunov exponent plotted against velocities v. Horizontal green line indicates the velocity axis, the solid black line is $\lambda(v)$ and the blue dotted line is our fit for $\lambda(v) \sim -(v - v_B)^\alpha$.

time to account for the possibility that the form in Eq. (SM24) fits better before the classical wave-front arrives. We therefore investigate and fit the contours given by,

$$t = \frac{x}{v} - t_s, \tag{SM26}$$

where t_s is the shift time we vary from $t_s = 0 \to 1$. We then select the time shift with the most numerical agreement with Eq. (SM24).

We find numerically that,

$$\alpha \approx 1.2801 \pm 0.0009, \;\; v_B = 1.29, \;\; t_s \approx 0.108 \tag{SM27}$$

IV. ALTERNATIVE EXAMPLE

In this section we discuss an example where $m(x)$ does not scale as $\sim b(x)^2$ demonstrating that this behavior is not generic and the ETH obeying models may have corrections to the scaling of $m(x)$ independent of $b(x)$. We start be re-parametrizing our Hamiltonian in Eq. (6) for convenience. We restrict the possible parameter choices in our Hamiltonian as,

$$\hat{H} = \sum_{n=1,2} J_n \sum_j \left(\hat{S}_j^X \hat{S}_{j+n}^X + \hat{S}_j^Y \hat{S}_{j+n}^Y + \Delta \hat{S}_j^Z \hat{S}_{j+n}^Z \right). \tag{SM28}$$

Here we choose values of $J_1 = -1$, $J_2 = 0.3703704$ and $\Delta = 0.75$ which corresponds to a chiral phase of the ground state [6]. We similarly determine the butterfly velocity as in section III, and find that,

$$\alpha \approx 1.2964 \pm 0.0004, \;\; v_B = 1.26, \;\; t_s \approx 0.06. \tag{SM29}$$

This then allows us to reconfirm that the Gaussian wave can be confirmed for each x, shown in Fig. SM3. The fitting interval was again on an interval of length $\Delta t = 1$ indicating a large dynamical regime of validity. With this we can extract the forms of $m(x)$ and $b(x)$ which again decay exponentially.

In Fig. SM4 we again see that,

$$b(x) \sim e^{-cx}, \;\; m(x) \sim e^{-wx}. \tag{SM30}$$

However this time, we get the behavior that, $c = 0.2666 \pm 0.0003$ and $w = 0.398 \pm 0.0009$, therefore we see that $w \not\approx 2c$. We can see why this might be the case with a simple derivation of the form of Eq. (5) in the main text.

We are interested solely in the dynamical region centred around $t = x/v_B$. With standard expansions one can arrive at the propagating Gaussian form. Let $\tau = t - \frac{x}{v_B}$ and $\Delta = \frac{\dot{C}\left(x, \frac{x}{v_B}\right)}{C\left(x, \frac{x}{v_B}\right)}$. Since $C(x,t)$ is a positive function for the regime we are interested in,

$$C(x,t) = \exp\left[\ln C(x,t)\right], \tag{SM31}$$

this allows us to expand inside the logarithm,

$$C(x,t) = Ke^{\ln\left(1+\Delta\tau+\mathbb{O}\left[\frac{\ddot{C}\left(x,\frac{x}{v_B}\right)}{C\left(x,\frac{x}{v_B}\right)}\tau^2\right]\right)}, \tag{SM32}$$

$$= Ke^{\ln(1+\Delta\tau)+\ln\left(1+\mathbb{O}\left[\frac{\ddot{C}\left(x,\frac{x}{v_B}\right)}{C\left(x,\frac{x}{v_B}\right)\Delta(1+\tau)}\tau^2\right]\right)}. \tag{SM33}$$

Expanding one more time we arrive at,

$$C(x,t) = Ke^{\Delta\tau-\frac{1}{2}\Delta^2\tau^2+\mathbb{O}\left(\frac{1}{3}\Delta^3\tau^3\right)+\mathbb{O}\left[\frac{\ddot{C}\left(x,\frac{x}{v_B}\right)}{\dot{C}\left(x,\frac{x}{v_B}\right)(1+\tau)}\tau^2\right]}. \tag{SM34}$$

In Eq. (SM34) we see that the first order term and the second order term are related by squaring the first order term if,

$$\frac{\ddot{C}\left(x,\frac{x}{v_B}\right)}{\dot{C}\left(x,\frac{x}{v_B}\right)(1+\tau)} \approx 0. \tag{SM35}$$

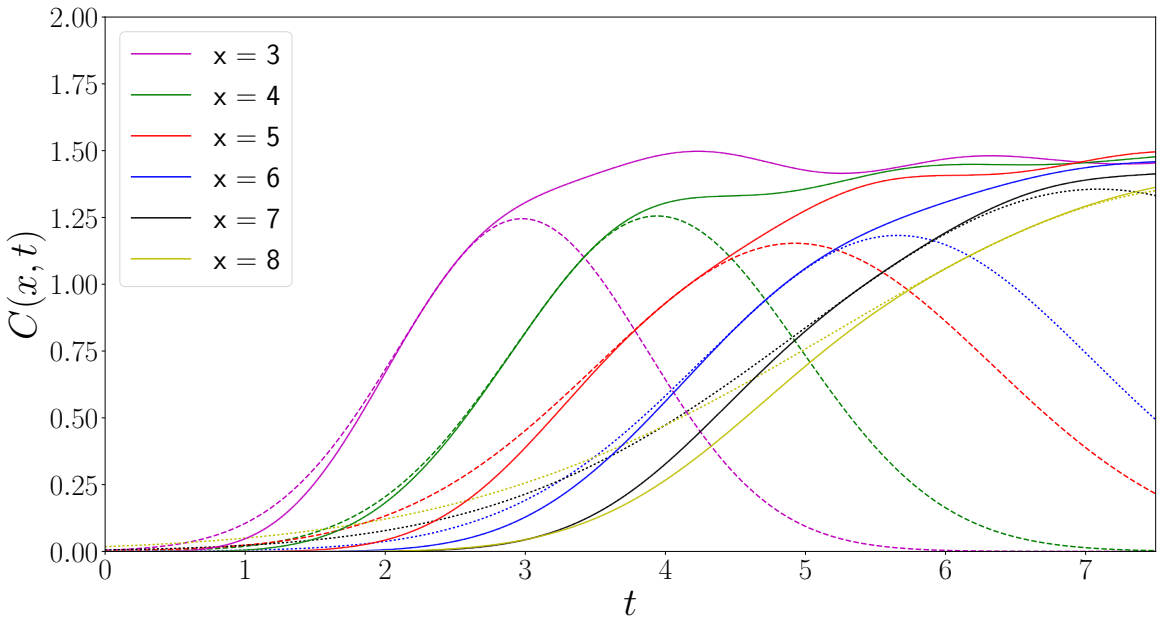

Figure SM3. $C(x,t)$ for the Hamiltonian in Eq. (SM28). Solid lines indicate the OTOC data, and dashed lines are the fitted Gaussian waveform given in Eq. (5) in the main text. Errors on the fits are on the order of 10^{-7} to 10^{-9} for all fitting parameters. The interval fitted is of total length $\Delta t = 1$ centred around $x = v_B t$.

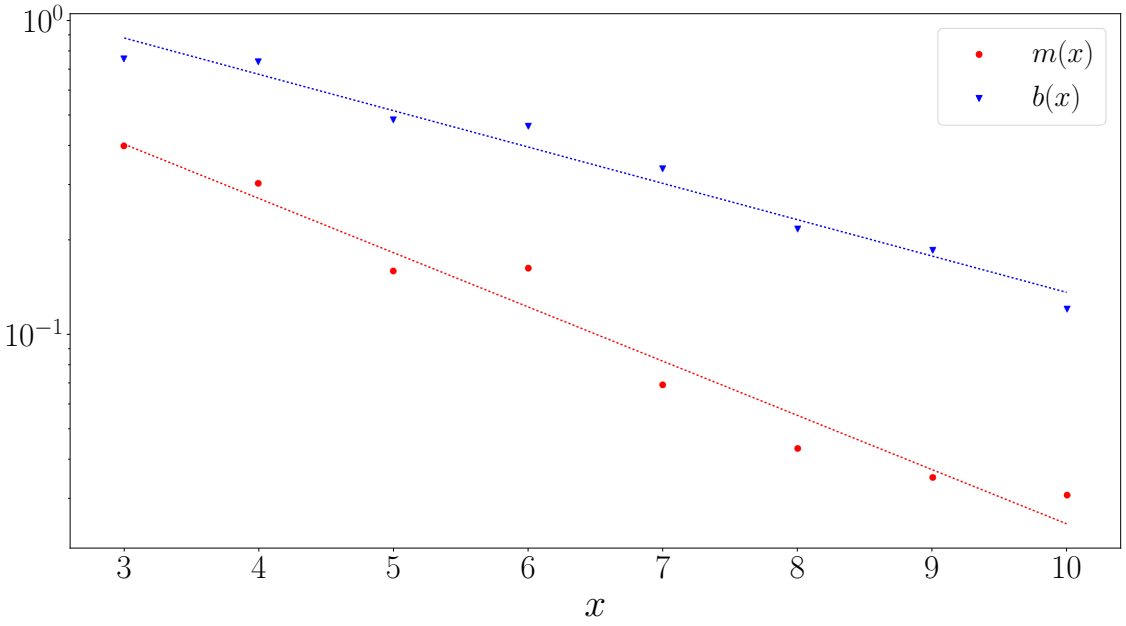

Figure SM4. Log-linear plot for $m(x)$ and $b(x)$ for the Hamiltonian characterized by the Hamiltonian in Eq. (SM28). Solid circles indicate data points from the fitting in Fig. SM3 and dashed lines indicate a fit to a linear equation. This rough linear scaling indicates the points are falling off exponentially fast.

This is of course not always the case. However for free fermions it turns out this is true for sufficiently large x. In the case of free fermions, the OTOC given in Eq. (7) in the main text experiences a change in curvature at the light cone. At a given fixed lattice point at large x, $C(x, t = \frac{x}{v_B})$ is an inflection point in a slice along the temporal direction. This property is inherited from the local Airy description, where $\mathrm{Ai}''[z] = z\mathrm{Ai}[z]$, and hence $\mathrm{Ai}''[0] = 0$. This interestingly allows one to approximate the butterfly velocity (for free models) as,

$$v_B \equiv \frac{x}{t_*} \quad , \tag{SM36}$$

for which one defines t_* such that,

$$\frac{d^2}{dt^2} C(x,t)\Big|_{t=t^*} = 0 \tag{SM37}$$

In Fig. SM5 we see that for free fermions this conjecture approximates the butterfly velocity to $v_B \approx 0.988$ which corresponds to a 1.21% difference. This method is however unreliable in the cases where only small x are accessible.

[1] G. B. Airy, On the intensity of light in the neighbourhood of a caustic, Trans. Cambridge Philos. Soc. **6**, 379 (1838).

[2] W. Kirkby, J. Mumford, and D. H. J. O'Dell, Quantum caustics and the hierarchy of light cones in quenched spin chains, Phys. Rev. Research **1**, 033135 (2019).

[3] NIST Digital Library of Mathematical Functions. http://dlmf.nist.gov/, Release 1.1.1 of 2021-03-15. F. W. J. Olver, A. B. Olde Daalhuis, D. W. Lozier, B. I. Schneider, R. F. Boisvert, C. W. Clark, B. R. Miller, B. V. Saunders, H. S. Cohl, and M. A. McClain, eds.

[4] V. Khemani, D. A. Huse, and A. Nahum, Velocity-dependent Lyapunov exponents in many-body quantum, semiclassical, and classical chaos, Phys. Rev. B **98**, 144304 (2018).

[5] Y.-L. Zhang and V. Khemani, Asymmetric butterfly velocities in 2-local hamiltonians, SciPost Phys. **9**, 24 (2020).

[6] S. Furukawa, M. Sato, and S. Onoda, Chiral order and electromagnetic dynamics in one-dimensional multiferroic cuprates, Phys. Rev. Lett. **105**, 257205 (2010).

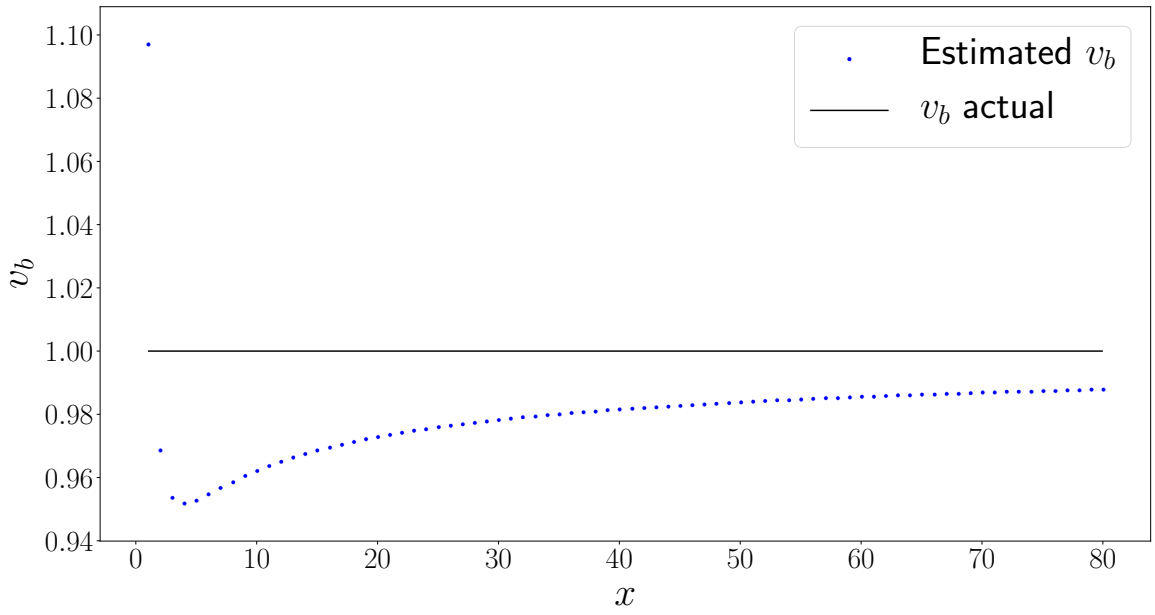

Figure SM5. Numerical estimate of v_B for the free model characterized by $\vec{c}_f$. Where $m = \frac{L}{2}$ and $x = |m - n|$. The system size used was $L = 1600$, and the data estimated roots with time steps of $\Delta t = 10^{-4}$. Roots were estimated within $\pm 10^{-5}$ of zero.

Chapter 6

Summary and conclusion

In this thesis we reviewed how statistical mechanics can emerge in isolated quantum systems in chapter 2. We did this by first establishing how static equilibrium can emerge for observables and subsystems. We found that the purity of the diagonal ensemble is a strong indicator of the emergence of static equilibrium,

$$\text{Tr}\left[\omega^2\right] \ , \omega = \sum_k |c_k|^2 |E_k\rangle\langle E_k|. \tag{6.1}$$

If equilibrium is well defined we came to the conclusion that the expectation values of the diagonal ensemble were the static equilibrium expectation values,

$$A(\infty) = \text{Tr}\left[\hat{A}\omega\right]. \tag{6.2}$$

It was briefly discussed that, despite a number of strong infinite time analytical results being available, the field has many open problems regarding finite time descriptions of the path to equilibrium.

We then derived the microcanonical ensemble $\tau_{u,\delta}$ and the Gibbs ensemble ρ_β using Jaynes' principle of maximum entropy. These are the traditional ensembles studied in statistical mechanics. It was noted that $\omega \neq \tau_{u,\delta} \neq \rho_\beta$ globally, but equivalence of ensemble results allow us to equate $\tau_{u,\delta}$ and ρ_β on subsystems of the total system. Eigenstate thermalization was introduced to equate the expectation values of the microcanonical ensemble and the diagonal ensemble,

$$A(\infty) = \text{Tr}\left[\hat{A}\omega\right] = \sum_k |c_k|^2 A_{k,k} \approx \text{Tr}\left[\hat{A}\tau_{u,\delta}\right] = \frac{1}{\Omega}\sum_{k\in T_{u,\delta}} A_{k,k}, \tag{6.3}$$

by requiring that the diagonal entries of the observable $\hat{A}$ are well approximated by a smooth function of energy $\hat{A}_{k,k} \approx A(E_k)$. We expect this to be an exact expression in the thermo-

dynamic limit. Eigenstate thermalization was the key ingredient introduced to connect our notion of static equilibrium to the predictions of statistical mechanics. Notably little progress has been made analytically on the validity of eigenstate thermalization despite an abundance of numerical work verifying it.

We next introduced the weak form of the eigenstate thermalization hypothesis that requires that typical eigenstates obey the hypothesis. We discussed analytical progress that has been made in this direction, which provides a proof of weak ETH for locally interacting, translation invariant interacting models. We then briefly derived consequences of these statements. Volume law scaling of eigenstate entanglement entropy was then discussed as an indicator of eigenstate thermalization.

We then finished the introductory section by introducing classes of models which do not fit into this description. These classes of models can be broadly put into two categories. Models which thermalize to a generalized Gibbs ensemble due to the presence of a large collection of conserved quantities in the dynamics. The second class of models are localized models, which lack the transport required to thermalize the systems in question.

In chapter 3 we investigated the early time relaxation of pure states towards equilibrium. We found that, if the initial condition lacked transport and was sufficiently well behaved, the initial dynamics looked identical to the dynamics of the Kubo formula from linear response theory, and the late time fluctuation correlation function defined in [9]. We proposed a possible equilibration, fluctuation, dissipation relation,

$$\sigma_A \approx \sigma_G \approx \sigma_K, \tag{6.4}$$

relating the early time relaxation of these three processes together. Random matrix theory arguments were used to show that in the infinite temperature regime the corrections to equation 6.4 should be on the order of $\mathbb{O}(1/d^N)$ where d^N is the Hilbert space size. Notably however, it was easy to find initial conditions where this was not true. Further work is required to investigate if the initial conditions that don't fall into this description can be potentially captured by higher order response theory or some other approach.

In chapter 4 we derived a number of results pertaining to equilibration and recurrence times. In particular we derived the equations 2.19, 2.20 and 2.134. We showed that the expectation value of $\langle\psi|\hat{A}(t)|\psi\rangle$ concentrates about the equilibrium point $A(\infty)$, and used this bound to show the average recurrence time would approach infinity in the thermodynamic limit for typical dynamics. Despite the strength of these results, they come at the cost of strong assumptions on the energies of the model, namely that the spectrum is non-degenerate, the frequencies are non-degenerate and so on. Further work is required to relax

the assumptions on the spectrum and investigate the consequences of doing so.

In chapter 5 we investigated the possibility of distinguishing quantum chaotic systems from non-chaotic systems with information from the OTOC wavefront. We conclude that, despite the universal waveform not carrying such information, the classical wavefront at $x = v_B t$ does in fact carry that information in the form of a Gaussian wave form,

$$C(x,t) \sim e^{-m(x)(x-v_B t)^2 + b(x)(x-v_B t)}, \tag{6.5}$$

where the functions $m(x), b(x)$ scaling like a power law in free models and exponentially in chaotic models. Further work is required to investigate if this Gaussian waveform tells us about the interacting integrable regime, and if similar descriptions and scaling are found in other models.

Bibliography

[1] Luca D'Alessio, Yariv Kafri, Anatoli Polkovnikov, and Marcos Rigol. From quantum chaos and eigenstate thermalization to statistical mechanics and thermodynamics. *Advances in Physics*, 65(3):239–362, 2016.

[2] Christian Gogolin and Jens Eisert. Equilibration, thermalisation, and the emergence of statistical mechanics in closed quantum systems. *Reports on Progress in Physics*, 79(5):056001, apr 2016.

[3] Immanuel Bloch, Jean Dalibard, and Wilhelm Zwerger. Many-body physics with ultracold gases. *Rev. Mod. Phys.*, 80:885–964, Jul 2008.

[4] Sandu Popescu, Anthony J. Short, and Andreas Winter. Entanglement and the foundations of statistical mechanics. *Nature Physics*, 2(11):754–758, 2006.

[5] Sheldon Goldstein, Joel L. Lebowitz, Roderich Tumulka, and Nino Zanghì. Canonical typicality. *Phys. Rev. Lett.*, 96:050403, Feb 2006.

[6] Noah Linden, Sandu Popescu, Anthony J. Short, and Andreas Winter. Quantum mechanical evolution towards thermal equilibrium. *Phys. Rev. E*, 79:061103, Jun 2009.

[7] Günter Mahler, Jochen Gemmer, and Mathias Michel. Emergence of thermodynamic behavior within composite quantum systems. *Physica E: Low-dimensional Systems and Nanostructures*, 29(1):53–65, 2005. Frontiers of Quantum.

[8] J. M. Deutsch. Quantum statistical mechanics in a closed system. *Phys. Rev. A*, 43:2046–2049, Feb 1991.

[9] M. Srednicki. The approach to thermal equilibrium in quantized chaotic systems. *Journal of Physics A: Mathematical and General*, 32(7):1163, 1999.

[10] Mark Srednicki. Chaos and quantum thermalization. *Phys. Rev. E*, 50:888–901, Aug 1994.

[11] A.J. Berlinsky and A.B. Harris. *Statistical Mechanics: An Introductory Graduate Course*. Graduate Texts in Physics. Springer International Publishing, 2020.

[12] R.K. Pathria. *Statistical Mechanics*. International series of monographs in natural philosophy. Elsevier Science & Technology Books, 1972.

[13] Chaitanya Murthy, Arman Babakhani, Fernando Iniguez, Mark Srednicki, and Nicole Yunger Halpern. Non-abelian eigenstate thermalization hypothesis, 2022.

[14] Christian Gramsch and Marcos Rigol. Quenches in a quasidisordered integrable lattice system: Dynamics and statistical description of observables after relaxation. *Phys. Rev. A*, 86:053615, Nov 2012.

[15] Jonathon Riddell and Erik S. Sørensen. Out-of-time-order correlations in the quasiperiodic aubry-andré model. *Phys. Rev. B*, 101:024202, Jan 2020.

[16] Lucas Hackl, Lev Vidmar, Marcos Rigol, and Eugenio Bianchi. Average eigenstate entanglement entropy of the xy chain in a transverse field and its universality for translationally invariant quadratic fermionic models. *Phys. Rev. B*, 99:075123, Feb 2019.

[17] Martí Perarnau-Llobet, Arnau Riera, Rodrigo Gallego, Henrik Wilming, and Jens Eisert. Work and entropy production in generalised gibbs ensembles. *New Journal of Physics*, 18(12):123035, 2016.

[18] Jonathon Riddell and Markus P. Müller. Generalized eigenstate typicality in translation-invariant quasifree fermionic models. *Phys. Rev. B*, 97:035129, Jan 2018.

[19] Sushruth Muralidharan, Kinjalk Lochan, and S. Shankaranarayanan. Generalized thermalization for integrable system under quantum quench. *Phys. Rev. E*, 97:012142, Jan 2018.

[20] Serge Aubry and Gilles André. Analyticity breaking and anderson localization in incommensurate lattices. *Proceedings, VIII International Colloquium on Group-Theoretical Methods in Physics*, 3, 01 1980.

[21] Rahul Nandkishore and David A. Huse. Many-body localization and thermalization in quantum statistical mechanics. *Annual Review of Condensed Matter Physics*, 6(1):15–38, 2015.

[22] Lev Vidmar and Marcos Rigol. Generalized gibbs ensemble in integrable lattice models. *Journal of Statistical Mechanics: Theory and Experiment*, 2016(6):064007, jun 2016.

[23] Luis Pedro García-Pintos, Noah Linden, Artur S. L. Malabarba, Anthony J. Short, and Andreas Winter. Equilibration time scales of physically relevant observables. *Phys. Rev. X*, 7:031027, Aug 2017.

[24] A. J. Short. Equilibration of quantum systems and subsystems. *New Journal of Physics*, 13(5):053009, 2011.

[25] A. J. Short and T. C. Farrelly. Quantum equilibration in finite time. *New Journal of Physics*, 14(1):013063, 2012.

[26] N. Linden, S. Popescu, A. J. Short, and A. Winter. Quantum mechanical evolution towards thermal equilibrium. *Phys. Rev. E*, 79:061103, Jun 2009.

[27] P. Reimann. Foundation of statistical mechanics under experimentally realistic conditions. *Physical Review Letters*, 101(19), Nov 2008.

[28] J. Eisert, M. Friesdorf, and C. Gogolin. Quantum many-body systems out of equilibrium. *Nature Physics*, 11:124 EP –, Feb 2015. Review Article.

[29] L. Campos Venuti. *Theory of Temporal Fluctuations in Isolated Quantum Systems*, pages 203–219.

[30] Lorenzo Campos Venuti and Paolo Zanardi. Universality in the equilibration of quantum systems after a small quench. *Physical Review A*, 81(3), mar 2010.

[31] Jonathon Riddell, Nathan Pagliaroli, and Álvaro M. Alhambra. Concentration of quantum equilibration and an estimate of the recurrence time, 2022.

[32] Martin C. Gutzwiller. Periodic orbits and classical quantization conditions. *Journal of Mathematical Physics*, 12(3):343–358, 1971.

[33] Michael Victor Berry, M. Tabor, and John Michael Ziman. Closed orbits and the regular bound spectrum. *Proceedings of the Royal Society of London. A. Mathematical and Physical Sciences*, 349(1656):101–123, 1976.

[34] Noah Linden, Sandu Popescu, Anthony J Short, and Andreas Winter. On the speed of fluctuations around thermodynamic equilibrium. *New Journal of Physics*, 12(5):055021, may 2010.

[35] P. Reimann. Canonical thermalization. *New Journal of Physics*, 12(5):055027, May 2010.

[36] G. Casati, F. Valz-Gris, and I. Guarnieri. On the connection between quantization of nonintegrable systems and statistical theory of spectra. *Lettere al Nuovo Cimento (1971-1985)*, 28(8):279–282, Jun 1980.

[37] O. Bohigas, M. J. Giannoni, and C. Schmit. Characterization of chaotic quantum spectra and universality of level fluctuation laws. *Phys. Rev. Lett.*, 52:1–4, Jan 1984.

[38] Thomas Guhr, Axel Müller–Groeling, and Hans A. Weidenmüller. Random-matrix theories in quantum physics: common concepts. *Physics Reports*, 299(4):189–425, 1998.

[39] H. Wilming, M. Goihl, I. Roth, and J. Eisert. Entanglement-ergodic quantum systems equilibrate exponentially well. *Phys. Rev. Lett.*, 123:200604, Nov 2019.

[40] Jonathon Riddell, Luis Pedro García-Pintos, and Álvaro M. Alhambra. Relaxation of non-integrable systems and correlation functions, 2021.

[41] Anatoly Dymarsky. Mechanism of macroscopic equilibration of isolated quantum systems. *Physical Review B*, 99(22), jun 2019.

[42] A. S. L. Malabarba, L. P. García-Pintos, N. Linden, T. C. Farrelly, and A. J. Short. Quantum systems equilibrate rapidly for most observables. *Phys. Rev. E*, 90:012121, Jul 2014.

[43] S. Goldstein, T. Hara, and H. Tasaki. Time scales in the approach to equilibrium of macroscopic quantum systems. *Phys. Rev. Lett.*, 111:140401, Oct 2013.

[44] Anatoly Dymarsky. Bound on eigenstate thermalization from transport, 2018.

[45] Jonathan Lux, Jan Müller, Aditi Mitra, and Achim Rosch. Hydrodynamic long-time tails after a quantum quench. *Phys. Rev. A*, 89:053608, May 2014.

[46] Mike Blake. Universal charge diffusion and the butterfly effect in holographic theories. *Phys. Rev. Lett.*, 117:091601, Aug 2016.

[47] W. Miller. *Symmetry Groups and Their Applications*. Computer Science and Applied Mathematics. Academic Press, 1972.

[48] Henrik Wilming, Thiago R. de Oliveira, Anthony J. Short, and Jens Eisert. *Equilibration Times in Closed Quantum Many-Body Systems*, pages 435–455. Springer International Publishing, Cham, 2018.

[49] Álvaro M. Alhambra, Jonathon Riddell, and Luis Pedro García-Pintos. Time evolution of correlation functions in quantum many-body systems. *Phys. Rev. Lett.*, 124:110605, Mar 2020.

[50] Jonas Richter, Jochen Gemmer, and Robin Steinigeweg. Impact of eigenstate thermalization on the route to equilibrium. *Phys. Rev. E*, 99:050104, May 2019.

[51] Jonas Richter and Robin Steinigeweg. Relation between far-from-equilibrium dynamics and equilibrium correlation functions for binary operators. *Phys. Rev. E*, 99:012114, Jan 2019.

[52] Elena Tartaglia, Pasquale Calabrese, , and Bruno Bertini. Real-Time Evolution in the Hubbard Model with Infinite Repulsion. *SciPost Phys.*, 12:28, 2022.

[53] Alvise Bastianello, Bruno Bertini, Benjamin Doyon, and Romain Vasseur. Introduction to the special issue on emergent hydrodynamics in integrable many-body systems. *Journal of Statistical Mechanics: Theory and Experiment*, 2022(1):014001, jan 2022.

[54] M. Gluza, C. Krumnow, M. Friesdorf, C. Gogolin, and J. Eisert. Equilibration via gaussification in fermionic lattice systems. *Phys. Rev. Lett.*, 117:190602, Nov 2016.

[55] Marek Gluza, Jens Eisert, and Terry Farrelly. Equilibration towards generalized gibbs ensembles in non-interacting theories. *arXiv:1809.08268*, 2018.

[56] Mark Srednicki Chaitanya Murthy. On relaxation to gaussian and generalized gibbs states in systems of particles with quadratic hamiltonians. *arXiv.org*, 2018.

[57] Lea F. Santos and E. Jonathan Torres-Herrera. Analytical expressions for the evolution of many-body quantum systems quenched far from equilibrium. *AIP Conference Proceedings*, 1912(1):020015, 2017.

[58] H. Poincaré. *Sur le problème des trois corps et les équations de la dynamique, par H. Poincaré*, volume 13 of *Acta Mathematica*. 1890.

[59] P. Bocchieri and A. Loinger. Quantum recurrence theorem. *Phys. Rev.*, 107:337–338, Jul 1957.

[60] Ian C. Percival. Almost periodicity and the quantal h theorem. *Journal of Mathematical Physics*, 2(2):235–239, 1961.

[61] L. S. Schulman. Note on the quantum recurrence theorem. *Phys. Rev. A*, 18:2379–2380, Nov 1978.

[62] T. Hogg and B. A. Huberman. Recurrence phenomena in quantum dynamics. *Phys. Rev. Lett.*, 48:711–714, Mar 1982.

[63] Rocco Duvenhage. Recurrence in quantum mechanics. *International Journal of Theoretical Physics*, 41(1):45–61, Jan 2002.

[64] David Wallace. Recurrence theorems: A unified account. *Journal of Mathematical Physics*, 56(2):022105, 2015.

[65] Lorenzo Campos Venuti. The recurrence time in quantum mechanics, 2015.

[66] Kamal Bhattacharyya and Debashis Mukherjee. On estimates of the quantum recurrence time. *The Journal of Chemical Physics*, 84(6):3212–3214, 1986.

[67] E. T. Jaynes. Information theory and statistical mechanics. *Phys. Rev.*, 106:620–630, May 1957.

[68] Ingemar Bengtsson and Karol Zyczkowski. *Geometry of Quantum States: An Introduction to Quantum Entanglement*. Cambridge University Press, 2006.

[69] Fabio Anza. New equilibrium ensembles for isolated quantum systems. *Entropy*, 20(10):744, sep 2018.

[70] Álvaro M. Alhambra. Quantum many-body systems in thermal equilibrium, 2022.

[71] Fernando G. S. L. Brandao and Marcus Cramer. Equivalence of statistical mechanical ensembles for non-critical quantum systems. *arXiv:1502.03263*, 2015.

[72] Markus P. Müller, Emily Adlam, Lluís Masanes, and Nathan Wiebe. Thermalization and canonical typicality in translation-invariant quantum lattice systems. *Communications in Mathematical Physics*, 340(2):499–561, Dec 2015.

[73] Hal Tasaki. On the local equivalence between the canonical and the microcanonical ensembles for quantum spin systems. *Journal of Statistical Physics*, 172(4):905–926, jun 2018.

[74] Takashi Mori. Macrostate equivalence of two general ensembles and specific relative entropies. *Phys. Rev. E*, 94:020101, Aug 2016.

[75] Francois Leyvraz and Stefano Ruffo. Ensemble inequivalence in systems with long-range interactions. *Journal of Physics A: Mathematical and General*, 35(2):285–294, jan 2002.

[76] Julien Barré, David Mukamel, and Stefano Ruffo. Inequivalence of ensembles in a system with long-range interactions. *Phys. Rev. Lett.*, 87:030601, Jun 2001.

[77] Alessandro Campa, Thierry Dauxois, and Stefano Ruffo. Statistical mechanics and dynamics of solvable models with long-range interactions. *Physics Reports*, 480(3):57–159, 2009.

[78] F. Bouchet and J. Barré. Classification of phase transitions and ensemble inequivalence, in systems with long range interactions. *Journal of Statistical Physics*, 118(5):1073–1105, Mar 2005.

[79] Julien Barré, David Mukamel, and Stefano Ruffo. *Ensemble Inequivalence in Mean-Field Models of Magnetism*, pages 45–67. Springer Berlin Heidelberg, Berlin, Heidelberg, 2002.

[80] Anurag Anshu. Concentration bounds for quantum states with finite correlation length on quantum spin lattice systems. *New Journal of Physics*, 18(8):083011, aug 2016.

[81] H. Wilming, M. Goihl, C. Krumnow, and J. Eisert. Towards local equilibration in closed interacting quantum many-body systems, 2017.

[82] R. A. Jalabert, H. U. Baranger, and A. D. Stone. Conductance fluctuations in the ballistic regime: A probe of quantum chaos? *Phys. Rev. Lett.*, 65:2442, 1990.

[83] C. M. Marcus, A. J. Rimberg, R. M. Westervelt, P. F. Hopkins, and A. C. Gossard. Conductance fluctuations and chaotic scattering in ballistic microstructures. *Phys. Rev. Lett.*, 69:506, 1992.

[84] V. Milner, J. L. Hanssen, W. C. Campbell, and M. G. Raizen. Optical billiards for atoms. *Phys. Rev. Lett.*, 86:1514, 2001.

[85] N. Friedman, A. Kaplan, D. Carasso, and N. Davidson. Observation of chaotic and regular dynamics in atom-optics billiards. *Phys. Rev. Lett.*, 86:1518, 2001.

[86] H. J. Stockmann and J. Stein. "Quantum" chaos in billiards studied by microwave absorption. *Phys. Rev. Lett.*, 64:2215, 1990.

[87] S. Sridhar. Experimental observation of scarred eigenfunctions of chaotic microwave cavities. *Phys. Rev. Lett.*, 67:785, 1991.

[88] F. L. Moore, J. C. Robinson, C. Bharucha, P. E. Williams, and M. G. Raizen. Observation of dynamical localization in atomic momentum transfer: A new testing ground for quantum chaos. *Phys. Rev. Lett.*, 73:2974, 1994.

[89] D. A. Steck, W. H. Oskay, and M. G. Raizen. Observation of chaos-assisted tunneling between islands of stability. *Science*, 293:274, 2001.

[90] W. K. Hensinger, H. Häffner, A. Browaeys, N. R. Heckenberg, K. Helmerson, C. McKenzie, G. J. Milburn, W. D. Phillips, S. L. Rolston, H. Rubinsztein-Dunlop, and B. Upcroft. Dynamical tunnelling of ultracold atoms. *Nature*, 412:52, 2001.

[91] S. Chaudhury, A. Smith, B. E. Anderson, S. Ghose, and P. S. Jessen. Quantum signatures of chaos in a kicked top. *Nature*, 461:768, 2009.

[92] Y. S. Weinstein, S. Lloyd, J. Emerson, and D. G. Cory. Experimental implementation of the quantum baker's map. *Phys. Rev. Lett.*, 89:157902, 2002.

[93] E. P. Wigner. On the statistical distribution of the widths and spacings of nuclear resonance levels. *Proc. Cambridge Philos. Soc.*, 47:790, 1951.

[94] C. E. Porter. *Statistical theories of spectra: fluctuations*. Academic Press, New York, 1965.

[95] M. V. Berry and M. Tabor. Level clustering in the regular spectrum. *Proc. R. Soc. A*, 356:375, 1977.

[96] M. V. Berry. Quantum chaology (The Bakerian Lecture). *Proc. R. Soc. A*, 413:183, 1987.

[97] M. Rigol, V. Dunjko, and M. Olshanii. Thermalization and its mechanism for generic isolated quantum systems. *Nature*, 452(7189):854–858, 2008.

[98] M. Rigol and M. Srednicki. Alternatives to eigenstate thermalization. *Phys. Rev. Lett.*, 108:110601, Mar 2012.

[99] A. Khodja, R. Steinigeweg, and J. Gemmer. Relevance of the eigenstate thermalization hypothesis for thermal relaxation. *Phys. Rev. E*, 91:012120, Jan 2015.

[100] Joshua M Deutsch. Eigenstate thermalization hypothesis. *Reports on Progress in Physics*, 81(8):082001, jul 2018.

[101] Alberto Rolandi and Henrik Wilming. Extensive rényi entropies in matrix product states, 2020.

[102] Jonas Haferkamp, Christian Bertoni, Ingo Roth, and Jens Eisert. Emergent statistical mechanics from properties of disordered random matrix product states. *PRX Quantum*, 2:040308, Oct 2021.

[103] Yichen Huang and Aram W. Harrow. Instability of localization in translation-invariant systems, 2019.

[104] Kazuya Kaneko, Eiki Iyoda, and Takahiro Sagawa. Work extraction from a single energy eigenstate. *Phys. Rev. E*, 99:032128, Mar 2019.

[105] Guillaume Roux. Finite-size effects in global quantum quenches: Examples from free bosons in an harmonic trap and the one-dimensional bose-hubbard model. *Phys. Rev. A*, 81:053604, May 2010.

[106] Giulio Biroli, Corinna Kollath, and Andreas M. Läuchli. Effect of rare fluctuations on the thermalization of isolated quantum systems. *Phys. Rev. Lett.*, 105:250401, Dec 2010.

[107] S. Genway, A. F. Ho, and D. K. K. Lee. Thermalization of local observables in small hubbard lattices. *Phys. Rev. A*, 86:023609, Aug 2012.

[108] Clemens Neuenhahn and Florian Marquardt. Thermalization of interacting fermions and delocalization in fock space. *Phys. Rev. E*, 85:060101, Jun 2012.

[109] R. Steinigeweg, A. Khodja, H. Niemeyer, C. Gogolin, and J. Gemmer. Pushing the limits of the eigenstate thermalization hypothesis towards mesoscopic quantum systems. *Phys. Rev. Lett.*, 112:130403, Apr 2014.

[110] Hyungwon Kim, Tatsuhiko N. Ikeda, and David A. Huse. Testing whether all eigenstates obey the eigenstate thermalization hypothesis. *Phys. Rev. E*, 90:052105, Nov 2014.

[111] R. Steinigeweg, J. Herbrych, and P. Prelovšek. Eigenstate thermalization within isolated spin-chain systems. *Phys. Rev. E*, 87(1):012118, January 2013.

[112] Marcos Rigol. Quantum quenches and thermalization in one-dimensional fermionic systems. *Phys. Rev. A*, 80:053607, Nov 2009.

[113] Marcos Rigol. Breakdown of thermalization in finite one-dimensional systems. *Phys. Rev. Lett.*, 103:100403, Sep 2009.

[114] Ehsan Khatami, Guido Pupillo, Mark Srednicki, and Marcos Rigol. Fluctuation-dissipation theorem in an isolated system of quantum dipolar bosons after a quench. *Phys. Rev. Lett.*, 111:050403, Jul 2013.

[115] Marcos Rigol and Lea F. Santos. Quantum chaos and thermalization in gapped systems. *Phys. Rev. A*, 82:011604, Jul 2010.

[116] Lea F. Santos and Marcos Rigol. Onset of quantum chaos in one-dimensional bosonic and fermionic systems and its relation to thermalization. *Phys. Rev. E*, 81:036206, Mar 2010.

[117] Tyler LeBlond, Krishnanand Mallayya, Lev Vidmar, and Marcos Rigol. Entanglement and matrix elements of observables in interacting integrable systems. *Phys. Rev. E*, 100:062134, Dec 2019.

[118] Chi-Fang Chen and Fernando G. S. L. Brandão. Fast thermalization from the eigenstate thermalization hypothesis, 2021.

[119] Shoki Sugimoto, Ryusuke Hamazaki, and Masahito Ueda. Eigenstate thermalization in long-range interacting systems, 2021.

[120] S. Sorg, L. Vidmar, L. Pollet, and F. Heidrich-Meisner. Relaxation and thermalization in the one-dimensional bose-hubbard model: A case study for the interaction quantum quench from the atomic limit. *Phys. Rev. A*, 90:033606, Sep 2014.

[121] Abdellah Khodja, Robin Steinigeweg, and Jochen Gemmer. Relevance of the eigenstate thermalization hypothesis for thermal relaxation. *Phys. Rev. E*, 91:012120, Jan 2015.

[122] A. Chandran, Marc D. Schulz, and F. J. Burnell. The eigenstate thermalization hypothesis in constrained hilbert spaces: A case study in non-abelian anyon chains. *Phys. Rev. B*, 94:235122, Dec 2016.

[123] David J. Luitz and Yevgeny Bar Lev. Anomalous thermalization in ergodic systems. *Phys. Rev. Lett.*, 117:170404, Oct 2016.

[124] Zhihao Lan and Stephen Powell. Eigenstate thermalization hypothesis in quantum dimer models. *Phys. Rev. B*, 96:115140, Sep 2017.

[125] Rubem Mondaini and Marcos Rigol. Eigenstate thermalization in the two-dimensional transverse field ising model. ii. off-diagonal matrix elements of observables. *Phys. Rev. E*, 96:012157, Jul 2017.

[126] Julian Sonner and Manuel Vielma. Eigenstate thermalization in the sachdev-ye-kitaev model. *Journal of High Energy Physics*, 2017(11):149, Nov 2017.

[127] Itai Arad, Tomotaka Kuwahara, and Zeph Landau. Connecting global and local energy distributions in quantum spin models on a lattice. *Journal of Statistical Mechanics: Theory and Experiment*, 2016(3):033301, 2016.

[128] Thiago R de Oliveira, Christos Charalambous, Daniel Jonathan, Maciej Lewenstein, and Arnau Riera. Equilibration time scales in closed many-body quantum systems. *New Journal of Physics*, 2018.

[129] Tomotaka Kuwahara and Keiji Saito. Gaussian concentration bound and ensemble equivalence in generic quantum many-body systems including long-range interactions. *Annals of Physics*, 421:168278, 2020.

[130] Tomotaka Kuwahara and Keiji Saito. Eigenstate thermalization from the clustering property of correlation. *Phys. Rev. Lett.*, 124:200604, May 2020.

[131] Giacomo De Palma, Alessio Serafini, Vittorio Giovannetti, and Marcus Cramer. Necessity of eigenstate thermalization. *Phys. Rev. Lett.*, 115:220401, Nov 2015.

[132] Fernando G. S. L. Brandão, Elizabeth Crosson, M. Burak Şahinoğlu, and John Bowen. Quantum error correcting codes in eigenstates of translation-invariant spin chains. *Phys. Rev. Lett.*, 123:110502, Sep 2019.

[133] Takashi Mori. Weak eigenstate thermalization with large deviation bound. *arXiv e-prints*, page arXiv:1609.09776, Sep 2016.

[134] M.A. Nielsen, I.L. Chuang, I. Chuang, and I.L. Chuang. *Quantum Computation and Quantum Information*. Cambridge Series on Information and the Natural Sciences. Cambridge University Press, 2000.

[135] G. Jaeger. *Quantum Information: An Overview*. Springer New York, 2007.

[136] Lev Vidmar and Marcos Rigol. Entanglement entropy of eigenstates of quantum chaotic hamiltonians. *Phys. Rev. Lett.*, 119:220603, Nov 2017.

[137] Ruihua Fan, Pengfei Zhang, Huitao Shen, and Hui Zhai. Out-of-time-order correlation for many-body localization. *Science Bulletin*, 62(10):707 – 711, 2017.

[138] Adam Nahum, Sagar Vijay, and Jeongwan Haah. Operator spreading in random unitary circuits. *Phys. Rev. X*, 8:021014, Apr 2018.

[139] J I Latorre and A Riera. A short review on entanglement in quantum spin systems. *Journal of Physics A: Mathematical and Theoretical*, 42(50):504002, 2009.

[140] M B Hastings. An area law for one-dimensional quantum systems. *Journal of Statistical Mechanics: Theory and Experiment*, 2007(08):P08024–P08024, aug 2007.

[141] Luigi Amico, Rosario Fazio, Andreas Osterloh, and Vlatko Vedral. Entanglement in many-body systems. *Rev. Mod. Phys.*, 80:517–576, May 2008.

[142] J. Eisert, M. Cramer, and M. B. Plenio. Colloquium: Area laws for the entanglement entropy. *Rev. Mod. Phys.*, 82:277–306, Feb 2010.

[143] Lev Vidmar, Lucas Hackl, Eugenio Bianchi, and Marcos Rigol. Entanglement entropy of eigenstates of quadratic fermionic hamiltonians. *Phys. Rev. Lett.*, 119:020601, Jul 2017.

[144] Lev Vidmar, Lucas Hackl, Eugenio Bianchi, and Marcos Rigol. Volume law and quantum criticality in the entanglement entropy of excited eigenstates of the quantum ising model. *Phys. Rev. Lett.*, 121:220602, Nov 2018.

[145] Ferenc Iglói, Zsolt Szatmári, and Yu-Cheng Lin. Entanglement entropy dynamics of disordered quantum spin chains. *Phys. Rev. B*, 85:094417, Mar 2012.

[146] Gabriele De Chiara, Simone Montangero, Pasquale Calabrese, and Rosario Fazio. Entanglement entropy dynamics of heisenberg chains. *Journal of Statistical Mechanics: Theory and Experiment*, 2006(03):P03001, 2006.

[147] R.J̃. Lewis-Swan et al. Unifying fast scrambling, thermalization and entanglement through the measurement of fotocs in the dicke model. *arXiv.org*, 2018.

[148] C. W. von Keyserlingk, Tibor Rakovszky, Frank Pollmann, and S. L. Sondhi. Operator hydrodynamics, otocs, and entanglement growth in systems without conservation laws. *Phys. Rev. X*, 8:021013, Apr 2018.

[149] Fabien Alet and Nicolas Laflorencie. Many-body localization: An introduction and selected topics. *Comptes Rendus Physique*, 2018.

[150] Hong Liu and S. Josephine Suh. Entanglement tsunami: Universal scaling in holographic thermalization. *Phys. Rev. Lett.*, 112:011601, Jan 2014.

[151] R. J. Lewis-Swan, A. Safavi-Naini, J. J. Bollinger, and A. M. Rey. Unifying scrambling, thermalization and entanglement through measurement of fidelity out-of-time-order correlators in the dicke model. *Nature Communications*, 10(1):1581, 2019.

[152] Don N. Page. Average entropy of a subsystem. *Phys. Rev. Lett.*, 71:1291–1294, Aug 1993.

[153] Piers Coleman. *Introduction to Many-Body Physics*. Cambridge University Press, 2015.

[154] G. C. Wick. The evaluation of the collision matrix. *Phys. Rev.*, 80:268–272, Oct 1950.

[155] Michel Gaudin. Une démonstration simplifiée du théorème de wick en mécanique statistique. *Nuclear Physics*, 15:89 – 91, 1960.

[156] Terry Farrelly. Equilibration of quantum gases. *New Journal of Physics*, 18(7):073014, jul 2016.

[157] Hsin-Hua Lai and Kun Yang. Entanglement entropy scaling laws and eigenstate typicality in free fermion systems. *Phys. Rev. B*, 91:081110, Feb 2015.

[158] Michelle Storms and Rajiv R. P. Singh. Entanglement in ground and excited states of gapped free-fermion systems and their relationship with fermi surface and thermodynamic equilibrium properties. *Phys. Rev. E*, 89:012125, Jan 2014.

[159] Sourav Nandy, Arnab Sen, Arnab Das, and Abhishek Dhar. Eigenstate gibbs ensemble in integrable quantum systems. *Phys. Rev. B*, 94:245131, Dec 2016.

[160] P. W. Anderson. Absence of diffusion in certain random lattices. *Phys. Rev.*, 109:1492–1505, Mar 1958.

[161] Houssam Abdul-Rahman, Bruno Nachtergaele, Robert Sims, and Günter Stolz. Localization properties of the disordered xy spin chain. *Annalen der Physik*, 529(7):1600280, 2017.

[162] Adam Nahum, Jonathan Ruhman, and David A. Huse. Dynamics of entanglement and transport in one-dimensional systems with quenched randomness. *Phys. Rev. B*, 98:035118, Jul 2018.

[163] Max McGinley, Andreas Nunnenkamp, and Johannes Knolle. Slow growth of entanglement and out-of-time-order correlators in integrable disordered systems. *arXiv:1807.06039*, 2018.

[164] Elliott Lieb, Theodore Schultz, and Daniel Mattis. Two soluble models of an antiferromagnetic chain. *Annals of Physics*, 16(3):407 – 466, 1961.

[165] Houssam Abdul-Rahman, Bruno Nachtergaele, Robert Sims, and Günter Stolz. Entanglement dynamics of disordered quantum xy chains. *Letters in Mathematical Physics*, 106(5):649–674, May 2016.

[166] Eman Hamza, Robert Sims, and Günter Stolz. Dynamical localization in disordered quantum spin systems. *Communications in Mathematical Physics*, 315(1):215–239, Oct 2012.

[167] Trithep Devakul and David A. Huse. Anderson localization transitions with and without random potentials. *Physical Review B*, 96(21), dec 2017.

[168] Jonathon Riddell and Erik S. Sørensen. Out-of-time ordered correlators and entanglement growth in the random-field xx spin chain. *Phys. Rev. B*, 99:054205, Feb 2019.

[169] G. Stolz. An introduction to the mathematics of anderson localization. *arXiv preprint arXiv:1104.2317*, 2011.

[170] Hisashi Hiramoto and Mahito Kohmoto. Scaling analysis of quasiperiodic systems: Generalized Harper model. *Physical Review B*, 40(12):8225–8234, October 1989.

[171] Christian Aulbach, André Wobst, Gert-Ludwig Ingold, Peter Hänggi, and Imre Varga. Phase-space visualization of a metal–insulator transition. *New Journal of Physics*, 6:70–70, jul 2004.

[172] Dave J. Boers, Benjamin Goedeke, Dennis Hinrichs, and Martin Holthaus. Mobility edges in bichromatic optical lattices. *Phys. Rev. A*, 75:063404, Jun 2007.

[173] Michele Modugno. Exponential localization in one-dimensional quasi-periodic optical lattices. *New Journal of Physics*, 11(3):033023, mar 2009.

[174] Mathias Albert and Patricio Leboeuf. Localization by bichromatic potentials versus anderson localization. *Phys. Rev. A*, 81:013614, Jan 2010.

[175] Pedro Ribeiro, Masudul Haque, and Achilleas Lazarides. Strongly interacting bosons in multichromatic potentials supporting mobility edges: Localization, quasi-condensation, and expansion dynamics. *Phys. Rev. A*, 87:043635, Apr 2013.

[176] Carlo Danieli, Kristian Rayanov, Boris Pavlov, Gaven Martin, and Sergej Flach. Approximating metal–insulator transitions. *International Journal of Modern Physics B*, 29(06):1550036, 2015.

[177] Xiao Li, Xiaopeng Li, and S. Das Sarma. Mobility edges in one-dimensional bichromatic incommensurate potentials. *Phys. Rev. B*, 96:085119, Aug 2017.

[178] Alejandro J. Martínez, Mason A. Porter, and P. G. Kevrekidis. Quasiperiodic granular chains and hofstadter butterflies. *Philosophical Transactions of the Royal Society A: Mathematical, Physical and Engineering Sciences*, 376(2127):20170139, 2018.

[179] J. Biddle, D. J. Priour, B. Wang, and S. Das Sarma. Localization in one-dimensional lattices with non-nearest-neighbor hopping: Generalized anderson and aubry-andré models. *Physical Review B*, 83(7), feb 2011.

[180] Yucheng Wang, Xu Xia, Yongjian Wang, Zuohuan Zheng, and Xiong-Jun Liu. Duality between two generalized aubry-andré models with exact mobility edges. *Phys. Rev. B*, 103:174205, May 2021.

[181] Giacomo Roati, Chiara D'Errico, Leonardo Fallani, Marco Fattori, Chiara Fort, Matteo Zaccanti, Giovanni Modugno, Michele Modugno, and Massimo Inguscio. Anderson localization of a non-interacting bose–einstein condensate. *Nature*, 453(7197):895–898, jun 2008.

[182] B. Deissler, M. Zaccanti, G. Roati, C. D'Errico, M. Fattori, M. Modugno, G. Modugno, and M. Inguscio. Delocalization of a disordered bosonic system by repulsive interactions. *Nature Physics*, 6(5):354–358, apr 2010.

[183] E Lucioni, B Deissler, L Tanzi, G Roati, M Zaccanti, M. Modugno, M. Larcher, F. Dalfovo, M. Inguscio, and G Modugno. Observation of Subdiffusion in a Disordered Interacting System. *Physical Review Letters*, 106(23):133–4, June 2011.

[184] L. Fallani, J. E. Lye, V. Guarrera, C. Fort, and M. Inguscio. Ultracold atoms in a disordered crystal of light: Towards a bose glass. *Phys. Rev. Lett.*, 98:130404, Mar 2007.

[185] Michael Schreiber, Sean S. Hodgman, Pranjal Bordia, Henrik P. Lüschen, Mark H. Fischer, Ronen Vosk, Ehud Altman, Ulrich Schneider, and Immanuel Bloch. Observation of many-body localization of interacting fermions in a quasirandom optical lattice. *Science*, 349(6250):842–845, aug 2015.

[186] Henrik P. Lüschen, Pranjal Bordia, Sean S. Hodgman, Michael Schreiber, Saubhik Sarkar, Andrew J. Daley, Mark H. Fischer, Ehud Altman, Immanuel Bloch, and Ulrich Schneider. Signatures of many-body localization in a controlled open quantum system. *Phys. Rev. X*, 7:011034, Mar 2017.

[187] Henrik P. Lüschen, Pranjal Bordia, Sebastian Scherg, Fabien Alet, Ehud Altman, Ulrich Schneider, and Immanuel Bloch. Observation of slow dynamics near the many-body localization transition in one-dimensional quasiperiodic systems. *Phys. Rev. Lett.*, 119:260401, Dec 2017.

[188] H. Bethe. Zur theorie der metalle. *Zeitschrift für Physik*, 71(3):205–226, Mar 1931.

[189] Vincenzo Alba. Eigenstate thermalization hypothesis and integrability in quantum spin chains. *Physical Review B*, 91(15), apr 2015.

[190] E. Ilievski, J. De Nardis, B. Wouters, J.-S. Caux, F. H. L. Essler, and T. Prosen. Complete generalized gibbs ensembles in an interacting theory. *Phys. Rev. Lett.*, 115:157201, Oct 2015.

[191] B. Wouters, J. De Nardis, M. Brockmann, D. Fioretto, M. Rigol, and J.-S. Caux. Quenching the anisotropic heisenberg chain: Exact solution and generalized gibbs ensemble predictions. *Phys. Rev. Lett.*, 113:117202, Sep 2014.

[192] B. Pozsgay, M. Mestyán, M. A. Werner, M. Kormos, G. Zaránd, and G. Takács. Correlations after quantum quenches in the xxz spin chain: Failure of the generalized gibbs ensemble. *Phys. Rev. Lett.*, 113:117203, Sep 2014.

[193] D.M. Basko, I.L. Aleiner, and B.L. Altshuler. Metal–insulator transition in a weakly interacting many-electron system with localized single-particle states. *Annals of Physics*, 321(5):1126–1205, 2006.

[194] Vadim Oganesyan and David A. Huse. Localization of interacting fermions at high temperature. *Phys. Rev. B*, 75:155111, Apr 2007.

[195] Arijeet Pal and David A. Huse. Many-body localization phase transition. *Phys. Rev. B*, 82:174411, Nov 2010.

[196] John Z. Imbrie. On many-body localization for quantum spin chains. *Journal of Statistical Physics*, 163(5):998–1048, Jun 2016.

[197] Wojciech De Roeck and Fran çois Huveneers. Stability and instability towards delocalization in many-body localization systems. *Phys. Rev. B*, 95:155129, Apr 2017.

[198] K.S. Tikhonov and A.D. Mirlin. From anderson localization on random regular graphs to many-body localization. *Annals of Physics*, 435:168525, 2021. Special Issue on Localisation 2020.

[199] David J. Luitz, Nicolas Laflorencie, and Fabien Alet. Many-body localization edge in the random-field heisenberg chain. *Phys. Rev. B*, 91:081103, Feb 2015.

[200] Jens H. Bardarson, Frank Pollmann, and Joel E. Moore. Unbounded growth of entanglement in models of many-body localization. *Phys. Rev. Lett.*, 109:017202, Jul 2012.

[201] Maksym Serbyn, Z. Papić, and Dmitry A. Abanin. Universal slow growth of entanglement in interacting strongly disordered systems. *Phys. Rev. Lett.*, 110:260601, Jun 2013.

[202] Dong-Ling Deng, Xiaopeng Li, J. H. Pixley, Yang-Le Wu, and S. Das Sarma. Logarithmic entanglement lightcone in many-body localized systems. *Phys. Rev. B*, 95:024202, Jan 2017.

[203] Marko Žnidarič, Toma ž Prosen, and Peter Prelovšek. Many-body localization in the heisenberg xxz magnet in a random field. *Phys. Rev. B*, 77:064426, Feb 2008.

[204] David M. Long, Philip J. D. Crowley, Vedika Khemani, and Anushya Chandran. Phenomenology of the prethermal many-body localized regime, 2022.

[205] D.A. Abanin, J.H. Bardarson, G. De Tomasi, S. Gopalakrishnan, V. Khemani, S.A. Parameswaran, F. Pollmann, A.C. Potter, M. Serbyn, and R. Vasseur. Distinguishing localization from chaos: Challenges in finite-size systems. *Annals of Physics*, 427:168415, 2021.

[206] Jan Šuntajs, Janez Bonča, Toma ž Prosen, and Lev Vidmar. Quantum chaos challenges many-body localization. *Phys. Rev. E*, 102:062144, Dec 2020.

[207] Scott R. Taylor and Antonello Scardicchio. Subdiffusion in a one-dimensional anderson insulator with random dephasing: Finite-size scaling, griffiths effects, and possible implications for many-body localization. *Phys. Rev. B*, 103:184202, May 2021.

[208] Dries Sels and Anatoli Polkovnikov. Dynamical obstruction to localization in a disordered spin chain. *Phys. Rev. E*, 104:054105, Nov 2021.

[209] Dries Sels and Anatoli Polkovnikov. Thermalization of dilute impurities in one dimensional spin chains, 2021.

[210] Alan Morningstar, Luis Colmenarez, Vedika Khemani, David J. Luitz, and David A. Huse. Avalanches and many-body resonances in many-body localized systems. *Phys. Rev. B*, 105:174205, May 2022.

[211] Piotr Sierant and Jakub Zakrzewski. Challenges to observation of many-body localization. *Phys. Rev. B*, 105:224203, Jun 2022.

[212] Beni Yoshida. Firewalls vs. scrambling. 2019.

[213] Brian Swingle and Debanjan Chowdhury. Slow scrambling in disordered quantum systems. *Phys. Rev. B*, 95:060201, Feb 2017.

[214] José Raúl González Alonso, Nicole Yunger Halpern, and Justin Dressel. Out-of-time-ordered-correlator quasiprobabilities robustly witness scrambling. *Phys. Rev. Lett.*, 122:040404, Feb 2019.

[215] Bin Yan, Lukasz Cincio, and Wojciech H. Zurek. Information scrambling and loschmidt echo. 2019.

[216] Jan Tuziemski. Out-of-time-ordered correlation functions in open systems: A feynman-vernon influence functional approach. 2019.

[217] Dan Mao, Debanjan Chowdhury, and T. Senthil. Slow scrambling and hidden integrability in a random rotor model. 2019.

[218] Shunsuke Nakamura, Eiki Iyoda, Tetsuo Deguchi, and Takahiro Sagawa. Universal scrambling in gapless quantum spin chains. 2019.

[219] Ron Belyansky, Przemyslaw Bienias, Yaroslav A. Kharkov, Alexey V. Gorshkov, and Brian Swingle. Minimal model for fast scrambling. *Phys. Rev. Lett.*, 125:130601, Sep 2020.

[220] Juan Maldacena, Stephen H. Shenker, and Douglas Stanford. A bound on chaos. *Journal of High Energy Physics*, 2016(8):106, Aug 2016.

[221] J. Lee, D. Kim, and D. H. Kim. Typical growth behavior of the out-of-time-ordered commutator in many-body localized systems. *arXiv:1812.00357*, 2018.

[222] Xiao Chen, Tianci Zhou, David A. Huse, and Eduardo Fradkin. Out-of-time-order correlations in many-body localized and thermal phases. *Annalen der Physik*, 529(7):1600332, 2017.

[223] Balázs Dóra and Roderich Moessner. Out-of-time-ordered density correlators in luttinger liquids. *Phys. Rev. Lett.*, 119:026802, Jul 2017.

[224] Daniel A. Roberts and Brian Swingle. Lieb-robinson bound and the butterfly effect in quantum field theories. *Phys. Rev. Lett.*, 117:091602, Aug 2016.

[225] Xiao Chen, Tianci Zhou, and Cenke Xu. Measuring the distance between quantum many-body wave functions. *Journal of Statistical Mechanics: Theory and Experiment*, 2018(7):073101, jul 2018.

[226] Cheng-Ju Lin and Olexei I. Motrunich. Out-of-time-ordered correlators in a quantum ising chain. *Phys. Rev. B*, 97:144304, Apr 2018.

[227] Jia-Hui Bao and Cheng-Yong Zhang. Out-of-time-order correlators in the one-dimensional XY model. *Communications in Theoretical Physics*, 72(8):085103, jul 2020.

[228] Shenglong Xu and Brian Swingle. Accessing scrambling using matrix product operators. *Nature Physics*, 16(2):199–204, nov 2019.

[229] Shenglong Xu and Brian Swingle. Locality, quantum fluctuations, and scrambling. *Physical Review X*, 9(3), sep 2019.

[230] Vedika Khemani, David A. Huse, and Adam Nahum. Velocity-dependent lyapunov exponents in many-body quantum, semiclassical, and classical chaos. *Phys. Rev. B*, 98:144304, Oct 2018.

[231] C. W. von Keyserlingk, Tibor Rakovszky, Frank Pollmann, and S. L. Sondhi. Operator hydrodynamics, otocs, and entanglement growth in systems without conservation laws. *Phys. Rev. X*, 8:021013, Apr 2018.

[232] Yingfei Gu, Xiao-Liang Qi, and Douglas Stanford. Local criticality, diffusion and chaos in generalized sachdev-ye-kitaev models. *Journal of High Energy Physics*, 2017(5):125, May 2017.

[233] Subhayan Sahu, Shenglong Xu, and Brian Swingle. Scrambling dynamics across a thermalization-localization quantum phase transition. *arXiv:1807.06086v1*, cond-mat.str-el, 2018.

[234] Tibor Rakovszky, Frank Pollmann, and C. W. von Keyserlingk. Diffusive hydrodynamics of out-of-time-ordered correlators with charge conservation. *Phys. Rev. X*, 8:031058, Sep 2018.

[235] Stephen H. Shenker and Douglas Stanford. Black holes and the butterfly effect. *Journal of High Energy Physics*, 2014(3):67, Mar 2014.

[236] Aavishkar A. Patel, Debanjan Chowdhury, Subir Sachdev, and Brian Swingle. Quantum butterfly effect in weakly interacting diffusive metals. *Phys. Rev. X*, 7:031047, Sep 2017.

[237] Debanjan Chowdhury and Brian Swingle. Onset of many-body chaos in the $o(n)$ model. *Phys. Rev. D*, 96:065005, Sep 2017.

[238] Shao-Kai Jian and Hong Yao. Universal properties of many-body quantum chaos at gross-neveu criticality. *arXiv:1805.12299*, 2018.

[239] Jonathon Riddell, Wyatt Kirkby, D. H. J. O'Dell, and Erik S. Sørensen. Scaling at the otoc wavefront: Integrable versus chaotic models, 2021.

[240] Yichen Huang, Yong-Liang Zhang, and Xie Chen. Out-of-time-ordered correlators in many-body localized systems. *Annalen der Physik*, 529(7):1600318, 2017.

[241] Beni Yoshida and Norman Y. Yao. Disentangling scrambling and decoherence via quantum teleportation. *Phys. Rev. X*, 9:011006, Jan 2019.

[242] Tianrui Xu, Thomas Scaffidi, and Xiangyu Cao. Does scrambling equal chaos? *Physical Review Letters*, 124(14), apr 2020.